

## Department of Precision and Microsystems Engineering

### Inherently balanced spherical pantograph-based mechanisms

K.T.Y. Durieux

Report no : 2024.023  
Coach : Dr. ir. V. van der Wijk  
Professor : Prof. dr. ir. J.L. Herder  
Specialisation : ED & MSD  
Type of report : Master Thesis  
Date : 23 May 2024





# Inherently balanced spherical pantograph-based mechanisms

by

K.T.Y. Durieux

to obtain the degree of Master of Science  
at the Delft University of Technology,  
to be defended publicly on Thursday May 23, 2024 at 15:30.

Student number: 4282051  
Project duration: February 7, 2023 – May 23, 2024  
Thesis committee: Prof. dr. ir. J.L. Herder, TU Delft, Chair  
Dr. ir. V. van der Wijk, TU Delft, Supervisor  
Dr. ir. R.A.J. van Ostayen, Tu Delft

An electronic version of this thesis is available at <http://repository.tudelft.nl/>.

# Preface

This thesis represents the results of a challenging yet rewarding journey, and I am grateful to those who have supported me along the way. My supervisor, Volkert van der Wijk, deserves special thanks for his guidance and support throughout this process. His expertise and encouragement has been instrumental in shaping this work, with the acceptance of a chapter of this thesis for the International Symposium for Advances in Robot Kinematics (ARK) 2024 as the cherry on the cake. I would also like to express my appreciation to my graduation committee consisting of Just Herder and Ron van Ostayen as well as the support staff for making my graduation possible. I am also thankful to my family for their constant love and encouragement, and to my friends and fellow students for their camaraderie, shared experiences discussions and feedback. As I present this thesis, I do so with deep appreciation for the collective efforts of those who have stood by me and helped me reach this milestone.

*K.T.Y. Durieux  
Delft, May 2024*

# Abstract

Dynamic balancing can offer significant benefits to applications where moving parts are present. It aims to reduce the reaction forces and moments due to inertia of the parts, thereby reducing vibrations. Dynamic balancing receives significant academic interest for planar and spatial applications, but limited attention for spherical mechanisms. This leads to the following goal of this thesis: Present novel force balanced spherical mechanisms design using inherent balancing planar pantograph theory for use in micro precision applications.

To achieve this goal, the thesis has been divided into three sub goals. First is defining the qualitative benefit of dynamic balancing for applications requiring micro-precision. This qualitative analysis looked into six different 'high speed precise' applications with motion and determined a potentially significant benefit exists for applications such as (space) telescopes, space manipulation, additive manufacturing, motions stages and beam steering. Engines and drives require new balancing methods to achieve significant benefit. However, the analysis also showed that many different aspects other than inertia also influence precision, thereby potentially reducing the gained benefit in precision. This is due to the addition of extra components or mass in most common dynamic balancing methods.

The second goal presents five new shaking force balanced spherical mechanisms using inherent balancing theory. Here the planar knowledge of inherently balanced shapes such as the pantograph as well as the use of projections are used to design three novel types of balanced spherical pantographs, namely the spherical pantograph, double spherical pantograph and the double S shaped mechanism with surrounding 4R four-bar linkage. Also, two additional variations of the spherical pantograph and the double spherical pantograph are presented, which leads to a total of five new designs. Each design has its required constraints and available design freedom described. Also, the balance conditions for the double spherical pantograph are presented.

The last goal shows ten novel force balanced remote center mechanisms, using the three types of inherently balanced spherical pantographs. These remote center mechanisms are either using a swivel joint or are a combination of spherical pantographs to form a parallel manipulator. This allows all end effectors to show spherical movement, around a fixed Center of Rotation. The pros and cons as well as feasible variations and constraints are also discussed. To show the use case of a force balanced remote center mechanism, a realistic design has been made for a beam steering application, where a mirror can perform a tip/tilt movement around a shared center of rotation. The mechanism uses three scaled shifted double spherical pantographs as legs to form a parallel manipulator, with a mirrored surfaced attached to the end effector and positioned in the center of rotation.

# Contents

Preface	ii
Abstract	iii
1 Introduction	1
1.1 Research goals . . . . .	2
1.2 Thesis outline . . . . .	2
2 Analysis of micro-precision applications for dynamic balancing	3
3 Inherently Balanced Spherical Pantograph Mechanisms	27
4 Inherently Balanced Remote Center Mechanisms	37
5 Discussion	57
5.1 Literature research . . . . .	57
5.2 Projections . . . . .	57
5.3 Reflection on state of the art . . . . .	57
5.4 Future work . . . . .	58
6 Conclusion	59
Bibliography	64
Appendices	64
A Precision factors and effects	65
B Overview researched force balanced spherical mechanisms	69
B.1 Functioning mechanisms . . . . .	69
B.2 Non-functioning mechanisms. . . . .	78
C Overview of spherical mechanisms	84
D Mini review Beam steering application	91

# 1

## Introduction

Mechanisms have been used for centuries to make life easier. Their ability to convert input force and movement to a desired type of output force and movement makes them useful in many applications. This ability can be achieved by using various components such as gears, bevels, chains, cams, linkages and joints or by bending material [1]–[3]. These types of components allow for varied movements, from large movements in scissors lifts and conveyor belts [4], [5] to microscopically small movements within Micro-Electro-Mechanical Systems (MEMS) devices [6].

Different applications warrant diverse types of mechanisms, which can be categorised into several distinctive types. A relevant distinction is the difference between serial or parallel mechanisms. Serial mechanisms have a single line of components connected in a chain between input and output. Benefits are a simpler design, less components, the absence of singularities, a large range of motion and potentially easier control [7]. On the other hand, parallel mechanisms have several chains connecting input with output, resulting in a higher stiffness, lower inertia, easier inverse kinematics, more advantageous mass positioning and are more energy efficient [8]. A additional categorisation could be made based on the type of movement a mechanism makes, namely planar, spatial or spherical. Planar mechanisms have their rigid bodies all moving within a plane, whereas spatial mechanisms can have parts move out of said plane [9]. Spherical mechanisms are a version of spatial mechanisms, where the end-effector is constrained to move along a spherical path, resulting in a motion around a single Center of Rotation (CoR) [10].

Different applications also mean varying desirable aspects for the mechanisms, ranging from a large range of motion, small form factor, precise and accurate movement to low losses and cost. Another desirable aspect is a minimal amount of vibrations caused by parts moving within the mechanism. These vibrations result from reaction forces and moments due to the inertia of the moving components within a mechanism. When accelerated a reaction force and/or moment is created, which can then result in a net reaction force at the base of the mechanism, generating to vibrations. Dynamic balancing aims to reduce these vibrations, using passive or active balancing methods.

Dynamic balancing can be split into 3 types, namely shaking force balance, shaking moment balance as well as partial balance. Shaking force balancing aims to balance reaction forces of parts by creating a correct mass placement and movement [11]. When all reaction forces are balanced, a situation occurs where the Center of Mass (CoM) is stationary, linear momentum remains constant and the net resulting reaction force in the base is equal to zero. This situation also means gravity cannot create any movement when the stationary CoM is located in the base. All that remains are the shaking moments, which can be balanced using various moment balancing methods, such as counter rotating counter masses or using Assur groups [12]. These methods use inertia which moves in opposite directions to counteract the remaining reaction moments, ensure a constant angular momentum and a net zero reaction moment. Since many force- and moment balancing methods require additional parts, resulting in an increase in mass, inertia and complexity, solutions that achieve partial balance such as optimisation methods or path planning are also investigated [13], [14]. Contrary to dynamic balancing, which is related to movement, are static balancing methods which focus on balancing potential forces such as gravity. These static balancing methods allow for a mechanism to remain stationary in any position by using for example springs [15].

Relevant to note is the manner in which dynamic balancing is applied within the design process. Many solutions mentioned here are solutions which balance an unbalanced design using various additional solutions. These solutions therefore tend to add complexity, mass and inertia resulting in reduced performance [11]. An

alternative design philosophy is inherent dynamic balancing which uses principal vectors and pantograph shaped mechanisms to achieve shaking force balance. These methods are included during the initial design and influence kinematics, mass location and inertia. The generated design with a certain kinematics might require adjustments to achieve the desired motion or be used in combination with other mechanisms but negates the drawbacks of common balance methods by in general being lighter and less complex.

## 1.1. Research goals

Research into dynamic balancing of mechanisms is quite active but focuses in large on planar or spatial solutions. On the contrary, spherical mechanisms being a subset of spatial solutions receive much less interest, which is why the goal of this thesis is to: **Present novel force balanced spherical mechanisms designed using inherently balanced planar pantograph theory and to show how this can be used for micro precision applications.**

To achieve this, the following 3 sub-goals have been formulated:

- Display the qualitative benefit of dynamic balancing for applications requiring micro precision;
- Present novel shaking force balanced spherical pantographs using planar inherent balance theory;
- Show novel shaking force balanced remote center mechanisms displaying spherical motion and present an exemplary realistic shaking force balanced design for beam steering solution.

Each sub-goal has been answered and written as a separate paper which can be read individually. However, combined each paper contributes towards to main research goal and aid the development of knowledge into the dynamic balancing of spherical mechanisms.

## 1.2. Thesis outline

The structure of this thesis results from the research goals, with chapter 2 containing literature research into the potential benefit of dynamic balancing for high speed high precision applications with motion. Here qualitative research is described into several distinctive high precision application, where influences, solutions and an evaluation of the potential benefit are provided. This chapter forms the basis of relevance for chapter 3 and chapter 4. Chapter 3 presents research into novel inherently shaking force balanced spherical pantographs, where possible spherical motion mechanisms are shown based of inherently balanced pantographs. Variations, requirements and constraints are also presented. Chapter 4 combines the inherently balanced spherical pantographs into novel remote center mechanisms, whilst also providing an example for balance conditions of a spherical pantograph variation as well as an exemplary design for use in beam steering applications. Chapter 5 evaluates choices and results as well as future recommendations based on this thesis. Chapter 6 concludes this thesis.

# 2

## Analysis of micro-precision applications for dynamic balancing

# Analysis of micro-precision applications for dynamic balancing

K.T.Y. Durieux  
High-tech Engineering  
Delft University of Technology  
Delft, the Netherlands  
K.T.Y.Durieux@student.tudelft.nl

**Abstract**— Dynamic balancing offers advantages related to reaction forces/ vibrations, and precision is an important aspect of many high tech micro precision applications. This literature research aims to answer the question what applications requiring micro precision could benefit from dynamic balancing. Dynamic balancing methods were researched, as well as literature for general factors influencing precision of a relevant selection of applications. The selection of applications is based on 6 selection criteria and consists of (space) telescopes, space manipulation, engines/drives, additive manufacturing, motion stages and beam steering. Based on dynamic balancing knowledge, acceleration related factors per application were analysed to see whether applying dynamic balancing could provide a significant benefit in precision. The qualitative analysis shows that all but engine/drive applications can see a significant benefit, especially active and scanning mirrors, mechanical beam steering, cryo-coolers and motion stages. Engines and drives already use dynamic balancing but require new methods of balancing to further increase precision. Noteworthy are the numerous other factors influencing precision, which can potentially lead to a trade-off in precision when dynamic balancing is applied.

## I INTRODUCTION

High tech applications are continuing to advance the world we live in. Micro scale systems such as organs on chips or high volume computer chip production such as lithography allow for incredible technological progress, creating faster, smaller and more powerful systems to satisfy the ever increasing demand for higher performance [1]–[3]. However, these technologies are still limiting progress in certain fields such as Artificial Intelligence (AI) [4] and health monitoring systems [5]. To overcome these challenges, high tech applications require ever more precision and speed.

Dynamic balancing of mechanisms are methods to reduce the reaction forces in the machine base due to movement of masses. They could therefore reduce induced vibrations in the base of a system and potentially increase precision. It therefore sounds logical to use this technique in many systems to improve precision, but surprisingly, dynamic balancing sees only limited use in applications such as dynamic balancing of rotating parts [6]–[8] or engines [9]. This absence in industry and especially high tech applications raised the question why and if dynamic balancing can provide a significant benefit. This leads to the following research question: *What current applications requiring micro precision could potentially benefit from using dynamic balancing?*

The first step in determining the feasibility of dynamic balancing in high precision applications is finding which factors per application influence precision and which type of factors can be solved using dynamic balancing. This requires broad research into relevant high precision applications as well as a fundamental knowledge of balancing. The next step is to analyse the related causes per application and use the dynamic balancing and application knowledge to determine whether dynamic balancing could improve precision.

This report will first explain the fundamentals of balancing and the research method in section II. Next, chosen applications and influence of relevant factors are explained, what current solutions are already developed and what applications can benefit from dynamic balancing in section III. In section IV the choices made in this research as well as interesting findings will be discussed. A conclusion and future recommendations are added in section V.

## II FUNDAMENTALS

This chapter explains the fundamentals of dynamic balancing as well as the methods used for conducting this literature research.

### II-A Balancing

Balancing of objects means a system will remain stationary when no force is applied, no matter the orientation or position of the related objects. This is achieved when the forces acting on the system are in equilibrium. Balancing can be split into 2 types, namely static balancing and dynamic balancing.

Static balancing means the potential energy within a mechanism remains constant [10]. This means potential external forces such as gravity or magnetic field are compensated using internal opposing forces. This is also known as gravity compensation [11], [12], when applied to a mechanism which compensates the gravity of a payload with a mechanical design. Examples of applied statically balanced mechanisms are spring balanced desk lamps or spring assisted wall mounts, visible in Figure 1.

Dynamic balancing aims to reduce not only potential forces but also the reaction forces and moments created by the movement of masses within a machine [14]. The forces required to overcome the inertia of the accelerated masses can create a reaction force which accumulates within the base of



Fig. 1: Gravity compensated desklamp [13]

the machine. As a result, a net force between the base of the machine and the world can occur. When the direction of this net force changes due to movement of the mechanism, vibrations can potentially occur influencing the mechanism as well as other parts of the machine. To reduce these vibrations, inertia forces can be compensated using opposing forces, which is considered (shaking) force balancing.

3 conditions hold if an object is force balanced, which are: a constant Center of Mass (CoM) (stationary), constant linear momentum and a net zero sum of forces at the base within the mechanism. A system is force balanced if any of these 3 conditions is met. A change in linear momentum can only occur when an external force is applied on the system, thus when no reaction forces due to inertia are present then the momentum remains constant. This constant momentum also means that any external vibrations on the base will not cause any relative movement within the mechanism i.e. the mechanism acts as a rigid body. If the CoM remains stationary (i.e. no translation globally), then no reaction force from the inertia of the masses is produced either. Additionally, if no net force exists between the base and the world, then the object is force balanced.

Some notable examples of force balancing are bascule bridges or passive camera stabilizers, see Figure 2.

Shaking moment balanced, also called fully dynamically balanced, moment balanced or reactionless [16], [17], means no reaction forces nor reaction moments act on the base. This is equivalent to no change in linear and angular momentum [14]. To compensate for reaction moments, an opposing moment related to the motion of the mechanism needs to occur. Examples of this are balance shafts within engines (frequency



Fig. 2: Bascule bridge [15]

specific) or pantographs, visible in Figure 3.

Dynamically balanced mechanisms benefit from generating no net base reaction force and moment, which could otherwise potentially induce resonance in other parts of the system. These vibrations could then result in undesired rigid body movement of the mechanism. Also, dynamic balancing can reduce the overall stresses within the base due to opposing forces [18], but opposite findings have also been found [19]. Additionally, since internal movement is not influenced by external forces when its momentum remains constant, no influence of gravity will be present in force- and moment-balanced mechanisms [14].

However, dynamically balanced mechanisms also have drawbacks. These include increased complexity, increased input torque, increased number parts and increased mass [20]–[22]. Additionally, designing for only force or moment balanced can actually increase dynamic unbalance, and therefore increase vibrations in the base. Moreover, unbalance in the drive as well as dynamic forces such as driving torques, joint friction and work loads can cause vibrations in the base, even when fully dynamically balanced [23]. Besides, most methods assume infinitely stiff links and joints, which leads to an oversimplification due to the absence of kineto-elastodynamic inertia forces [24]. Also, certain methods are only balanced at certain trajectories, thus the benefit is not applied to its full workspace [25]. Furthermore, methods of dynamic balancing for varying payloads are currently limited in their vibration

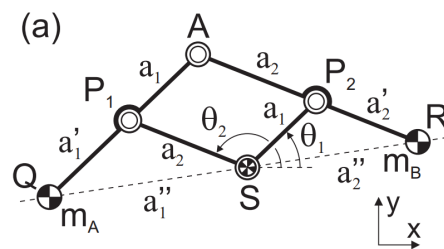


Fig. 3: Dynamically balanced pantograph [14]

reduction or payload variability, reducing their efficacy [26].

## **II-B Research method**

The first step to determine the viability of dynamic balancing within high tech applications is to investigate a relevant selection of high precision applications for limitations to their precision. This selection is required to limit the scope of this research due to the large amount of existing high tech applications as well as a limited amount of available time.

To find this relevant selection, the following criteria have been used:

- 1) Includes related internally moving parts;
- 2) Precision required is of micro scale;
- 3) Type of task (manipulation, orientation or transferring);
- 4) Type of base (free floating or fixed);
- 5) Type of movement (Planar, spatial or rotating).
- 6) High speed

This selection shall function as a varied base of high tech applications and should allow for both general insights based on commonalities as well as application specific conclusions. Since many applications share similar traits, and could therefore replace each other, making the chosen applications are only a single set out of many possible sets.

## **II-C Selection criteria**

The first criteria of internal moving parts relate to the methods for dynamic balancing, discussed in subsection II-A. For a mechanism to be dynamically balanced, a fixed or controllable relation between internally moving parts needs to exist. This makes for example fluid-, current- or magnetism-based systems impossible to be balanced with the current proposed methods. Additionally, physical movement of parts is required for dynamic balancing to be applied. The second criteria is the exclusion of the precision applications for which specifically micro scale precision is not required since these fall outside of the scope of this research.

To find a relevant selection, applications are selected based on type of task, base and movement. The 3 types of tasks are: manipulation, orientation or transferring. Manipulation is the act of moving a separate object over a fixed trajectory (including orientation). Orientation moves an internal part of the system to a specific location, without change in payload. Transferring means guided transmission of forces between 2 locations, such as a fluid piston or drilling. These 3 types of tasks cover in essence the different tasks a mechanism/ linkage can perform.

The fourth selection criteria is the type of base, since at the base forces can enter or exit the system when attached to the world. Including also free floating systems will allow for the possible finding of specific limitations to, for example, space or aquatic applications. The fifth criteria is related to the type of movement, to include limitations that occur specifically in each type of movement. The last criteria is high speed since accelerations need to be present for dynamic balancing to be useful.

## **II-D Search method**

To search for the limitations in precision and their sources, a combination of a search plan and snowball method on relevant papers was used.

The search plan consisted of the search terms visible in Table I, but not limited to. Review papers and handbooks were focused for a broad overview on the applications in order to find their workings, relevant factors for precision as well as solutions to counteract said factors. These papers also provided a good base for using the snowball method into papers related to mentioned problems or interesting solutions.

The research was mainly performed using google scholar, which shows results from publishers as well as reputable sources such as universities or large institutes. Google web search has also been used for finding specific sources or information outside of academic literature. Theses from predecessors at TU Delft as well as from other universities have been used to find information concerning dynamic balancing and interesting starting points for using the snowball method.

## **III MICRO PRECISION APPLICATIONS**

This chapter explains the workings of every selected application, followed by the limitations to their precision and the current state of the art solutions for improving precision. Lastly, based on the research results and dynamic balancing knowledge from subsection II-A, a qualitative answer is formed whether the benefit of dynamic balancing per application could be significant or not.

This chapter contains the results from researching the following selected set of applications:

- A (Space) Telescopes;
- B Space manipulation;
- C Engines/drives;
- D Additive manufacturing;
- E Motion stage;
- F Beam steering

The research results indicate a large number of factors influencing precision, but since the scope of this report is limited to dynamic balancing, only acceleration related causes are considered. Influence of the other factors as well as other choices made in this research will be discussed in section IV.

### **III-A (Space) Telescopes**

Telescopes, on land or in space, measure rays/ waves emitted or reflected by objects at large distances, using highly sensitive sensors and various systems to guide the information between source and sensors. This information can be different frequencies of electromagnetic waves, mostly between radio waves ( $>$ kHz) and gamma rays ( $>>$ THz), being limited by sensitivity of sensors and external noise sources [27], [28]. To receive precise images of space, a high angular resolution is required to define clear outlines of objects at large distances [29]. Current modern ground-based telescopes have angular resolutions of 0.015-1.0 arcsec within a Field Of View (FOV) between  $0.01^\circ$  and  $4.2^\circ$  [30], [31]. Space telescopes are usually

Search queries			
Micro	Dynamic balan*	Manipulator	High speed
Mini	Vibration isolation	Mechanism	Comparison
	Balan*	Application X	Parallel
	Performance		Passive OR Active
	Dynamics		Review
	Evaluation		Challenges
	Vibrations		
	Precision		

TABLE I: Search plan

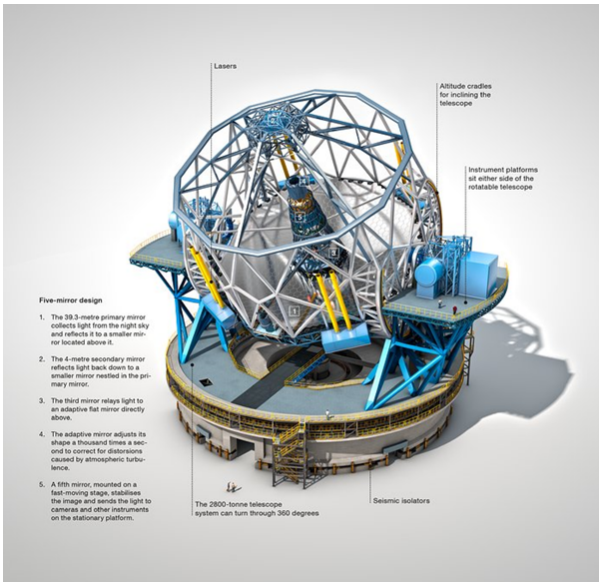


Fig. 4: Ground based telescope [34]

more precise by 1-2 orders of magnitude, with a resolution between 0.0003 and 0.1 arcsec [32], [33].

The precision of these telescopes is limited by vibrations from either internal or external sources, which causes blur and noise in measurements [36]–[38]. These vibrations can arise from internal components, external sources or due to movement of parts within the system. Several functions of



Fig. 5: ALMA radio array [35]

a telescope require the movement of parts, such as the orientation of the optics to track an object. This means for large adjustments the entire body of space telescopes or the instrument on top of the base of ground based telescope has to rotate, as visible in Figure 4. If a ground based telescope is using multiple smaller telescopes in an array (see Figure 5), then multiple movements will have to occur simultaneously for accurate pointing [39]. For small movements, beam steering mirrors or active optics are often used, either in series or parallel. These can create low amplitude vibrations at high and low frequencies [33], [40], [41]. Another function of modern day ground based telescopes is adjustment for varying atmospheric conditions, by altering the received image using adaptive optics. These optics will move sections of mirrors to adjust for aberrations [42]. These active and adaptive optics are also used in other high tech applications and will therefore be analysed in more detail in subsection III-F. Additionally, the focus of the telescope has to be adjusted during tracking to retain a sharp image, which is achieved by moving lenses or mirrors. This can occur in series for lenses or parallel if multiple mirrors have to be adjusted to capture light [43]. Also, most satellites will have folding parts due to size constraints inside the launch vehicle, as visible in Figure 6, which requires movement.

Within space telescopes several sources of internal vibrations exist, which are described as Micro-vibrations. These vibrations are caused by sensors, cry-coolers for heat management, reaction flywheels, Control Moment Gyroscopes (CMG) and solar array drives [36]. Their frequency ranges from below

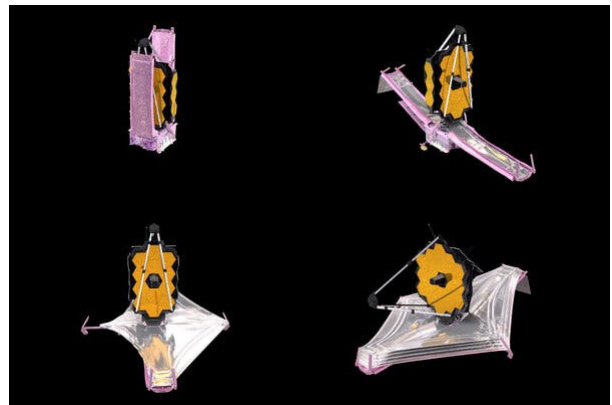


Fig. 6: James Webb space telescope unfolding [44]

1Hz up to 1kHz and are relatively small amplitude. However, they have a significant influence due to a lack of damping within the satellite [33]. Ground-based telescopes also have vibrations, either external vibrations from ground or wind, or internal due to mechanical components such as coolers, shutters, tracking errors, actuator imperfections or movement for telescope orientation. These vibrations tend to be low frequency ( $<80$  Hz), due to the large masses of the system [45].

#### *Current solutions*

Solutions for the previously mentioned micro-vibrations are prevalent in literature, due to a large interest from academics. Most solutions are either passive [36], [46], [47] semi-active [48], [49] or active [45], [50]–[53] Vibration Isolation Solutions (VIS). Additionally, choices in the system can be made to reduce vibrations [36], [54], [55] as well as reduce vibrations in the sources by combining components with isolation systems [56]. Many of these isolation systems can compensate for vibrations at low frequencies ( $\sim 10$  Hz [36] and low amplitude, which are generally the natural frequencies of the entire system. Regular viscous or elastic damping can be used to dampen high frequency vibrations (up to 1kHz [57]).

#### *Evaluation*

Precision of telescopes is affected by vibrations, but a significant difference can be made between internal and external sources. External forces cannot be dynamically balanced according to subsection II-A, thus only internal sources could potentially see a benefit. Since dynamic balancing reduces forces originating from inertia, movement with large masses or high accelerations will benefit most from dynamic balancing.

Due to the required movement of ground-based telescopes with their tracking and large mass, dynamic balancing could be beneficial in reducing the vibrations. However, it must be noted that for observing space related effects a relatively low tracking speed is required (only  $\sim 15$  arcsec per second to compensate for rotation of and orbit of earth [58]) and thus limited forces will be generated.

Active mirrors, parallel mirror arrays, pointing mechanisms and adaptive mirrors have high frequencies and vibrations, which could therefore also see a significant benefit. Current regenerative cryo-coolers have moving parts which create vibrations and could potentially be dynamically balanced. However, recuperative coolers or alternative types such as sorption-cooling can reduce or even remove the accelerations and thereby solve the vibration problems as well [40]. The solar array mechanisms could potentially be dynamically balanced as well, but since accelerations and masses are small, the benefits would be limited.

This means dynamic balancing could provide a significant benefit in active mirrors & cry-coolers and less in tracking and solar array mechanisms.

### **III-B Space manipulation**

Space manipulation is the act of moving and/of positioning objects within space, which can be done by astronauts during ExtraVehicular Activities (EVAs) or by manipulators attached



Fig. 7: Canadarm (right) and Canada hand as end effector(left) [65]

to spacecrafts or satellites (see Figure 7). This is useful for On-Orbit Servicing (OOS), which could be maintenance, upgrading or decommissioning of space systems [59]. Since (almost) no resistances exists within space, any undesired movement of the manipulator directly translates in unwanted movement of the object or satellite. This could also potentially damage both, resulting in costly and dangerous situations. Precise manipulation requires therefore precise mechanisms, actuators, motion planning, control, contact dynamic models, system identification, feedback as well as verification [36], [46], [48], [60]. The current positional accuracy of space manipulators ranges between  $\pm 5$  to 50 mm and rotational accuracy of  $\pm 1^\circ$  degree [61]–[64].

Undesired movement can be the result of vibrations, which can originate from external or internal sources. One of these internal sources can be the manipulator of the satellite or space station. These tend to be multi Degree of Freedom (DoF) serial manipulators, allowing for a large workspace and great range of orientations of the end-effector without movement of the base [59]. This flexibility is especially useful since many different tasks have to be executed using the same manipulator. However, serial manipulators also have drawbacks, such as being slower, less accurate and less rigid compared to parallel manipulators [36]. This lack of rigidity could cause eigenmodes to be excited during movement, reducing precision.

Additionally, space applies specific constraints on the manipulator such as launch weight, compact storage dimensions, built-in redundancy, joint lubrication, temperature differences and launch vibration [37], [66]–[68]. These constraints mean many manipulators cannot be properly tested before launching, due to an apparent lack of a constant momentum and gravity free environment or setup as well as a lack of joint stiffness and power in earth conditions [60]. Additionally, some vibration sources present in space telescopes are also present in space manipulators, such as coolers, reaction wheels, gyroscopes, thrusters, solar array drives and sensors [36].

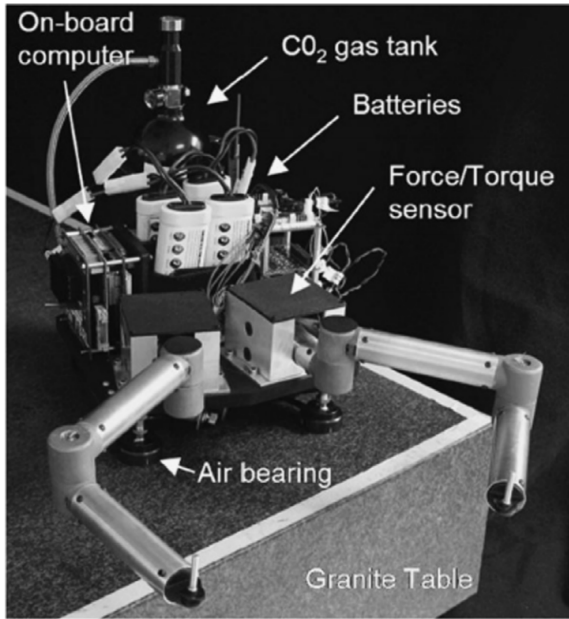


Fig. 8: Air bearing testing [59]

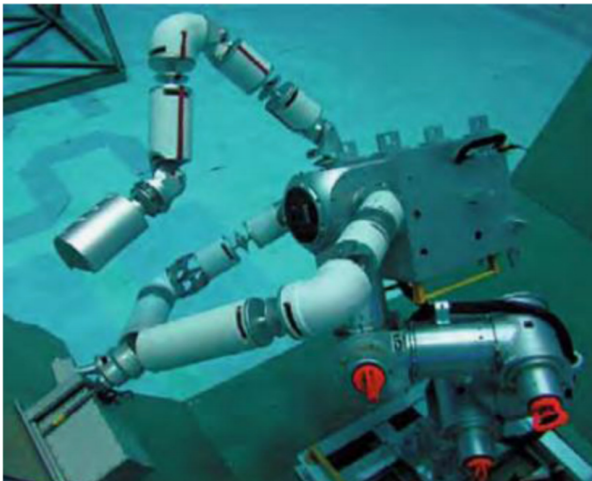


Fig. 9: Buoyancy testing [59]

#### Current solutions

Some vibration sources are like ones found in space telescopes, which means isolation systems or damping solutions as mentioned in subsection III-A can also be applied.

Current solutions for testing of 0g manipulators is performed using either suspension testing, air-bearing supported testing, cable suspension, neutral buoyancy testing, free-fall, magnetic suspension, large rotating wheels or hardware-in-the-loop simulations [59]. Of these types, air-bearing supported testing is the most applied method, which allows for planar zero momentum movement but no vertical compensation, visible in Figure 8. Neutral buoyancy tests are also commonly applied during space related training and validation, but accuracy is hampered because of the resistances due to the fluid as

well as having to modify the manipulator for the test due to the risk of contamination (see Figure 9) [59]. Another method is to adjust the control of the manipulator based on a model of the free-floating base. This method is called HIL (Hardware In Line) and uses a similar physical manipulator. The model of the manipulator in space will define the reactions the base would make upon manipulation, and then the resulting influence is implemented in the manipulator control [60]. Other test methods also differ, either in environment (momentum or resistances) or capabilities (range of motion or forces) [59].

#### Evaluation

Since vibrations can arise from movement of the manipulator, using a dynamically balanced design can reduce these reaction forces. Even though the mass and accelerations of the manipulator are relatively small, a significant benefit can be had by using dynamic balancing. This is due to the free-floating mode of the satellite (no thruster use) during manipulation, eliminating sudden motions caused by these thrusters and conserves propellant and power [59], [60]. This means the correct attitude in this mode can only be guaranteed if control gyroscopes or reaction wheels are applied or if no reaction force is exerted during movement. This is why dynamic balancing can reduce energy consumption, make control easier and improve precision. Additionally, the momentum of the system remains constant eliminating gravity's influence and resembling the constant momentum conditions of space.

Another aspect where dynamic balancing of the manipulator could yield a significant benefit is within testing and verification. A dynamically balancing system is minimally influenced by gravity and has a constant momentum. This means no difference would occur when environments change from here on earth to space, concerning tested gravity and momentum. A good verification and test would allow for better fine tuning of control thereby improving precision of the manipulator. However, it must be noted that this holds for the manipulator and only for gravity and momentum. Other conditions, such as temperature, vacuum and overall satellite constant momentum would have to be accounted for in a different manner. Also, since some vibration causes are like ones found in the space telescopes, dynamically balancing cryo-coolers could also increase precision, see subsection III-A.

Manipulator satellites are preferably in free-floating (no thruster use) mode during manipulation, since this This is where a dynamically balanced manipulator can aid in potentially increasing precision, reducing energy consumed and making control easier since no compensation is required.

This means a significant benefit by dynamically balancing can be had concerning manipulation and cryo-coolers.

#### III-C Engines/drives

Engines and drives either turn continuously or in steps around a single axis of rotation, turning potential energy into kinetic energy. This makes them useful for many applications where controlled rotations are required, such as in vehicles, power tools or fans. Within drives and engines, mass is accelerated per step or constantly accelerated to maintain a

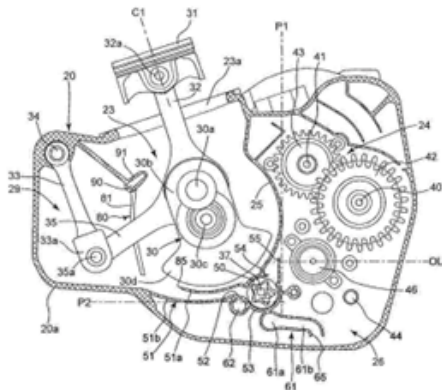


Fig. 10: Suzuki single cylinder ICE with dummy piston (left linkage) [76]

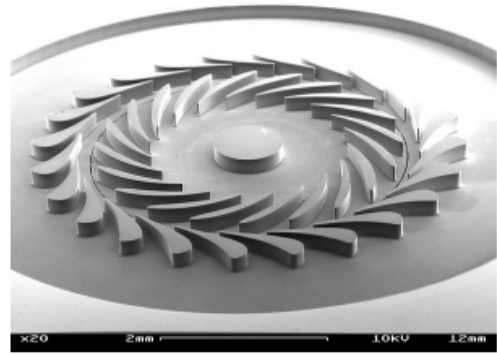


Fig. 12: Micro turbine [71]

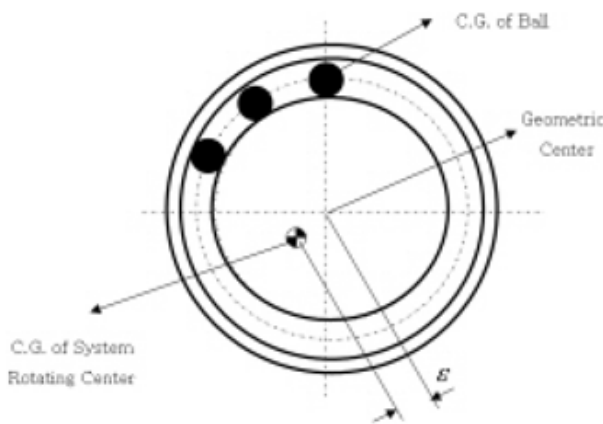


Fig. 11: Dynamic automatic balancer [77]

set rotation speed due to losses in the system. If the rotating object has an unbalance (i.e. Center of Mass (CoM) not aligned with Center of Rotation (CoR)), then a reaction force will be generated upon acceleration [69]. This can result in vibrations, especially at high rotations speeds or fast accelerations. These vibrations could result in frame vibrations [70], fluid leakage [71] and wear.

For micro-precision applications high precision of drives and engines is required to perform the tasks. This precision can be described as the minimum difference between the expected amount of rotation of the axle and the real amount for a given amount of input energy, also called resolution [72]. Precise drives currently have an angular resolution between 100 and 0.1 microns [73], [74]. When fluids are involved, such as turbines, Internal Combustion Engines (ICE) or pumps, precision becomes linked to the amount of mass moved for a given input [75].

#### Current solutions

Vibrations within engines or drives are a common problem, due to unbalance [69]. Solutions for reduction of these vibrations are either (dynamic) balancing or damping. Dynamic balancing is achieved by adding or subtracting mass at specific

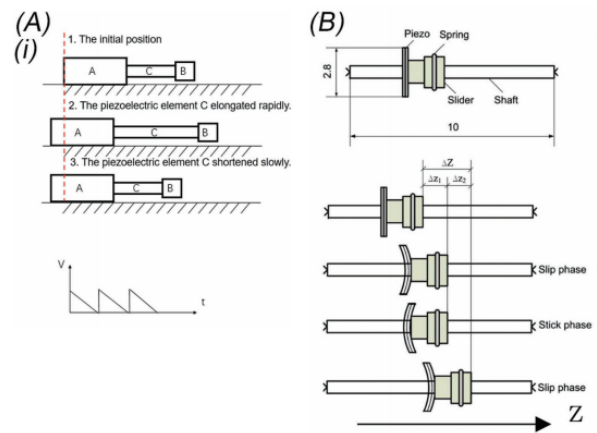


Fig. 13: Workings inertial motors [81]

spots of the rotating part, to create a more uniform inertia around the axis of rotation and thereby reduce reaction forces [69], [71], [78]. Perfect balance using addition or subtraction of mass is however limited to axially symmetric components and relatively simple components. This is not applicable to for example camshafts or turbines, due to their eccentric designs or complex shapes. Balancing using additional linkages and separate masses is also a solution. This is applied in various engine configuration, such as a boxer motor, inline 6 or by using dummy pistons (see Figure 10). Here the movement of a single piston cancels the reaction forces of the in opposite direction moving piston, and thereby reduces the vibrations.

An alternative solution to reduce the created accelerations from the unbalance is either by damping the vibrations or increasing inertia to reduce impact of smaller deviations. Damping is achieved by viscous/ viscous-elastic dampers, actively controlled bearings, input control or automatic balancing (passive or active) [79], [80]. Additionally, adding inertia by using free running balls in a concentric ring reduces unbalance, visible in Figure 11 [77].

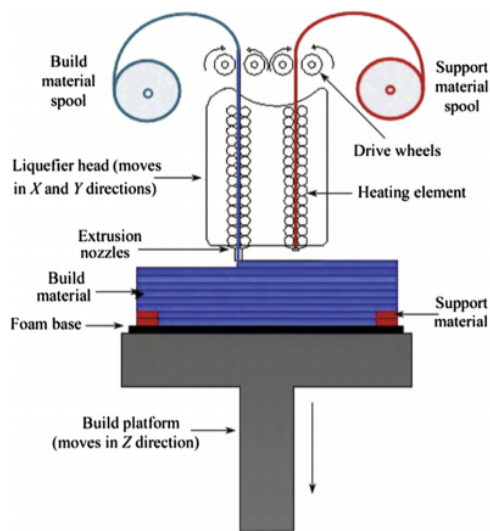


Fig. 14: Fused Deposition Modeling (FDM) workings [86]

### Evaluation

Dynamic balancing is already adding significant value to engines and drives, due to the large accelerations of masses. These solutions, such as balance shafts [82] or dummy pistons [76], [83], provide a significant reduction, proving the benefit of dynamic balancing methods. However, it must be noted that current solutions cannot be applied on small scale very high precision applications (nano- or sub-micrometer precision), such as micro turbines (see Figure 12) or Piezoelectric (PZT) rotating stages. This is due to scale not allowing subtraction or addition of mass [71], [84], or vibrations being part of how motion is generated, visible in Figure 13. This last limitation occurs for example in ultrasonic motors or inertial motors [81]. Improving precision for these small and precise types of systems requires new dynamic balancing methods to be developed.

This means a significant benefit exist for dynamic balancing, but less for very high precision and small scale applications due to a lack of suitable methods.

### III-D Additive manufacturing

Additive Manufacturing (AM) relies on creating detailed 3d objects by placing material at specific locations [85]. This can be achieved with various methods, such as Selective Laser Sintering or Melting (SLS & SLM), Fused Deposition Modeling (FDM), Stereo-Lithography Apparatus (SLA) or less common methods such as Direct Energy deposition (DED), Inkjet printing and Laminated Object Manufacturing (LOM). To get a high quality 3d product, the printer has to have a high precision. This is in AM defined as the print resolution which indicates the smallest possible producible detail. Resolutions range from 250  $\mu\text{m}$  for DED to 5  $\mu\text{m}$  for inkjet printing, with resolutions of common methods being 80-250  $\mu\text{m}$  for SLS/SLM, 50-200  $\mu\text{m}$  for FDM and 5  $\mu\text{m}$  for SLA [85].

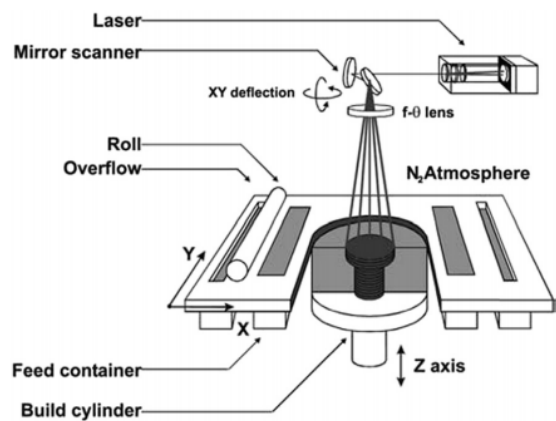


Fig. 15: Workings of Selective Laser Sintering (SLS) [86]

Since all these methods rely on adding 2d layers of material on top of one another to realise a 3d object, precise placement of materials or energy (light or heat) is required. For this precise placement, parts such as the printhead (see Figure 14), steering mirrors or motion stages for print beds need to be moved. This movement can create vibrations as well as be negatively influenced by vibrations [87]. Some additional sources of vibrations can be the wiper mechanism for powder or resin based printers (SLS/SLA) (See Figure 15) or auxiliary components such as power sources and fans.

Vibrations negatively influence mainly positioning of the printer head nozzle [88]–[91] or laser optics [86]. These vibrations mainly arise when a high production speed is desired, resulting in increased accelerations of components and thus vibrations due to inertia. The effects of these vibrations are commonly known as layer shifting [92] visible in Figure 16 or ringing, rippling or ghosting, indicating a wavy or irregular shift of layers (see Figure 17). Ghosting reduces dimensional accuracy and layer quality of the 3d part [93].

Another source of vibrations is the wiper mechanism, related to SLS or SLA printing. Here every new layer in z direction requires a smooth and homogeneous layer, visible in Figure 15. This is achieved by moving a blade across the material, thereby spreading and/or compacting the new layer. The action of the wiper is currently the limiting factor for process speed of SLS [86], as well as influencing quality and density of layer. This influences the dimensional accuracy and material properties of the produced part [94]–[96]. However, for SLA a new technology called CLIP (Continuous Liquid Interface Production) has been developed. This uses an optical window in the resin bath, through which the laser will point and form the layer on a moving z stage, visible in Figure 18. This means only a small layer of resin is required and no wiper movement. CLIP can be combined with Digital Light Processing (DLP), which exposes a full layer simultaneously with a light pattern, which will drastically increase production speed and reduce vibrations [86].



Fig. 16: Layers of FDM print shifting [88]

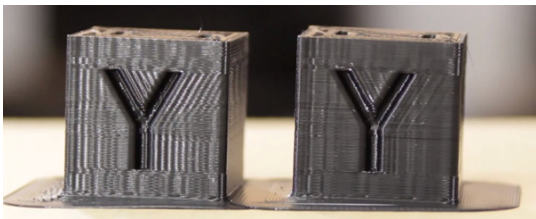


Fig. 17: Ghosting (Wavy pattern) in FDM print [97]

#### Current solutions

Current solutions for the reduction of vibrations are control based (slicer/motion planning) [88], [89], [92], [98], [99] as well as limiting print [100]–[103], scanning [104] and/or travel speed [89]. Additionally, damping or isolation (springs) of the entire system can be applied as well as using high speed manipulator designs which allow for higher speeds without increased vibrations (such as delta robots) [87], [105]. However, results also show that using a delta printer for FDM still displays a lack of rigidity due to the long link lengths causing little advantage compared to a gantry or serial solution [106]. Additionally, many enthusiasts also develop solutions such as home made dampers/ springs or DIY printer designs to increase printing speed and reduce vibrations in name of the speedbench challenge [107]. These solutions do however often lack scientific testing, and thus quantifiable results are difficult to find.

#### Evaluation

Since many parts within the printer move and any undesired movement directly negatively influences the result, a significant benefit can be had by using dynamic balancing. Reducing vibrations from moving masses such as the motion stage for the print head in FDM printers or the scanning mechanism in SLS/SLA printers, would increase overall accuracy and resolution at similar speeds. It could potentially also allow for better precision at higher print speeds. This could aid in tackling a major hurdle inhibiting mass production, which is the limited production speed compared to more traditional methods [85]. Dynamic balancing is for inkjet printing even more relevant, since a relation between jetting and stage speed

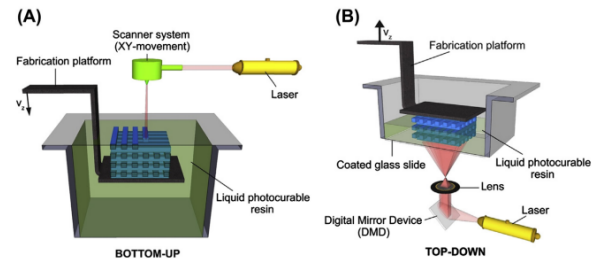


Fig. 18: SLA with regular (A) and CLIP (B) method [86]

exist [108]. This relation means a mismatch in speeds can lead to a decrease in dimensional accuracy of the created part, meaning more faster jetting is only possible when the stage is faster, making dynamic balancing of the stage even more relevant.

Dynamic balancing of the print bed could be beneficial for improving precision, but would currently see less benefit due to the changing mass on the bed. This mass variability significantly reduces the benefit of dynamic balancing, as discussed in subsection II-A. Dynamic balancing of the wiper could have a benefit on the precision, by reducing vibrations in the system and creating a more equal layer and thus material density.

This means a significant benefit can be had when applied to motion stages and scanning mirrors and less for wiper mechanisms and print beds.

#### III-E Motion stage

Motion stages or manipulators revolve around moving an end effector in space, either in planar or spatial movements. These movements can be used for point to point movement of a payload (i.e. pick and place machine) or orientating a fixed payload (such as a pointing mechanism for a laser). Having an accurate and precise stage allows for less positional errors, which can be important for many high tech applications, such as lithography, surgery or micro assembly. However, a trade-off exists between range of motion and precision [109] This means very precise motion stages (precision  $< 5\text{nm}$ ) tend to have a limited range of motion ( $100\text{--}200\ \mu\text{m}$ ) [110]. Alternatively, larger range of motion ( $100\text{ to }25000\ \text{mm}$ ) means in general less precision ( $6\text{--}50\ \mu\text{m}$ ) [111]–[113]. A relation between precision and speed does also exist, noticeable as settling time. Here a higher stiffness will decrease settling time and thus allow for a higher bandwidth. This means the controller can control the system at higher frequencies, which results in higher precision at higher speeds [114].

While various types and variations of stages and manipulators exist, they can generally be split into 2 types. These are either serial or parallel type stage, which have distinct differences [115], [116]. The type of stage refers to the orientation and layout of links between the end effector and the base, see Figure 19. Parallel type motion stages have a higher precision, but at the cost of less range of motion, increased coupling and introduction of singularities.

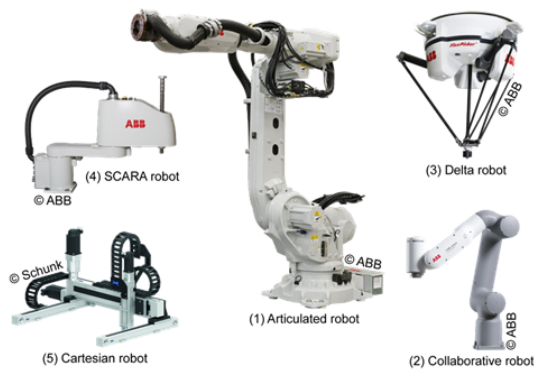


Fig. 19: Various types of manipulators (serial: 1,2&4, parallel: 3&5) [86]

Motion stages are negatively influenced by both internal and external vibrations [88], [117]–[121], reducing precision and possibly exciting natural frequencies. A relevant internal source are vibrations caused by elastic deformations during movement within the machine. These elastic deformations are caused by the inertia of accelerated masses, causing links to bend and potentially vibrate. Transmission of these vibrations to other parts of the system is also a relevant aspect to consider. Focusing on the transmission of vibrations within the structure of the system can reduce their transmission or dampen vibrations, thereby improving overall precision [56], [87], [106], [122]. Additionally, coupling of DoFs can reduce precision, but design can be optimised for as little isotropic coupling behaviour as possible [53], [123].

#### Current solutions

Since vibrations have a negative influence on the precision of motion stages, many solutions have been developed. These solutions can be either isolation or reduction of vibrations [56], [124]. Vibration isolation solutions for stages and manipulators can be active [57], [125]–[127], passive [120], [128] active-passive hybrids [129] or semi-active systems. These solutions vary in complexity from mechanical frame designs [130], [131] and control schemes [132]–[137] to complete dual stage system with actuators and sensors for verification [138]. Vibration isolation is also applied in space application, mentioned as VIS solutions in subsection III-A.

#### Evaluation

Since vibrations within motion stages are both from internal and external sources, current solutions focus mainly on mitigating them. However, the internal sources of these vibrations are not addressed. Since some of these internal vibrations are due to the accelerations of parts, dynamic balancing could provide a considerable benefit here. Most dynamic balancing solutions and methods create a mechanism/system where a single point can be moved without generating reaction forces and/or moments. These solutions exist for serial or parallel types of motion stages, planar or spatial movement as well as solutions which are purely control based. This means many solutions are already developed and implementing these

could relatively simply create a significant benefit in precision. It must however be noted that if payload variation occurs, dynamic balancing will see a reduced benefit, as mentioned in subsection II-A.

This means a significant benefit could be had within motion stages and manipulators.

### III-F Beam steering

Beam steering is used to adjust the path of light to allow for precise positioning of light or sound waves. Since reflection and refraction are related to the wavelength of the light or sound, mechanisms designed to steer sound are bound to have large dimensions. This means other solutions, such as phased arrays [139], are more commonly used instead for steering sound. Beam steering using reflection or refraction is more readily applied in light based applications, such as LiDAR (Laser imaging Detection And Ranging), optical tweezers, laser micro-machining, atmosphere compensation or optical storage [140]–[142]. Precision within beam steering is the resolution of the mechanisms, which is also described as the number of resolvable spots. This is related to the maximum number of steps that can be addressed within the maximum steering angle. Precision of current beam steering solutions range between 1 and  $10^4$  spots, at maximum angles between 0.05 and 1 rad [141]. Further angles are possible with either using arrays [143], lenses [144], [145], resonance [145], [146] or having a continuous rotation [143], [147].

Beam steering can be separated into 2 categories, namely mechanical and non-mechanical [144]. Mechanical beam steering either orientates a mirror to reflect the wave or positions a refractive prism and thereby changing the steering angle. Variants of mechanical beam steering are Fast Steering Mirrors (FSM), Gimbals, Risley Prisms, Rotating polygons, lenslet arrays or MOEMS (Micro-Opto-Electro-Mechanical-System) [141], [144], [145], see Figure 20. Important to note when steering using reflection and/or refraction is the addition of phase change. Phase difference in light from multiple sources or mirrors can create destructive interference at certain places and thus reduce the intensity of the light source. It is therefore relevant when the system is an array or serial chain to not only orientate a mirror in tip or tilt, but also piston (z movement) [148].

Mechanical beam steering means it includes moving parts to alter the direction of the wave. These movements will create vibrations due to the inertia of the moving parts. This has led to an 'inertia' gap in random-access (not continuously rotating) beam steering, which is a range of steering angle and frequency where vibrations are too large for acceptable performance from mechanical solutions [141]. Higher frequencies can be achieved using resonance, continuous rotation or non-mechanical solutions such as Electro- or Acoustic-Optic Deflectors (AOD & EOD) [141], electro wetting [149], Liquid Crystals (LC) [140] or adaptive optics [150], see Figure 21. Passive solutions are also feasible, but require additional equipment to perform steering of the incoming light [151]. Additionally, combination of beam steering solutions can

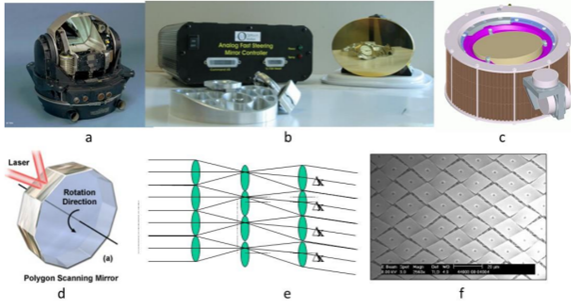


Figure 1 : Mechanical Approaches to Beam Steering, a) Gimbal, b) Fast Steering Mirror (FSM), c) Risley prism, d) Rotating Polygon, e) Lenslet Array, and f) MEMs array.

Fig. 20: Mechanical beam steering options [144]

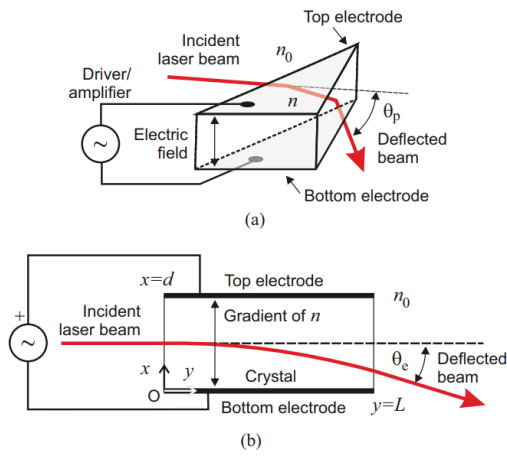


Fig. 21: Non-mechanical beam steering workings [141]

provide an overall larger steering angle and a higher steering frequency. However, coupling within the active mechanisms can decrease precision [152]. Also, actuators such as PZT can show hysteresis, which has a significant influence on precision [153] but can be fixed with model based control [154], [155].

#### Current solutions

Vibrations from these beam steering solutions are mentioned as sources for precision loss in space telescopes and additive manufacturing, see subsection III-A and subsection III-D. Several solutions to reduce these vibrations have been developed, such as force balancing using opposing actuators [142], [156], [157] or counter rotating frames [158], [159] as well as passive/active (vibrations) isolation solutions discussed in subsection III-A.

#### Evaluation

Since beam steering requires high frequency adjustments, mechanical solutions are negatively influenced by the reaction forces generated by the inertia of the moving parts such as mirrors or prisms. Dynamic balancing of these solutions could thus provide a considerable benefit, improving the resolution and reducing negative influences on other parts of a full system. MOEMS systems or adaptive optics, which rely on the

deformation of monolithic sections are difficult to dynamically balance using current methods [160], [161], and would thus see limited benefit from dynamic balancing. It must however be noted that non-mechanical beam steering solutions are currently receiving more attention in academics, due to the lack of movement and thus vibrations as well noise, wear and tear, drift and higher deflection angle velocities [141]. These non-mechanical beam steering would see little to no benefit from dynamic balancing and could eventually remove the need for dynamic balancing for this application.

This means dynamic balancing could provide a significant benefit for mechanical beam steering, but only a limited benefit for adaptive optics.

## IV DISCUSSION

Several choices as well as observations have been made during this literature research, which led to the following remarks.

Research into the chosen applications started by looking for what factors influence precision and what effects are visible as precision loss. This interestingly resulted in many more factors other than just inertia or acceleration related. Since many factors and effects were mentioned, an attempt was made to determine whether common sources of precision loss could be found across applications. This led to the following division: Machine, process and environmental related factors. Environmental and process related factors, visible in Table III and Table II respectively, show many factors influencing the chosen applications. The environmental factors are external sources which negatively influence precision, with notable examples being temperature influence, external vibration sources or external forces. Design of the machine can be adjusted to mitigate some of these effects, but applying dynamic balancing would provide limited to no benefit in reducing these effects, see subsection II-A. Similarly, process related factors are inherent to the process or functionality of system. They depend on parts, processes and parameters which cannot be influenced by machine design. Examples are material properties of feedstock in Additive Manufacturing (AM), cavitation in pumps or axial forces in drives. Reducing these factors requires either adjustment of the process or input of the system, and dynamic balancing can therefore offer little to no significant benefit. Both process and environmental factors do have an influence on precision, thus adjusting design or process for these factors would be good general engineering practice to achieve higher precision. Machine aspect related factors as visible in Table IV have many sources and consequences influencing precision of the applications. Visible are a large number of causes and consequences related to manufacturing and assembly, indicating a large influence on precision. Similar importance can be attributed to control, followed by stiffness and acceleration related factors. Smart design choices, production methods as well as quality control can aid in reducing the negative consequences, but aspects such as wear, noise or expansion are more difficult to control or design for. Since they vary over time, a solution would need

Process aspect	Sources	Consequence	Present in:
<i>Heating</i>	Solar arrays	Disturbances, inconsistency layer width, strength & height, thermally induced structural vibrations/ disturbances	A, B, D
<i>Cooling</i>	Combustor	Combustor heat loss (Area to Volume), shrinkage	C, D
<i>Curing</i>	Dynamics (MJ)	Inconsistency layer width, strength & height	D
<i>Feedstock properties</i>	Filament conductivity dynamics, feedstock shape, feedstock consistency, droplet physical size properties, process parameters (IJ, DW)	Inconsistency layer height, width, surface quality & strength, feedrate (stringing or over extrusion/ over pumping), overspreading, reactive small particles	D
<i>Parameter</i>	Air gap	Inconsistency layer height & width, small influence on surface quality	D
<i>Parameter</i>	Building direction	layer fusion strength, inconsistency layer height & width	D
<i>Parameter</i>	Layer height (tension & viscosity) (SLM)	Inconsistency thickness, circularity surface roughness and surface waviness	D
<i>Process</i>	Gas pressure pulses	Fluid loss, deformation machine	C
<i>Process</i>	Cavitation	Damaging shock waves	C
<i>Process</i>	Interaction with object	Incorrect control, potential damage	B
<i>Process</i>	Payload identification	Incorrect control, potential damage	B
<i>Process</i>	Viscous forces	Higher forces, larger heat transfer	C
<i>Process</i>	Chemical reaction	Incomplete reaction	C
<i>Process</i>	Tip leakage		C
<i>Parameter</i>	Raster shape/ orientation		D
<i>Process</i>	Recoating/ compaction layer (SLS & SLA)		D
<i>Process</i>	Mixing (binder/particle ratio) (IJ)		D
<i>Process</i>	Droplet evaporation (AJP)		D
<i>Parameter</i>	Hatch spacing		D
<i>Process</i>	Splatter (droplet velocity) (IJ)		D
<i>Process</i>	Axial force		C
<i>Process</i>	jetting to stage speed relation (IJ)	Skewed cone jet, wavy filament	D
<i>Parameter</i>	Scan speed of non-mechanical element	Cylindrical focusing	F
<i>Parameter</i>	Nozzle pressure	Inconsistency layer height & width, feedrate (stringing or over extrusion)	D

TABLE II: Process aspects

Environment aspect	Source	Consequence	Present in:
<i>Thermal</i>	Temperature environment	Disturbances, inconsistency layer width, strength & height, expansion	D, E
<i>External vibration sources</i>	RWA, CMG, Cooler fans, systems & motors, sensors, solar array drives, adaptive optics, thrusters, scanning/pointing mechanism, motor driver, ground vibrations, rocket launch, shutters	Vibrations, fretting,	A, B, E, F
<i>External forces</i>	Aerodynamics, solar radiation pressure, uneven gravity, collisions, noise, pressure, wind, gravity	Vibrations, translations & rotations, resistance, vertical (static) load	A, B, C, D, E
<i>Conditions</i>	Air turbulences, convection, varying index of refraction, air flow, humidity	Wavelength alterations, warping of prints	A, D, F

TABLE III: Environmental aspects

to be variable, requiring adjustable designs or control methods to counteract. These solutions can exist based on feedback, but are more difficult to implement. The solution to reduce the influence from wear, noise and expansion is to control the environment with constant conditions and apply frequent maintenance.

Relevant to note is the potential trade-off for using dynamic balancing. As stated in subsection II-A, the benefits of dynamic balancing are reduced or removed reaction force in base, stationary CoM and constant momentum. Some potential general drawbacks of using dynamic balancing are increased complexity in design and production, weight, lower or combined eigenmodes due to increased number of links, increased influence from expansion and control due to larger number of parts as well as additional parts to wear down. Furthermore, increasing the number of parts increases the chance of manufacturing or assembly errors. This could thus potentially result in an overall net precision loss, when the

previously mentioned machine aspects are considered.

The full list of factors/ effects per application is present in Appendix A, including sources.

The current chosen set of applications is one of many possible sets. Applications such as machining with lathes, mills or drill as well as paper printing, MRI scanners, auto-focus system and Coordinate Measuring Machines (CMM) have also been considered, but were too similar to other applications due to their common types of movement and bases. The final selection was therefore based on interest as well as activeness of research topic in academics. The found factors as visible in Table IV cover a wide base of aspects and can thereby function as a base for more general insights related to the machine. A different set of applications could lead to different precision influencing factors, but most likely mainly different application specific factors related to process or different names for similar sources or consequences. Relevant to note is the high speed selection criterion. Dynamic

Machine aspect	Source	Consequence	Present in:
<i>Manufacturing</i>	Etching, forging, casting, machining, clearances, PZT actuator, inhomogeneous & anisotropic material, laser optics, scanning mechanism, laser source, nozzle diameter/ shape	Shaft whirling, abbe error, lens/mirror defects (aberrations), kinematic model error, dynamic balance vibrations, laser quality, fluid leakage, backlash, actuator drift, non-linearity, irregular scanning rotation motion, PZT hysteresis, spot size inconsistency, printhead resolution (MJ), voltage slamming, astigmatism, inconsistency layer height & width, feedrate (stringing or over extrusion)	A, B, C, D, E, F
<i>Assembly</i>	Preload, lubrication, assembly, mounting, bearing, consistency	Beam diameter, cosine error, friction/stiction, misalignment, non-linearity, wobble, assembly error	A, C, D, E, F
<i>Calibration/ verification</i>	Optics, 1g test validation	Kinematic model error, unaccounted transmission, sensor drift, first layer adhesion	A, B, D, F
<i>Expansion</i>	Thermal isolation, centrifugal growth	Lens/mirror defects, kinematic model error, bearing friction/stiction, deformation, thermal drift	A, C, D, E, F
<i>Stiffness</i>	Belt deformation, bearing stiffness, joint, frame/ appendage, elastic forces, transmission flexibility	Eigenmodes, coupling, hysteresis, backlash	A, B, C, D, E, F
<i>Accelerations</i>	Inertia, print speed, travel speed, scanning speed, reaction torque, wiper SLA/SLS, continuous scanning	LOS control jitter, jitter, payload vibrations, frame/ appendage vibrations	A, B, C, D, E, F
<i>Wear</i>	Bearing, joints, nozzle, belt, aging, lubricant migration, friction	Friction/stiction, hysteresis, creep, ferroelectric mirror creep, oxidation, inconsistency printer parts, pneumatic hammer, drift, bearing wobble, tracking error, repeatability, jitter	C, D, E, F
<i>Noise</i>	Motion stage	Control & sensor deviations	E
<i>Control</i>	Motion planning, assembly planning, modelling of system, sensing, system dynamics, resolution feedback, bearing control stability, thermal measuring, telescope tracking, joint sensors	Stepper backlash, stability, linearity, actuator error, mathematical error, model dimension mismatch, measuring error, tracking error, bias error, controller integer rounding, arc shape over extrusion, retraction and jerk vibrations, slamming, audible noise, noise magnification, drift, fringing field effect	A, B, C, D, E, F

TABLE IV: Machine aspects

balancing can be applied when reaction forces occur due to inertia and accelerations. This means reaction forces are large when either accelerations or inertias are large. Initial research also investigated medical applications [162], [163], robotics [116], [164] or offshore [165], but precision loss due to accelerations was not due to inertia, but due to control and actuation. This led to the creation of high speed as a selection criteria, to limit the scope of this research. Inclusion of high inertia applications could however lead to potential new candidates for dynamic balancing. The research method is qualitative of nature, since impact of vibrations due to accelerations and inertia is a difficult metric to determine. Most sources state causes or effects on precision, many without any quantitative values. This makes qualitative interpretation the best metric for whether dynamic balancing can add a significant benefit. Determining a metric would allow for better comparison as well as determine the severity of precision loss within an application. Additionally, academic literature tends to focus more onto theoretical limitations whereas practical limitations within applications are more often only found in industry, hobbyist sources or occasionally textbooks. There are potentially more factors to be found if a search is widened to include non-academic literature, but these sources might be unfounded or not properly verified.

## V CONCLUSION

This research analysed 6 representative micro-precision applications for factors influencing precision, to answer the research question what micro-precision applications could benefit from dynamic balancing. This required explanation of the principles of dynamic balancing, which was used to determine that acceleration related (aka vibrations) factors are

relevant for this research. The workings and limitations of each application were discussed, which was used for a qualitative analysis whether the benefit of dynamic balancing would be significant or not. Research shows all applications can benefit from dynamic balancing, of which dynamic balancing of active mirrors, cryo-coolers, manipulators, scanning mirrors, motion stages and mechanical beam steering could provide a significant benefit. Limited benefit would be gained from dynamic balancing of telescope tracking, solar arrays, wiper mechanisms and adaptive optics. Drives and engines do currently use dynamic balancing to great benefit, but for further improvement of precision new dynamic balancing methods will have to be developed.

Research also showed a large number of other factors then accelerations influencing precision from different sources. These other factors would see no precision benefit from dynamic balancing and could potentially cause a trade-off in precision gain. A recommendation for further research would therefore be to investigate this trade-off point and determine best engineering practices for high precision dynamic balancing. Another recommendation would be researching a vibration influence metric which would allow for description and comparison of vibration severity, as well as describe effectiveness of dynamic balancing. A further recommendation would be to research high inertia applications which were excluded from this research due to the high speed selection criteria. Researching these high inertia applications could potentially lead to new insights into uses or limitations of dynamic balancing at lower accelerations.

## REFERENCES

- [1] *Organ on a chip: Interfacing with living tissue*, Delft, The Netherlands: TU Delft. [Online]. Available: <https://www.tudelft.nl/en/eemcs/research/facilities/else-kooi-lab/applications/organ-on-a-chip-interfacing-with-living-tissue>.
- [2] *MEMS overview: MEMS devices & uses in IoT*, ARROW, Feb. 2019. [Online]. Available: <https://www.arrow.com/en/research-and-events/articles/mems-and-iot-applications>.
- [3] Gustavo Santos de M. Chagas, *The evolution of processors performance over the past 10 years*, medium.com, Dec. 2020. [Online]. Available: <https://gustavosantosmc.medium.com/the-evolution-of-processors-performance-over-the-past-10-years-976ac38e1cce>.
- [4] Rakesh Kumar, *We need more powerful processors for the A.I. revolution. Too bad the chip industry is not keeping up*, fortune.com, Jun. 2023. [Online]. Available: <https://fortune.com/2023/06/12/computer-chips-ai-computing-power-innovation-rakesh-kumar/>.
- [5] memsstar, *Challenges and Opportunities Facing Next-Generation MEMS Devices*, memsstar.com, Jun. 2021. [Online]. Available: <https://memsstar.com/challenges-and-opportunities-facing-next-generation-mems-devices/>.
- [6] *What is Dynamic Balancing?* Halesowen, United Kingdom: WDB Group. [Online]. Available: <https://wdbgroup.co.uk/blog/dynamic-balancing-explained/>.
- [7] David Manney, *Eight common benefits of dynamic balancing*, Downers Grove, IL, United States: Plant Engineering, Jul. 2016. [Online]. Available: <https://www.plantengineering.com/articles/eight-common-benefits-of-dynamic-balancing/>.
- [8] *Balancing Applications*, Gainesville, TX, United States: Probal Dynamic Balancing. [Online]. Available: <https://probaldynamicbalancing.com/applications/>.
- [9] *Dynamic Balancing*, Cleveland, GA, United States: Raby's Aircooled Technology, Jul. 2023. [Online]. Available: <https://aircooledtechnology.com/dynamic-balancing/>.
- [10] L. Wang and F. Xi, *Smart devices and machines for advanced manufacturing*. Springer Science & Business Media, 2008.
- [11] V. Arakelian and S. Briot, *Balancing of linkages and robot manipulators: advanced methods with illustrative examples*. Springer, 2015, vol. 27.
- [12] V. ARAKELIAN, *Gravity compensation in robotics—a review*, 2019.
- [13] *SPRING BALANCED | table*, Hamburg, Germany: Midgard. [Online]. Available: <https://midgard.com/pages/spring-balanced-table>.
- [14] V. van der Wijk, “Methodology for analysis and synthesis of inherently force and moment-balanced mechanisms,” English, Ph.D. dissertation, University of Twente, Netherlands, Apr. 2014, ISBN: 978-90-365-3630-1. DOI: 10.3990/1.9789036536301.
- [15] Alan Wenbourne, *Pegasus Rolling Lift Bascule Bridge*, South East London, United Kingdom: SELMEC, Feb. 2022. [Online]. Available: <https://selmec.org.uk/articles/116-pegasus-rolling-lift-bascule-bridge>.
- [16] D. Zhang and B. Wei, *Dynamic Balancing of Mechanisms and Synthesizing of Parallel Robots*. Springer, 2016.
- [17] *On the Development of Reactionless Parallel Manipulators*, vol. Volume 7A: 26th Biennial Mechanisms and Robotics Conference, International Design Engineering Technical Conferences and Computers and Information in Engineering Conference, Sep. 2000, pp. 493–502. DOI: 10.1115/DETC2000/MECH-14098. eprint: [https://asmedigitalcollection.asme.org/IDETC-CIE/proceedings-pdf/IDETC-CIE2000/35173/493/6610082/493\\_1.pdf](https://asmedigitalcollection.asme.org/IDETC-CIE/proceedings-pdf/IDETC-CIE2000/35173/493/6610082/493_1.pdf). [Online]. Available: <https://doi.org/10.1115/DETC2000/MECH-14098>.
- [18] V. Van Der Wijk, S. Krut, F. Pierrot, and J. L. Herder, “Design and experimental evaluation of a dynamically balanced redundant planar 4-rrr parallel manipulator,” *The International Journal of Robotics Research*, vol. 32, no. 6, pp. 744–759, 2013.
- [19] G. Lowen, F. Tepper, and R. Berkof, “The quantitative influence of complete force balancing on the forces and moments of certain families of four-bar linkages,” *Mechanism and Machine Theory*, vol. 9, no. 3, pp. 299–323, 1974, ISSN: 0094-114X. DOI: [https://doi.org/10.1016/0094-114X\(74\)90017-2](https://doi.org/10.1016/0094-114X(74)90017-2). [Online]. Available: <https://www.sciencedirect.com/science/article/pii/0094114X74900172>.
- [20] B. Wei and D. Zhang, “A review of dynamic balancing for robotic mechanisms,” *Robotica*, vol. 39, no. 1, pp. 55–71, 2021. DOI: 10.1017/S0263574720000168.
- [21] I. Kochev, “General theory of complete shaking moment balancing of planar linkages: A critical review,” *Mechanism and Machine Theory*, vol. 35, no. 11, pp. 1501–1514, 2000, ISSN: 0094-114X. DOI: [https://doi.org/10.1016/S0094-114X\(00\)00015-X](https://doi.org/10.1016/S0094-114X(00)00015-X). [Online]. Available: <https://www.sciencedirect.com/science/article/pii/S0094114X0000015X>.
- [22] V. van der Wijk, J. L. Herder, and B. Demeulenaere, “Comparison of Various Dynamic Balancing Principles Regarding Additional Mass and Additional Inertia,” *Journal of Mechanisms and Robotics*, vol. 1, no. 4, p. 041006, Sep. 2009, ISSN: 1942-4302. DOI: 10.1115/1.3211022. eprint: [https://asmedigitalcollection.asme.org/mechanismsrobotics/article-pdf/1/4/041006/5931432/041006\\_1.pdf](https://asmedigitalcollection.asme.org/mechanismsrobotics/article-pdf/1/4/041006/5931432/041006_1.pdf). [Online]. Available: <https://doi.org/10.1115/1.3211022>.
- [23] V. Kamenskii, “On the question of the balancing of plane linkages,” *Journal of Mechanisms*, vol. 3, no. 4, pp. 303–322, 1968, ISSN: 0022-2569. DOI: <https://doi.org/10.1115/1.3211022>.

- doi.org/10.1016/0022-2569(68)90006-2. [Online]. Available: <https://www.sciencedirect.com/science/article/pii/S0022256968900062>.
- [24] V. Arakelian, M. Dahan, and M. Smith, "A historical review of the evolution of the theory on balancing of mechanisms," in *International Symposium on History of Machines and Mechanisms Proceedings HMM 2000*, M. Ceccarelli, Ed., Dordrecht: Springer Netherlands, 2000, pp. 291–300, ISBN: 978-94-015-9554-4.
- [25] D. Zhang and B. Wei, "Critical review on complete dynamic balancing of mechanisms," *Proceedings of the 14th IFToMM World Congress*, no. 14th-4, pp. 69–74, Nov. 2015. DOI: 10.6567/IFToMM.14TH.WC.OPS10.001.
- [26] V. van der Wijk and J. L. Herder, "Force balancing of variable payload by active force-balanced reconfiguration of the mechanism," in *2009 ASME/IFToMM International Conference on Reconfigurable Mechanisms and Robots*, 2009, pp. 323–330.
- [27] *What radio frequency ranges are most beneficial for astronomy?* astronomy.stackexchange.com, Apr. 2021. [Online]. Available: <https://astronomy.stackexchange.com/questions/43508/what-radio-frequency-ranges-are-most-beneficial-for-astronomy>.
- [28] *Short wavelength astronomy*, astronomywa.net.au. [Online]. Available: <https://www.astronomywa.net.au/short-wavelength-astronomy.html>.
- [29] *astronomy*, britannica.com. [Online]. Available: <https://www.britannica.com/science/astronomy/The-techniques-of-astronomy#ref910526>.
- [30] C. Mackay, R. Rebolo-López, B. F. Castellá, *et al.*, "AOLI: Adaptive Optics Lucky Imager: diffraction limited imaging in the visible on large ground-based telescopes," in *Ground-based and Airborne Instrumentation for Astronomy IV*, I. S. McLean, S. K. Ramsay, and H. Takami, Eds., International Society for Optics and Photonics, vol. 8446, SPIE, 2012, p. 844 621. DOI: 10.1117/12.925618. [Online]. Available: <https://doi.org/10.1117/12.925618>.
- [31] H. Zhang, H. Liu, W. Xu, and Z. Lu, "Large aperture diffractive optical telescope: A review," *Optics & Laser Technology*, vol. 130, p. 106 356, 2020, ISSN: 0030-3992. DOI: <https://doi.org/10.1016/j.optlastec.2020.106356>. [Online]. Available: <https://www.sciencedirect.com/science/article/pii/S0030399220309890>.
- [32] L. Li, L. Wang, L. Yuan, *et al.*, "Micro-vibration suppression methods and key technologies for high-precision space optical instruments," *Acta Astronautica*, vol. 180, pp. 417–428, 2021, ISSN: 0094-5765. DOI: <https://doi.org/10.1016/j.actaastro.2020.12.054>. [Online]. Available: <https://www.sciencedirect.com/science/article/pii/S0094576520307979>.
- [33] L. LI, L. YUAN, L. WANG, R. ZHENG, Y. WU, and X. WANG, "Recent advances in precision measurement & pointing control of spacecraft," *Chinese Journal of Aeronautics*, vol. 34, no. 10, pp. 191–209, 2021, ISSN: 1000-9361. DOI: <https://doi.org/10.1016/j.cja.2020.11.018>. [Online]. Available: <https://www.sciencedirect.com/science/article/pii/S1000936120305847>.
- [34] *The Extremely Large Telescope (annotated)*, ESO, Aug. 2012. [Online]. Available: [https://www.eso.org/public/images/E-ELT\\_labels\\_5000/](https://www.eso.org/public/images/E-ELT_labels_5000/).
- [35] *ALMA array from the air*, ESO, Mar. 2013. [Online]. Available: <https://www.eso.org/public/images/eso1312a/>.
- [36] C. Qin, Z. Xu, M. Xia, S. He, and J. Zhang, "Design and optimization of the micro-vibration isolation system for large space telescope," *Journal of Sound and Vibration*, vol. 482, p. 115 461, 2020, ISSN: 0022-460X. DOI: <https://doi.org/10.1016/j.jsv.2020.115461>. [Online]. Available: <https://www.sciencedirect.com/science/article/pii/S0022460X20302935>.
- [37] Z. Dong, A. Jiang, Y. Dai, and J. Xue, "Space-qualified fast steering mirror for an image stabilization system of space astronomical telescopes," *Appl. Opt.*, vol. 57, no. 31, pp. 9307–9315, Nov. 2018. DOI: 10.1364/AO.57.009307. [Online]. Available: <https://opg.optica.org/ao/abstract.cfm?URI=ao-57-31-9307>.
- [38] S. Altarac, P. Berlioz-Arthaud, E. Thiébaud, *et al.*, "Effect of telescope vibrations upon high angular resolution imaging," *Monthly Notices of the Royal Astronomical Society*, vol. 322, no. 1, pp. 141–148, Mar. 2001, ISSN: 0035-8711. DOI: 10.1046/j.1365-8711.2001.04111.x. eprint: <https://academic.oup.com/mnras/article-pdf/322/1/141/18409992/322-1-141.pdf>. [Online]. Available: <https://doi.org/10.1046/j.1365-8711.2001.04111.x>.
- [39] L. F. DeSandre, "Agile beam-steering technologies for laser radar transceivers," in *Design, Modeling, and Control of Laser Beam Optics*, Y. Kohanzadeh, G. N. Lawrence, J. G. McCoy, and H. Weichel, Eds., International Society for Optics and Photonics, vol. 1625, SPIE, 1992, pp. 62–77. DOI: 10.1117/12.58935. [Online]. Available: <https://doi.org/10.1117/12.58935>.
- [40] H. Cao, "Vibration control for mechanical cryocoolers," *Cryogenics*, vol. 128, p. 103 595, 2022, ISSN: 0011-2275. DOI: <https://doi.org/10.1016/j.cryogenics.2022.103595>. [Online]. Available: <https://www.sciencedirect.com/science/article/pii/S0011227522001771>.
- [41] *OWL - FREQUENTLY ASKED QUESTIONS*, ESO, May 2007. [Online]. Available: [https://www.eso.org/sci/facilities/eelt/owl/Print\\_files/FAQs\\_PRINT.html](https://www.eso.org/sci/facilities/eelt/owl/Print_files/FAQs_PRINT.html).
- [42] P.-Y. Madec, "Overview of deformable mirror technologies for adaptive optics and astronomy," in *Adaptive Optics Systems III*, B. L. Ellerbroek, E. Marchetti, and J.-P. Véran, Eds., International Society for Optics and Photonics, vol. 8447, SPIE, 2012, p. 844 705. DOI: 10.1117/12.924892. [Online]. Available: <https://doi.org/10.1117/12.924892>.

- [43] M. J. Santer and K. A. Seffen, "Optical space telescope structures: The state of the art and future directions," *The Aeronautical Journal*, vol. 113, no. 1148, pp. 633–645, 2009. DOI: 10.1017/S0001924000003304.
- [44] D. O. Joey Roulette, *What We Know About Unfolding the James Webb Space Telescope*, nytimes.com, Jan. 2022. [Online]. Available: <https://www.nytimes.com/2022/01/08/science/webb-telescope-nasa-time-livestream.html>.
- [45] G. Palacios-Navarro, F. Arranz Martínez, R. Martín Ferrer, and P. Ramos Lorente, "Compensation techniques aimed at mitigating vibrations in optical ground-based telescopes: A systematic review," *Sensors*, vol. 21, no. 11, 2021, ISSN: 1424-8220. DOI: 10.3390/s21113613. [Online]. Available: <https://www.mdpi.com/1424-8220/21/11/3613>.
- [46] D. Kamesh, R. Pandiyan, and A. Ghosal, "Passive vibration isolation of reaction wheel disturbances using a low frequency flexible space platform," *Journal of Sound and Vibration*, vol. 331, no. 6, pp. 1310–1330, 2012, ISSN: 0022-460X. DOI: <https://doi.org/10.1016/j.jsv.2011.10.033>. [Online]. Available: <https://www.sciencedirect.com/science/article/pii/S0022460X11008558>.
- [47] H. Luo, C. Fan, Y. Li, G. Liu, and C. Yu, "Design and experiment of micro-vibration isolation system for optical satellite," *European Journal of Mechanics-A/Solids*, vol. 97, p. 104833, 2023.
- [48] D.-O. Lee, G. Park, and J.-H. Han, "Hybrid isolation of micro vibrations induced by reaction wheels," *Journal of Sound and Vibration*, vol. 363, pp. 1–17, 2016.
- [49] D. Kamesh, R. Pandiyan, and A. Ghosal, "Modeling, design and analysis of low frequency platform for attenuating micro-vibration in spacecraft," *Journal of sound and vibration*, vol. 329, no. 17, pp. 3431–3450, 2010.
- [50] Q. Hu, Y. Jia, and S. Xu, "Adaptive suppression of linear structural vibration using control moment gyroscopes," *Journal of Guidance, Control, and Dynamics*, vol. 37, no. 3, pp. 990–996, 2014. DOI: 10.2514/1.62267. eprint: <https://doi.org/10.2514/1.62267>. [Online]. Available: <https://doi.org/10.2514/1.62267>.
- [51] C. Brackett, K. Denoyer, J. Jacobs, and T. Davis, "Miniature vibration isolation system (mvis)," in *2000 IEEE Aerospace Conference. Proceedings (Cat. No.00TH8484)*, vol. 4, 2000, 335–344 vol.4. DOI: 10.1109/AERO.2000.878445.
- [52] Y. Zhang, C. Sheng, Q. Hu, M. Li, Z. Guo, and R. Qi, "Dynamic analysis and control application of vibration isolation system with magnetic suspension on satellites," *Aerospace Science and Technology*, vol. 75, pp. 99–114, 2018, ISSN: 1270-9638. DOI: <https://doi.org/10.1016/j.ast.2017.12.041>. [Online]. Available: <https://www.sciencedirect.com/science/article/pii/S1270963817315900>.
- [53] Y. Wu, K. Yu, J. Jiao, D. Cao, W. Chi, and J. Tang, "Dynamic isotropy design and analysis of a six-dof active micro-vibration isolation manipulator on satellites," *Robotics and Computer-Integrated Manufacturing*, vol. 49, pp. 408–425, 2018, ISSN: 0736-5845. DOI: <https://doi.org/10.1016/j.rcim.2017.08.003>. [Online]. Available: <https://www.sciencedirect.com/science/article/pii/S073658451530185X>.
- [54] H. W. Brandhorst, "Space power — emerging opportunities," *Acta Astronautica*, vol. 16, pp. 335–342, 1987, ISSN: 0094-5765. DOI: [https://doi.org/10.1016/0094-5765\(87\)90122-6](https://doi.org/10.1016/0094-5765(87)90122-6). [Online]. Available: <https://www.sciencedirect.com/science/article/pii/0094576587901226>.
- [55] N. Jedrich, D. Zimbelman, M. Turczyn, *et al.*, "Cryo cooler induced micro-vibration disturbances to the hubble space telescope," 2002.
- [56] X. Jiao, J. Zhang, W. Li, Y. Wang, W. Ma, and Y. Zhao, "Advances in spacecraft micro-vibration suppression methods," *Progress in Aerospace Sciences*, vol. 138, p. 100898, 2023, ISSN: 0376-0421. DOI: <https://doi.org/10.1016/j.paerosci.2023.100898>. [Online]. Available: <https://www.sciencedirect.com/science/article/pii/S0376042123000143>.
- [57] C. Wang, Y. Chen, and Z. Zhang, "Simulation and experiment on the performance of a passive/active micro-vibration isolator," *Journal of Vibration and Control*, vol. 24, no. 3, pp. 453–465, 2018.
- [58] Connor Kragh, *Auto-Guiding*, Baltimore, MD, United States: UMBC, Jan. 2023. [Online]. Available: <https://observatory.umbc.edu/modernization/auto-guiding/>.
- [59] A. Flores-Abad, O. Ma, K. Pham, and S. Ulrich, "A review of space robotics technologies for on-orbit servicing," *Progress in Aerospace Sciences*, vol. 68, pp. 1–26, 2014, ISSN: 0376-0421. DOI: <https://doi.org/10.1016/j.paerosci.2014.03.002>. [Online]. Available: <https://www.sciencedirect.com/science/article/pii/S0376042114000347>.
- [60] E. Papadopoulos, F. Aghili, O. Ma, and R. Lampariello, "Robotic manipulation and capture in space: A survey," *Frontiers in Robotics and AI*, vol. 8, 2021, ISSN: 2296-9144. DOI: 10.3389/frobt.2021.686723. [Online]. Available: <https://www.frontiersin.org/articles/10.3389/frobt.2021.686723>.
- [61] H. Liu, "An overview of the space robotics progress in china," *System (ConeXpress ORS)*, vol. 14, p. 15, 2014.
- [62] *The Shuttle Remote Manipulator System – The Canadarm*, MacDonald Dettwiler Space and Advanced Robotics Ltd. [Online]. Available: [https://ewh.ieee.org/reg/7/millennium/canadarm/canadarm\\_technical.html](https://ewh.ieee.org/reg/7/millennium/canadarm/canadarm_technical.html).
- [63] *European Robotic Arm*, ESA. [Online]. Available: [https://www.esa.int/Science\\_Exploration/Human\\_and\\_Robotic\\_Exploration/International\\_Space\\_Station/European\\_Robotic\\_Arm](https://www.esa.int/Science_Exploration/Human_and_Robotic_Exploration/International_Space_Station/European_Robotic_Arm).

- [64] *Japanese Experiment Module Remote Manipulator System*, JAXA. [Online]. Available: <https://iss.jaxa.jp/en/kibo/about/kibo/rms/>.
- [65] *Space Station Robotic Arms Have a Long Reach*, medium.com, Nov. 2019. [Online]. Available: [https://www.nasa.gov/mission\\_pages/station/research/news/b4h-3rd/hh-robotic-arms-reach](https://www.nasa.gov/mission_pages/station/research/news/b4h-3rd/hh-robotic-arms-reach).
- [66] J. Plante and B. Lee, "Environmental conditions for space flight hardware: A survey," 2005.
- [67] E. W. Roberts, "Space tribology: Its role in spacecraft mechanisms," *Journal of Physics D: Applied Physics*, vol. 45, no. 50, p. 503001, Nov. 2012. DOI: 10.1088/0022-3727/45/50/503001. [Online]. Available: <https://dx.doi.org/10.1088/0022-3727/45/50/503001>.
- [68] M. H. Krim, "Mechanical design of optical systems for space operation," in *Optomechanical Design: A Critical Review*, SPIE, vol. 10265, 1992, pp. 5–19.
- [69] C. W. De Silva, *Vibration: fundamentals and practice*. CRC press, 2006.
- [70] S. Riabzev, A. Veprik, H. Vilenchik, and N. Pundak, "Vibration generation in a pulse tube refrigerator," *Cryogenics*, vol. 49, no. 1, pp. 1–6, 2009, ISSN: 0011-2275. DOI: <https://doi.org/10.1016/j.cryogenics.2008.08.002>. [Online]. Available: <https://www.sciencedirect.com/science/article/pii/S001122750800115X>.
- [71] *Millimeter-Scale, MEMS Gas Turbine Engines*, vol. Volume 4: Turbo Expo 2003, Turbo Expo: Power for Land, Sea, and Air, Jun. 2003, pp. 669–696. DOI: 10.1115/GT2003-38866. eprint: [https://asmedigitalcollection.asme.org/GT/proceedings-pdf/GT2003/36878/669/4547397/669\\_1.pdf](https://asmedigitalcollection.asme.org/GT/proceedings-pdf/GT2003/36878/669/4547397/669_1.pdf). [Online]. Available: <https://doi.org/10.1115/GT2003-38866>.
- [72] *Resolution*, Boxborough, MA, United States: Dover Motion. [Online]. Available: <https://dovermotion.com/resources/motion-control-handbook/resolution/>.
- [73] *Precision Rotary Stages*, Boxborough, MA, United States: Dover Motion. [Online]. Available: <https://dovermotion.com/rotary-stages/>.
- [74] *Precision Rotary Stages*, Auburn, MA, United States: Physik Instrumente. [Online]. Available: <https://www.pi-usa.us/en/products/motorized-rotary-stages-goniometers/stepper-motor-rotation-stages>.
- [75] C. Lewin, *Precision Fluid Handling: It's All In The Pump*, Boxborough, MA, United States: Performance Motion Devices. [Online]. Available: <https://www.pmdcorp.com/resources/type/articles/precision-fluid-handling-its-all-in-the-pump>.
- [76] B. Verhoeven, *Suzuki Supermono: Verrassend*, Motor.nl, May 2019. [Online]. Available: <https://www.motor.nl/nieuws/suzuki-supermono-verrassend/>.
- [77] K.-O. Olsson *et al.*, "Limits for the use of auto-balancing," *International Journal of Rotating Machinery*, vol. 10, pp. 221–226, 2004.
- [78] Y. Dai, X. Tao, Z. Li, S. Zhan, Y. Li, and Y. Gao, "A review of key technologies for high-speed motorized spindles of cnc machine tools," *Machines*, vol. 10, no. 2, p. 145, 2022.
- [79] C.-W. Lee, "Mechatronics in rotating machinery," in *IFTOMM International Conference on Rotor Dynamics*, International Conference on Rotor Dynamics, 2006.
- [80] A. B. Palazzolo, R. R. Lin, R. M. Alexander, A. F. Kascak, and J. Montague, "Test and Theory for Piezoelectric Actuator-Active Vibration Control of Rotating Machinery," *Journal of Vibration and Acoustics*, vol. 113, no. 2, pp. 167–175, Apr. 1991, ISSN: 1048-9002. DOI: 10.1115/1.2930165. eprint: [https://asmedigitalcollection.asme.org/vibrationacoustics/article-pdf/113/2/167/5716477/167\\_1.pdf](https://asmedigitalcollection.asme.org/vibrationacoustics/article-pdf/113/2/167/5716477/167_1.pdf). [Online]. Available: <https://doi.org/10.1115/1.2930165>.
- [81] X. Gao, J. Yang, J. Wu, *et al.*, "Piezoelectric actuators and motors: Materials, designs, and applications," *Advanced Materials Technologies*, vol. 5, no. 1, p. 1900716, 2020. DOI: <https://doi.org/10.1002/admt.201900716>. eprint: <https://onlinelibrary.wiley.com/doi/pdf/10.1002/admt.201900716>. [Online]. Available: <https://onlinelibrary.wiley.com/doi/abs/10.1002/admt.201900716>.
- [82] A. Wheeler, *The LC4 wizard: How the KTM 690 DUKE flies along the road*, KTM, Dec. 2015. [Online]. Available: <https://blog.ktm.com/the-lc4-wizard-how-the-ktm-690-duke-flies-along-the-road/>.
- [83] J. Scaysbrook, *Ducati Supermono: A single purpose*, Old bike australia, Dec. 2022. [Online]. Available: <https://www.oldbikemag.com.au/ducati-supermono-single-purpose/>.
- [84] C. T. Leondes, *Mems/Nems:(1) Handbook techniques and applications design methods,(2) Fabrication techniques,(3) manufacturing methods,(4) Sensors and actuators,(5) Medical applications and MOEMS*. Springer, 2006.
- [85] T. D. Ngo, A. Kashani, G. Imbalzano, K. T. Nguyen, and D. Hui, "Additive manufacturing (3d printing): A review of materials, methods, applications and challenges," *Composites Part B: Engineering*, vol. 143, pp. 172–196, 2018, ISSN: 1359-8368. DOI: <https://doi.org/10.1016/j.compositesb.2018.02.012>. [Online]. Available: <https://www.sciencedirect.com/science/article/pii/S1359836817342944>.
- [86] R. H. Awad, S. A. Habash, and C. J. Hansen, "Chapter 2 - 3d printing methods," in *3D Printing Applications in Cardiovascular Medicine*, S. J. Al'Aref, B. Mosadegh, S. Dunham, and J. K. Min, Eds., Boston: Academic Press, 2018, pp. 11–32, ISBN: 978-0-12-803917-5. DOI: <https://doi.org/10.1016/B978-0-12-803917-5.00002-X>. [Online]. Available: <https://www.sciencedirect.com/science/article/pii/B978012803917500002X>.
- [87] J. Go and A. J. Hart, "Fast desktop-scale extrusion additive manufacturing," *Additive Manufacturing*, vol. 18, pp. 276–284, 2017, ISSN: 2214-8604. DOI:

- <https://doi.org/10.1016/j.addma.2017.10.016>. [Online]. Available: <https://www.sciencedirect.com/science/article/pii/S2214860416303220>.
- [88] M. Duan, D. Yoon, and C. E. Okwudire, "A limited-preview filtered b-spline approach to tracking control – with application to vibration-induced error compensation of a 3d printer," *Mechatronics*, vol. 56, pp. 287–296, 2018, ISSN: 0957-4158. DOI: <https://doi.org/10.1016/j.mechatronics.2017.09.002>. [Online]. Available: <https://www.sciencedirect.com/science/article/pii/S0957415817301277>.
- [89] E. E. Kopets, D. A. Protasova, V. S. Andreev, I. I. Loginov, K. A. Kurtova, and A. D. Skuratov, "Relation between 3d printer printhead positioning rate and detail quality," in *2022 Conference of Russian Young Researchers in Electrical and Electronic Engineering (ElConRus)*, 2022, pp. 700–703. DOI: 10.1109/ElConRus54750.2022.9755569.
- [90] M. Kam, H. Saruhan, and A. İpekçi, "Investigation the effects of 3d printer system vibrations on mechanical properties of the printed products," *Sigma Journal of Engineering and Natural Sciences*, vol. 36, no. 3, pp. 655–666, 2018, ISSN: 1304-7191.
- [91] E. E. Kopets, G. Yu. Kolev, V. M. Vatnik, A. I. Karimov, and V. G. Rybin, "Mechanical vibration analysis of a gantry 3d printer," in *2021 IEEE Conference of Russian Young Researchers in Electrical and Electronic Engineering (ElConRus)*, 2021, pp. 956–960. DOI: 10.1109/ElConRus51938.2021.9396599.
- [92] N. Edoimioya, C.-H. Chou, and C. E. Okwudire, "Vibration compensation of delta 3d printer with position-varying dynamics using filtered b-splines," *The International Journal of Advanced Manufacturing Technology*, vol. 125, no. 5-6, pp. 2851–2868, 2023.
- [93] H. K. Jackson O'Connell, *3D Print Ghosting & Ringing: 3 Easy Fixes*, all3dp.com, Feb. 2022. [Online]. Available: <https://all3dp.com/2/3d-printer-ringing-3d-print-ghosting/>.
- [94] T. Petsch, P. Regenfuß, R. Ebert, *et al.*, "Industrial laser micro sintering," in *International Congress on Applications of Lasers & Electro-Optics*, Laser Institute of America, vol. 2004, 2004, p. M705.
- [95] S.-J. John Lee, E. Sachs, and M. Cima, "Powder layer position accuracy in powder-based rapid prototyping," in *1993 International Solid Freeform Fabrication Symposium*, 1993.
- [96] J. Weinberg, "A precision blade mechanism for powder recoating in selective laser melting," Ph.D. dissertation, Massachusetts Institute of Technology, 2018.
- [97] K. Harter, *What Causes 3D Print Ghosting + How to Fix Them*, 3dtechvalley.com. [Online]. Available: <https://www.3dtechvalley.com/3d-print-ghosting/>.
- [98] L. Bochmann, C. Bayley, M. Helu, R. Transchel, K. Wegener, and D. Dornfeld, "Understanding error generation in fused deposition modeling," *Surface Topography: Metrology and Properties*, vol. 3, no. 1, p. 014002, Jan. 2015. DOI: 10.1088/2051-672X/3/1/014002. [Online]. Available: <https://dx.doi.org/10.1088/2051-672X/3/1/014002>.
- [99] D. D. Hernandez, "Factors affecting dimensional precision of consumer 3d printing," *International Journal of Aviation, Aeronautics, and Aerospace*, vol. 2, no. 4, p. 2, 2015.
- [100] M. Doshi, A. Mahale, S. Kumar Singh, and S. Deshmukh, "Printing parameters and materials affecting mechanical properties of fdm-3d printed parts: Perspective and prospects," *Materials Today: Proceedings*, vol. 50, pp. 2269–2275, 2022, 2nd International Conference on Functional Material, Manufacturing and Performances (ICFMMP-2021), ISSN: 2214-7853. DOI: <https://doi.org/10.1016/j.matpr.2021.10.003>. [Online]. Available: <https://www.sciencedirect.com/science/article/pii/S2214785321064671>.
- [101] J. Žarko, G. Vladić, M. Pál, and S. Dedijer, "Influence of printing speed on production of embossing tools using fdm 3d printing technology," *Journal of graphic engineering and design*, vol. 8, no. 1, pp. 19–27, 2017.
- [102] W. T. Nugroho, Y. Dong, and A. Pramanik, "Dimensional accuracy and surface finish of 3d printed polyurethane (pu) dog-bone samples optimally manufactured by fused deposition modelling (fdm)," *Rapid Prototyping Journal*, vol. 28, no. 9, pp. 1779–1795, 2022.
- [103] A. Dine and G.-C. Vosniakos, "On the development of a robot-operated 3d-printer," *Procedia Manufacturing*, vol. 17, pp. 6–13, 2018, 28th International Conference on Flexible Automation and Intelligent Manufacturing (FAIM2018), June 11-14, 2018, Columbus, OH, US-AGlobal Integration of Intelligent Manufacturing and Smart Industry for Good of Humanity, ISSN: 2351-9789. DOI: <https://doi.org/10.1016/j.promfg.2018.10.004>. [Online]. Available: <https://www.sciencedirect.com/science/article/pii/S235197891831120X>.
- [104] R.-J. Wang, L. Wang, L. Zhao, and Z. Liu, "Influence of process parameters on part shrinkage in sls," *The International Journal of Advanced Manufacturing Technology*, vol. 33, pp. 498–504, 2007.
- [105] F. Cavas-Martinez, M. D. M. Granados, R. M. Buil, and O. D. de-Cózar-Macias, *Advances in Design Engineering III: Proceedings of the XXXI INGEGRAF International Conference 29–30 June, 1 July 2022, Málaga, Spain*. Springer Nature, 2023.
- [106] O. V. Zakharov, K. G. Pugin, and T. N. Ivanova, "Modeling and analysis of delta kinematics fdm printer," *Journal of Physics: Conference Series*, vol. 2182, no. 1, p. 012069, Mar. 2022. DOI: 10.1088/1742-6596/2182/1/012069. [Online]. Available: <https://dx.doi.org/10.1088/1742-6596/2182/1/012069>.
- [107] Matt, *The 100*, Mar. 2023. [Online]. Available: <https://github.com/MSzturc/the100>.
- [108] K. Muldoon, Y. Song, Z. Ahmad, X. Chen, and M.-W. Chang, "High precision 3d printing for micro to nano

scale biomedical and electronic devices,” *Micromachines*, vol. 13, no. 4, p. 642, 2022.

- [109] D. B. Hiemstra, “The design of moving magnet actuators for large-range flexure-based nanopositioning,” *Mechanical Engineering, University of Michigan*, 2014.
- [110] *P-541.2 & P-542.2 XY Piezo Stage*, Auburn, MA, United States: Physik Instrumente. [Online]. Available: <https://www.physikinstrumente.nl/en/products/nanopositioning-piezo-flexure-stages/xy-piezo-flexure-stages/p-5412-p-5422-xy-piezo-stage-201530#specification>.
- [111] *Robot Repeatability vs. Accuracy*, robotsdoneright.com. [Online]. Available: <https://robotsdoneright.com/Articles/robot-repeatability-vs-accuracy.html>.
- [112] *V-855 High-Speed Linear Stage*, Auburn, MA, United States: Physik Instrumente. [Online]. Available: <https://www.physikinstrumente.nl/en/products/linear-stages/stages-with-magnetic-direct-drive-linear-motor/v-855-high-speed-linear-stage-412418507#specification>.
- [113] *IRB 4600*, ABB. [Online]. Available: <https://new.abb.com/products/robotics/robots/articulated-robots/irb-4600>.
- [114] A. Y. C. Nee, *Handbook of manufacturing engineering and technology*. Springer Publishing Company, Incorporated, 2014.
- [115] S. Briot and I. A. Bonev, “Are parallel robots more accurate than serial robots?” *Transactions of the Canadian Society for Mechanical Engineering*, vol. 31, no. 4, pp. 445–455, 2007. DOI: 10.1139/tcsme-2007-0032. eprint: <https://doi.org/10.1139/tcsme-2007-0032>. [Online]. Available: <https://doi.org/10.1139/tcsme-2007-0032>.
- [116] Y. Patel, P. George, *et al.*, “Parallel manipulators applications—a survey,” *Modern Mechanical Engineering*, vol. 2, no. 03, p. 57, 2012.
- [117] L. Zhang, Z. Long, J. Cai, Y. Liu, J. Fang, and M. Y. Wang, “Active vibration isolation of macro–micro motion stage disturbances using a floating stator platform,” *Journal of Sound and Vibration*, vol. 354, pp. 13–33, 2015, ISSN: 0022-460X. DOI: <https://doi.org/10.1016/j.jsv.2015.06.024>. [Online]. Available: <https://www.sciencedirect.com/science/article/pii/S0022460X15005064>.
- [118] A. Rugbani and K. Schreve, “The use of parallel mechanism micro-cmm in micrometrology,” in *Presented at the 4th Robotics and Mechatronics Conference of South Africa (ROBMECH 2011)*, vol. 23, 2011, p. 25.
- [119] L.-f. Zhang, X.-l. Li, J.-w. Fang, *et al.*, “Vibration isolation of extended ultra-high acceleration macro–micro motion platform considering floating stator stage,” *International Journal of Precision Engineering and Manufacturing*, vol. 20, pp. 1265–1287, 2019.
- [120] X. LI, L. ZHANG, B. JIANG, J. FANG, and Y. ZHENG, “Research trends in china for macro-micro motion platform for microelectronics manufacturing industry,” *Journal of Advanced Mechanical Design, Systems, and Manufacturing*, vol. 15, no. 3, JAMDSM0032–JAMDSM0032, 2021. DOI: 10.1299/jamdsm.2021jamdsm0032.
- [121] M. Serge, T. Patrick, and F. Duquenoy, “Chapter 6 - motion systems: An overview of linear, air bearing, and piezo stages,” in *Three-Dimensional Microfabrication Using Two-photon Polymerization*, ser. Micro and Nano Technologies, T. Baldacchini, Ed., Oxford: William Andrew Publishing, 2016, pp. 148–167, ISBN: 978-0-323-35321-2. DOI: <https://doi.org/10.1016/B978-0-323-35321-2.00008-X>. [Online]. Available: <https://www.sciencedirect.com/science/article/pii/B978032335321200008X>.
- [122] J. R. Rogers and K. Craig, “On-hardware optimization of stepper-motor system dynamics,” *Mechatronics*, vol. 15, no. 3, pp. 291–316, 2005, ISSN: 0957-4158. DOI: <https://doi.org/10.1016/j.mechatronics.2004.09.004>. [Online]. Available: <https://www.sciencedirect.com/science/article/pii/S0957415804001023>.
- [123] A. A. Allais, J. E. McInroy, and J. F. O’Brien, “Locally decoupled micromanipulation using an even number of parallel force actuators,” *IEEE Transactions on Robotics*, vol. 28, no. 6, pp. 1323–1334, 2012. DOI: 10.1109/TRO.2012.2209229.
- [124] C. Liu, X. Jing, S. Daley, and F. Li, “Recent advances in micro-vibration isolation,” *Mechanical Systems and Signal Processing*, vol. 56-57, pp. 55–80, 2015, ISSN: 0888-3270. DOI: <https://doi.org/10.1016/j.ymsp.2014.10.007>. [Online]. Available: <https://www.sciencedirect.com/science/article/pii/S0888327014004014>.
- [125] Y. Dong, F. Gao, and Y. Yue, “Modeling and experimental study of a novel 3-rpr parallel micro-manipulator,” *Robotics and Computer-Integrated Manufacturing*, vol. 37, pp. 115–124, 2016, ISSN: 0736-5845. DOI: <https://doi.org/10.1016/j.rcim.2015.07.006>. [Online]. Available: <https://www.sciencedirect.com/science/article/pii/S073658451500085X>.
- [126] G. Wu, J. Li, R. Fei, X. Wang, and D. Liu, “Analysis and design of a novel micro-dissection manipulator based on ultrasonic vibration,” in *Proceedings of the 2005 IEEE International Conference on Robotics and Automation*, 2005, pp. 466–471. DOI: 10.1109/ROBOT.2005.1570162.
- [127] A. Elfizy, G. Bone, and M. Elbestawi, “Design and control of a dual-stage feed drive,” *International Journal of Machine Tools and Manufacture*, vol. 45, no. 2, pp. 153–165, 2005, ISSN: 0890-6955. DOI: <https://doi.org/10.1016/j.ijmachtools.2004.07.008>. [Online]. Available: <https://www.sciencedirect.com/science/article/pii/S0890695504001749>.
- [128] Y. Zhao, J. Cui, X. Bian, L. Zou, S. Liang, and L. Wang, “Study on performance of an air spring isolator for large-scale precision optical micro-vibration isolation,” in *Proceedings of the 3rd International Con-*

ference on Information Technologies and Electrical Engineering, 2020, pp. 173–178.

- [129] M.-S. Tsai and Y.-S. Sun, “Robust control of pendulum-type micro-vibration isolation system,” *Journal of Vibroengineering*, vol. 17, no. 5, pp. 2410–2421, 2015.
- [130] X. Feng, X. Jing, and Y. Guo, “Vibration isolation with passive linkage mechanisms,” *Nonlinear Dynamics*, vol. 106, pp. 1891–1927, 2021.
- [131] Z. Wu, X. Jing, B. Sun, and F. Li, “A 6dof passive vibration isolator using x-shape supporting structures,” *Journal of Sound and Vibration*, vol. 380, pp. 90–111, 2016, ISSN: 0022-460X. DOI: <https://doi.org/10.1016/j.jsv.2016.06.004>. [Online]. Available: <https://www.sciencedirect.com/science/article/pii/S0022460X16302255>.
- [132] Y.-l. Yang, Y.-d. Wei, J.-q. Lou, L. Fu, and X.-w. Zhao, “Nonlinear dynamic analysis and optimal trajectory planning of a high-speed macro-micro manipulator,” *Journal of Sound and Vibration*, vol. 405, pp. 112–132, 2017, ISSN: 0022-460X. DOI: <https://doi.org/10.1016/j.jsv.2017.05.047>. [Online]. Available: <https://www.sciencedirect.com/science/article/pii/S0022460X17304510>.
- [133] O. Sörnmo, B. Olofsson, U. Schneider, A. Robertsson, and R. Johansson, “Increasing the milling accuracy for industrial robots using a piezo-actuated high-dynamic micro manipulator,” in *2012 IEEE/ASME International Conference on Advanced Intelligent Mechatronics (AIM)*, 2012, pp. 104–110. DOI: 10.1109/AIM.2012.6265942.
- [134] S. Wang, Y.-l. Yang, G.-p. Li, H.-l. Du, and Y.-d. Wei, “Microscopic vibration suppression for a high-speed macro-micro manipulator with parameter perturbation,” *Mechanical Systems and Signal Processing*, vol. 179, p. 109332, 2022, ISSN: 0888-3270. DOI: <https://doi.org/10.1016/j.ymsp.2022.109332>. [Online]. Available: <https://www.sciencedirect.com/science/article/pii/S088832702200468X>.
- [135] Y. Li, F. Marcassa, R. Horowitz, R. Oboe, and R. Evans, “Track-Following Control With Active Vibration Damping of a PZT-Actuated Suspension Dual-Stage Servo System,” *Journal of Dynamic Systems, Measurement, and Control*, vol. 128, no. 3, pp. 568–576, Nov. 2005, ISSN: 0022-0434. DOI: 10.1115/1.2229257. eprint: [https://asmedigitalcollection.asme.org/dynamicsystems/article-pdf/128/3/568/5694551/568\\_1.pdf](https://asmedigitalcollection.asme.org/dynamicsystems/article-pdf/128/3/568/5694551/568_1.pdf). [Online]. Available: <https://doi.org/10.1115/1.2229257>.
- [136] Y.-t. Liu, R.-f. Fung, and C.-c. Wang, “Application of the nonlinear, double-dynamic taguchi method to the precision positioning device using combined piezovcm actuator,” *IEEE Transactions on Ultrasonics, Ferroelectrics, and Frequency Control*, vol. 54, no. 2, pp. 240–250, 2007. DOI: 10.1109/TUFFC.2007.239.
- [137] X. Shan, Y. Li, H. Liu, and T. Huang, “Residual vibration reduction of high-speed pick-and-place parallel robot using input shaping,” *Chinese Journal of Mechanical Engineering*, vol. 35, no. 1, pp. 1–8, 2022.
- [138] X. Sun, B. Yang, Y. Gao, and Y. Yang, “Integrated design, fabrication, and experimental study of a parallel micro-nano positioning-vibration isolation stage,” *Robotics and Computer-Integrated Manufacturing*, vol. 66, p. 101988, 2020, ISSN: 0736-5845. DOI: <https://doi.org/10.1016/j.rcim.2020.101988>. [Online]. Available: <https://www.sciencedirect.com/science/article/pii/S073658452030199X>.
- [139] *Phased array*, Wikipedia.org. [Online]. Available: [https://en.wikipedia.org/wiki/Phased\\_array](https://en.wikipedia.org/wiki/Phased_array).
- [140] Z. He, F. Gou, R. Chen, K. Yin, T. Zhan, and S.-T. Wu, “Liquid crystal beam steering devices: Principles, recent advances, and future developments,” *Crystals*, vol. 9, no. 6, p. 292, 2019.
- [141] G. Römer and P. Bechtold, “Electro-optic and acousto-optic laser beam scanners,” *Physics Procedia*, vol. 56, pp. 29–39, 2014, 8th International Conference on Laser Assisted Net Shape Engineering LANE 2014, ISSN: 1875-3892. DOI: <https://doi.org/10.1016/j.phpro.2014.08.092>. [Online]. Available: <https://www.sciencedirect.com/science/article/pii/S1875389214002375>.
- [142] J. L. Miller, “Pointing, scanning, and stabilization mechanisms,” in *Principles of Infrared Technology: A Practical Guide to the State of the Art*, Springer, 1994, pp. 284–323.
- [143] G. Garcia-Torales, “Risley prisms applications: an overview,” in *Advances in 3OM: Opto-Mechatronics, Opto-Mechanics, and Optical Metrology*, V.-F. Duma, J. P. Rolland, and A. G. H. Podoleanu, Eds., International Society for Optics and Photonics, vol. 12170, SPIE, 2022, 121700H. DOI: 10.1117/12.2616071. [Online]. Available: <https://doi.org/10.1117/12.2616071>.
- [144] P. F. McManamon and A. Ataei, “Progress and opportunities in optical beam steering,” in *Quantum Sensing and Nano Electronics and Photonics XVI*, M. Razeghi, J. S. Lewis, E. Tournié, and G. A. Khodaparast, Eds., International Society for Optics and Photonics, vol. 10926, SPIE, 2019, p. 1092610. DOI: 10.1117/12.2511987. [Online]. Available: <https://doi.org/10.1117/12.2511987>.
- [145] S. T. S. Holmström, U. Baran, and H. Urey, “Mems laser scanners: A review,” *Journal of Microelectromechanical Systems*, vol. 23, no. 2, pp. 259–275, 2014. DOI: 10.1109/JMEMS.2013.2295470.
- [146] A. Yalcinkaya, H. Urey, D. Brown, T. Montague, and R. Sprague, “Two-axis electromagnetic microscanner for high resolution displays,” *Journal of Microelectromechanical Systems*, vol. 15, no. 4, pp. 786–794, 2006. DOI: 10.1109/JMEMS.2006.879380.

- [147] W. D. Rogatto, J. S. Accetta, and D. L. Shumaker, "The infrared & electro-optical systems handbook. electro-optical components, volume 3," 1993.
- [148] F. M. Tapos, D. J. Edinger, T. R. Hilby, M. S. Ni, B. C. Holmes, and D. M. Stubbs, "High bandwidth fast steering mirror," in *Optomechanics 2005*, A. E. Hatheway, Ed., International Society for Optics and Photonics, vol. 5877, SPIE, 2005, p. 587 707. DOI: 10.1117/12.617960. [Online]. Available: <https://doi.org/10.1117/12.617960>.
- [149] J. Lee, J. Lee, and Y. H. Won, "Beam steering and forming in compact electrowetting prism array with separate electrode control," *OSA Continuum*, vol. 4, no. 9, pp. 2400–2409, Sep. 2021. DOI: 10.1364/OSAC.430925. [Online]. Available: <https://opg.optica.org/osac/abstract.cfm?URI=osac-4-9-2400>.
- [150] *OWL Concept Design Report*, ESO, May 2004. [Online]. Available: [https://www.eso.org/sci/facilities/eelt/owl/Phase\\_A\\_Review.html](https://www.eso.org/sci/facilities/eelt/owl/Phase_A_Review.html).
- [151] F. Ahmed, K. Singh, and K. P. Esselle, "State-of-the-art passive beam-steering antenna technologies: Challenges and capabilities," *IEEE Access*, vol. 11, pp. 69 101–69 116, 2023. DOI: 10.1109/ACCESS.2023.3278570.
- [152] S. Shao, Z. Tian, S. Song, and M. Xu, "Two-degrees-of-freedom piezo-driven fast steering mirror with cross-axis decoupling capability," *Review of Scientific Instruments*, vol. 89, no. 5, p. 055 003, May 2018, ISSN: 0034-6748. DOI: 10.1063/1.5001966. eprint: [https://pubs.aip.org/aip/rsi/article-pdf/doi/10.1063/1.5001966/15634386/055003\\_1\\_online.pdf](https://pubs.aip.org/aip/rsi/article-pdf/doi/10.1063/1.5001966/15634386/055003_1_online.pdf). [Online]. Available: <https://doi.org/10.1063/1.5001966>.
- [153] S. H. Chang, C. K. Tseng, and H. C. Chien, "An ultra-precision xy/spl theta/sub z/ piezo-micropositioner. i. design and analysis," *IEEE Transactions on Ultrasonics, Ferroelectrics, and Frequency Control*, vol. 46, no. 4, pp. 897–905, 1999. DOI: 10.1109/58.775656.
- [154] H. C. Liaw and B. Shirinzadeh, "Enhanced adaptive motion tracking control of piezo-actuated flexure-based four-bar mechanisms for micro/nano manipulation," *Sensors and Actuators A: Physical*, vol. 147, no. 1, pp. 254–262, 2008, ISSN: 0924-4247. DOI: <https://doi.org/10.1016/j.sna.2008.03.020>. [Online]. Available: <https://www.sciencedirect.com/science/article/pii/S0924424708001775>.
- [155] H. C. Liaw and B. Shirinzadeh, "Robust generalised impedance control of piezo-actuated flexure-based four-bar mechanisms for micro/nano manipulation," *Sensors and Actuators A: Physical*, vol. 148, no. 2, pp. 443–453, 2008, ISSN: 0924-4247. DOI: <https://doi.org/10.1016/j.sna.2008.09.006>. [Online]. Available: <https://www.sciencedirect.com/science/article/pii/S092442470800472X>.
- [156] B. Ran, P. Yang, L. Wen, *et al.*, "Design and analysis of a reactionless large-aperture fast steering mirror with piezoelectric actuators," *Appl. Opt.*, vol. 59, no. 4, pp. 1169–1179, Feb. 2020. DOI: 10.1364/AO.379344. [Online]. Available: <https://opg.optica.org/ao/abstract.cfm?URI=ao-59-4-1169>.
- [157] J. D. Medbery and L. M. Germann, "Six degree-of-freedom magnetically suspended fine-steering mirror," in *Acquisition, Tracking, and Pointing V*, M. K. Masten and L. A. Stockum, Eds., International Society for Optics and Photonics, vol. 1482, SPIE, 1991, pp. 397–405. DOI: 10.1117/12.45713. [Online]. Available: <https://doi.org/10.1117/12.45713>.
- [158] S. Andreou and E. G. Papadopoulos, "Design of a reactionless pointing mechanism for satellite antennas," in *11th ESA Workshop on Advanced Space Technologies for Robotics and Automation (ASTRA 2011)*, 2011, pp. 12–14.
- [159] E. I. Williams, R. T. Summers, and M. A. Ostaszewski, "High-performance reactionless scan mechanism," in *NASA. Johnson Space Center, The 29th Aerospace Mechanisms Symposium*, 1995.
- [160] J. Meijaard and V. van der Wijk, "Dynamic balancing of mechanisms with flexible links," English, *Mechanism and Machine Theory*, vol. 172, 2022, ISSN: 0094-114X. DOI: 10.1016/j.mechmachtheory.2022.104784.
- [161] Y.-Q. Yu and B. Jiang, "Analytical and experimental study on the dynamic balancing of flexible mechanisms," *Mechanism and Machine Theory*, vol. 42, no. 5, pp. 626–635, 2007, ISSN: 0094-114X. DOI: <https://doi.org/10.1016/j.mechmachtheory.2004.09.002>. [Online]. Available: <https://www.sciencedirect.com/science/article/pii/S0094114X05001680>.
- [162] A. A. Moshaii and F. Najafi, "A review of robotic mechanisms for ultrasound examinations," *Industrial Robot: An International Journal*, vol. 41, no. 4, pp. 373–380, 2014.
- [163] A. Vilchis, J. Troccaz, P. Cinquin, K. Masuda, and F. Pellissier, "A new robot architecture for tele-echography," *IEEE Transactions on Robotics and Automation*, vol. 19, no. 5, pp. 922–926, 2003. DOI: 10.1109/TRA.2003.817509.
- [164] G. Singh and V. Banga, "Robots and its types for industrial applications," *Materials Today: Proceedings*, vol. 60, pp. 1779–1786, 2022.
- [165] A. Shukla and H. Karki, "Application of robotics in offshore oil and gas industry— a review part ii," *Robotics and Autonomous Systems*, vol. 75, pp. 508–524, 2016, ISSN: 0921-8890. DOI: <https://doi.org/10.1016/j.robot.2015.09.013>. [Online]. Available: <https://www.sciencedirect.com/science/article/pii/S0921889015002018>.
- [166] S. Gao and H. Huang, "Recent advances in micro-and nano-machining technologies," *Frontiers of Mechanical Engineering*, vol. 12, pp. 18–32, 2017.
- [167] M. Remedias, G. Aglietti, and G. Richardson, "A stochastic methodology for predictions of the environment created by multiple microvibration sources,"

- Journal of Sound and Vibration*, vol. 344, pp. 138–157, 2015.
- [168] M. C. Roggemann, B. M. Welsh, and R. Q. Fugate, “Improving the resolution of ground-based telescopes,” *Reviews of Modern Physics*, vol. 69, no. 2, p. 437, 1997.
- [169] C. J. Dennehy and O. S. Alvarez-Salazar, “A survey of the spacecraft line-of-sight jitter problem,” in *AAS Annual Guidance and Control Conference*, 2019.
- [170] I. Trumper, B. T. Jannuzi, and D. W. Kim, “Emerging technology for astronomical optics metrology,” *Optics and Lasers in Engineering*, vol. 104, pp. 22–31, 2018.
- [171] T. D. Ngo, A. Kashani, G. Imbalzano, K. T. Nguyen, and D. Hui, “Additive manufacturing (3d printing): A review of materials, methods, applications and challenges,” *Composites Part B: Engineering*, vol. 143, pp. 172–196, 2018, ISSN: 1359-8368. DOI: <https://doi.org/10.1016/j.compositesb.2018.02.012>. [Online]. Available: <https://www.sciencedirect.com/science/article/pii/S1359836817342944>.
- [172] A. Qattawi, B. Alrawi, A. Guzman, *et al.*, “Experimental optimization of fused deposition modelling processing parameters: A design-for-manufacturing approach,” *Procedia Manufacturing*, vol. 10, pp. 791–803, 2017.
- [173] D. Behera and M. Cullinan, “Current challenges and potential directions towards precision microscale additive manufacturing—part i: Direct ink writing/jetting processes,” *Precision Engineering*, vol. 68, pp. 326–337, 2021.
- [174] J. Cai, Y. Wu, Y. Wang, and H. Wen, “Investigation of gas separation force balancing em mechanism for micro-scroll machines,” in *2022 International Conference on Electrical Machines (ICEM)*, IEEE, 2022, pp. 893–899.
- [175] B. Shaqour, M. Abuabiah, S. Abdel-Fattah, *et al.*, “Gaining a better understanding of the extrusion process in fused filament fabrication 3d printing: A review,” *The International Journal of Advanced Manufacturing Technology*, vol. 114, pp. 1279–1291, 2021.
- [176] K. Tiwari and S. Kumar, “Analysis of the factors affecting the dimensional accuracy of 3d printed products,” *Materials Today: Proceedings*, vol. 5, no. 9, pp. 18 674–18 680, 2018.
- [177] T. Nancharaiah, D. R. Raju, V. R. Raju, *et al.*, “An experimental investigation on surface quality and dimensional accuracy of fdm components,” *International Journal on Emerging Technologies*, vol. 1, no. 2, pp. 106–111, 2010.
- [178] O. A. Mohamed, S. H. Masood, and J. L. Bhowmik, “Mathematical modeling and fdm process parameters optimization using response surface methodology based on q-optimal design,” *Applied Mathematical Modelling*, vol. 40, no. 23-24, pp. 10 052–10 073, 2016.
- [179] B. Banjanin, G. Vladić, M. Pál, V. Dimovski, S. Adamović, and G. Delić, “Production factors influencing mechanical and physical properties of fdm printed embossing dies,” in *9th international symposium on graphic engineering and design*, 2018.
- [180] M. Vocetka, Z. Bobovský, J. Babjak, *et al.*, “Influence of drift on robot repeatability and its compensation,” *Applied Sciences*, vol. 11, no. 22, p. 10 813, 2021.
- [181] J. Wang, X. Dong, O. R. Barry, and C. Okwudire, “Friction-induced instability and vibration in a precision motion stage with a friction isolator,” *Journal of Vibration and Control*, vol. 28, no. 15-16, pp. 1879–1893, 2022.
- [182] A. V. Kochetkov, T. Ivanova, L. V. Seliverstova, and O. V. Zakharov, “Kinematic error modeling of delta 3d printer,” in *Materials Science Forum*, Trans Tech Publ, vol. 1037, 2021, pp. 77–83.



# 3

## Inherently Balanced Spherical Pantograph Mechanisms

# Inherently Balanced Spherical Pantograph Mechanisms

K.T.Y. Durieux and V. van der Wijk

**Abstract** This paper investigates the possibilities for designing shaking force balanced spherical pantograph mechanisms using inherent balancing theory. Three different spherical designs are presented, which are a balanced general spherical pantograph, a balanced double spherical pantograph and double S shaped mechanism with surrounding 4R four-bar linkage. Also, three variations of the balanced designs are presented. As compared to the planar pantograph, the same underlying system of principal vectors exists, of which the geometries can be visualized in the orthogonal planes. The feasible variations of link length for which force balance is maintained are discussed.

## 1 Introduction

Mechanisms used in applications with high accelerations or large moving masses, such as manipulators, combustion engines or land-based telescopes [1, 2, 3] can suffer from vibrations due to the generated shaking force and shaking moments, which can be significant [4]. These can be fully reduced by applying dynamic balancing which requires a specific distribution of the masses of the links [1].

Contrary to the balancing of planar and spatial mechanisms, of which a significant amount of research is known, the balancing of spherical mechanisms in specific has received limited attention. Gosselin [5] applied static balancing to spherical mechanisms, using springs to reduce the overall mass and inertia as compared to shaking force balancing using mass redistribution. Moore [6] created an algebraic method for force balancing of spherical four-bar mechanisms, using complex variables and Laurent polynomial factorisation. Borugadda [7] applied a counterweight and adjustable kinematic parameters with real time control to achieve force balance and partial

---

K.T.Y. Durieux · V. van der Wijk

This chapter has been accepted as article for the International Symposium on Advances in Robot Kinematics (ARK) 2024, Ljubljana, Slovenia.

moment balancing of a spherical mechanism. Partial force and moment balancing was also achieved by Gill et al. [8] using optimisation of the mass distribution. Most solutions for dynamic balancing of spherical mechanisms are based on the placement of additional mass and inertia, resulting in more complex systems with often larger power requirements or reduced performance [1]. Inherent balancing, on the contrary, is known for resulting in balanced solutions with relatively low mass, inertia and complexity which however has not yet been explored for spherical mechanisms.

The goal of this paper is to investigate a new approach for the design of shaking force balanced spherical mechanisms using inherently balanced spherical pantograph mechanisms. First, the transformation of a force balanced planar pantograph into a force balanced spherical pantograph is shown and subsequently four force balanced spherical variations are presented.

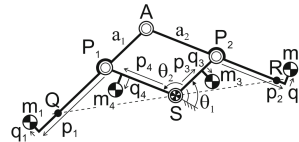
## 2 Balanced Spherical Pantograph

First the planar force balanced pantograph will be explained in chapter 2.1, which is used in chapter 2.2 as the basis for a spherical force balanced pantograph.

### 2.1 Planar pantograph

The planar pantograph shown in Fig. 1 is an inherently balanced planar geometry, which functions as the basis for a multitude of inherently balanced designs [1, 9]. The basic geometry is a parallelogram ( $SP_1AP_2$ ) with two sets of parallel and equally long links of lengths  $a_1$  and  $a_2$ , which are connected using revolute joints.

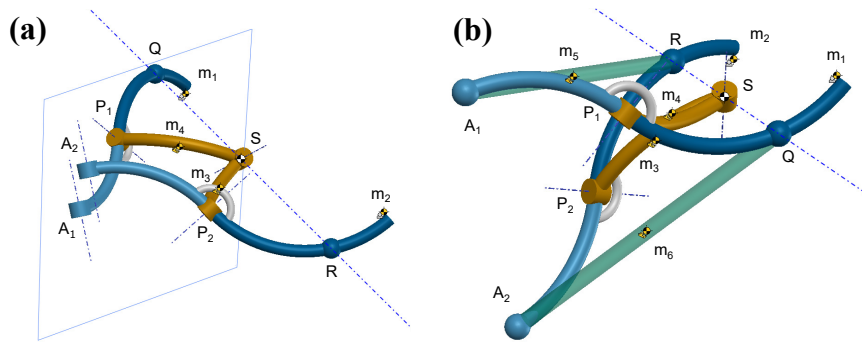
**Fig. 1** Planar shaking force balanced pantograph consisting of four moving elements with a common center of mass located in base point  $S$  for any motion of the linkage. [10]



The position of link masses  $m_i$  are described by distances  $p_i$  along a link and  $q_i$  normal to the link as illustrated. For specific conditions, the balance conditions, the common Center of Mass (CoM) is stationary in point  $S$ , invariable to the movement of the linkage. The balance conditions for a planar pantograph are based on the principal vectors [1], which was shown to also apply for spatial pantographs [10]. Additionally, a principle of mirrored motion is visible within this geometry, with similarity point  $Q$  moving similarly and oppositely to similarity point  $R$ , resulting in zero net reaction forces in point  $S$ . Other planar geometries also show this principle when balanced [9].

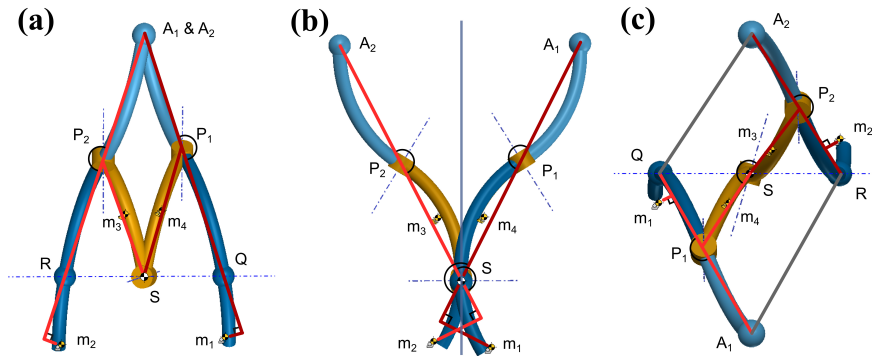
## 2.2 Spherical pantograph

Fig. 2a shows the spherical version of the balanced planar pantograph which is obtained when links are curved with equal radius in alternating directions. The curvatures cannot be in the same direction for a shaking force balanced design, since 2-fold radial symmetry is required to have the common CoM align in base pivot  $S$  for any pose of the linkages. Due to the alternating curves of the links of this mechanism, joint  $A$  can no longer exist and both links connecting in  $A$  obtain their own extremity  $A_1$  and  $A_2$  which move separately. These points move towards and away from one another by links  $SP_1$  and  $SP_2$  rotating in opposite directions, resulting in mirrored spherical trajectories.



**Fig. 2** a) Balanced spherical pantograph design with the similarity plane through point  $S$  normal to the line through  $Q$ ,  $S$  and  $R$ ; b) Additional links with spherical joints are needed to constrain the pantograph properly and have the common CoM in base pivot  $S$  for all motions.

The force balance of the spherical pantograph can be evaluated by the projections of the linkages onto the orthogonal planes. Figure 3a shows the projection onto the plane through  $Q$ ,  $R$  and  $A$ , Fig. 3b shows the projection onto the similarity plane through point  $S$  and normal to the line through  $Q$ ,  $S$  and  $R$ , as shown in Fig. 2a, and Fig. 3c shows the projection on the third orthogonal plane. The projection in Fig. 3a can be referred to as the in-plane projection, which shows a planar balanced pantograph as in Fig. 1. The projection in Fig. 3b can be referred to as the similarity projection, showing a mirrored geometry with respect to the vertical line through point  $S$  and resulting in similar but opposite movements of  $m_1$  and  $m_3$  compared to  $m_2$  and  $m_4$  which is a known force balanced geometry. The projection in Fig. 3c consists of parallelograms, which therefore forms a balanced planar pantograph, but with a different geometry as compared to Fig. 1. For each projection, the mass parameters for force balance can be calculated with the equations of the planar balanced pantograph. Due to the limited space of the paper, this has not been elaborated here.



**Fig. 3** Projections of the balanced spherical pantograph onto the three orthogonal planes: a) In-plane pantograph; b) Similarity projection; and c) Third projection.

The design in Fig. 3a is not properly constrained to move as a spherical pantograph, since points  $A_1$  and  $A_2$  can move independently. These two points have to move within the similarity plane as well as have their rotational axes remain parallel as illustrated with dashed lines in fig 2a. This can be accomplished by introducing two new equal links which connect points  $A_1$  with  $R$  and  $A_2$  with  $Q$  using ball joints, as shown in Fig. 2b. The mass of these links can be included for force balance by modelling their link mass as two equivalent masses located in the joints and combining the four equivalent masses with the mass of their respective connecting link. For balance of the spherical pantograph it is necessary for the pair of links  $SP_1$  and  $SP_2$  to have equal length, which also applies for pair of links  $P_1A_1$  and  $P_2A_2$ , while the length of each pair may be different. Additionally, links  $QA_2$  and  $RA_1$  need an equal length for balance. Proportional scaling of both pairs is also feasible if the same scaling is applied, including the constraint links  $A_1R$  and  $A_2Q$ .

### 3 Variations of the Balanced Spherical Pantograph

Variations of the inherently balanced spherical pantograph are presented here, with an alternative configuration of the spherical pantograph in Chapter 3.1. Chapter 3.2 and chapter 3.3 show spherical versions of two planar balanced pantograph variations from [9], namely a double pantograph and a double S shaped mechanism within a connecting 4R four-bar linkage. See Appendix B for more information about functioning and non-functioning additional variations.

### 3.1 Alternative configuration of Spherical Pantograph

Figure 4 shows an interesting configuration of the spherical pantograph when links  $SP_2$  and  $SP_1$  are made colinear, thereby forming a H shaped geometry. Balanced is achieved due to  $QP_1$  and  $RP_2$  being parallel, causing points  $A_1$  and  $A_2$  as well as  $m_1$  and  $m_2$  to move in opposite directions. This required constraint for points  $A$  and  $m$  can be enforced by attaching rigid links (visible as grey lines) between  $A_1$  and  $R$  as well as between  $A_2$  and  $Q$ , connected with ball joints. These links form two opposing parallelograms which balance each other. The out of plane geometry is shown in Fig. 4b. The link lengths can be varied, however the geometry must remain symmetrical about point  $S$  for force balance.

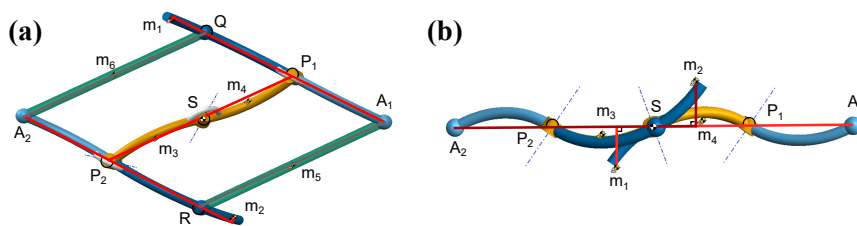


**Fig. 4** a) Variation of the balanced spherical pantograph when links  $SP_2$  and  $SP_1$  are collinear; b) Side view.

### 3.2 Balanced Double Pantograph

Figure 5a shows the design of a balanced double spherical pantograph, which can be considered as a combination of two mirrored spherical parallelograms using solely revolute joints. The parallelograms are positioned such that the curvature of the links is 2-fold radially symmetrical in point  $S$ . Link  $SP_1$  is rigidly connected to link  $SP_4$  and link  $SP_2$  to link  $SP_3$ , which makes both sides move synchronously with the joints of each side moving along the surface of a sphere. Each parallelogram can have a separate radius if each link within the parallelogram has equal radius and thereby allowing for spherical motion. Different link lengths are also feasible if similarity between parallelograms is retained, allowing for alternative shapes such as a Kite (near links equal and distant links equal) or Rhombus (all links equal). However, to achieve force balance, both parallelograms will have to be proportionate.

Also, here the projections of the mechanism onto the three orthogonal planes in Fig. 5b, 5c and 5d show planar balanced geometries from which the mass parameters can be derived as known.

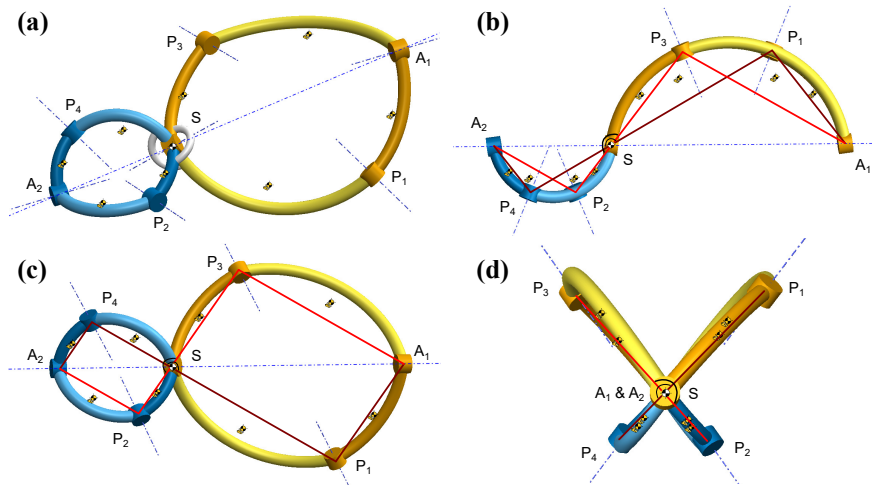
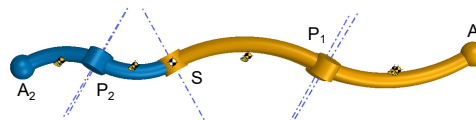


**Fig. 5** a) Balanced double spherical pantograph with one side twice as large as the other; b) Orthogonal projection; c) In-plane projection; and d) Projection onto the similarity plane.

An alternative version of this mechanism is obtained when the link curvatures are altered four times to create a wave like shape as shown in Fig. 6. This mechanism, however, requires ball joints in joints  $A_1$  and  $A_2$  to retain motion as well as link lengths near point  $S$  being equal or larger than distant links.

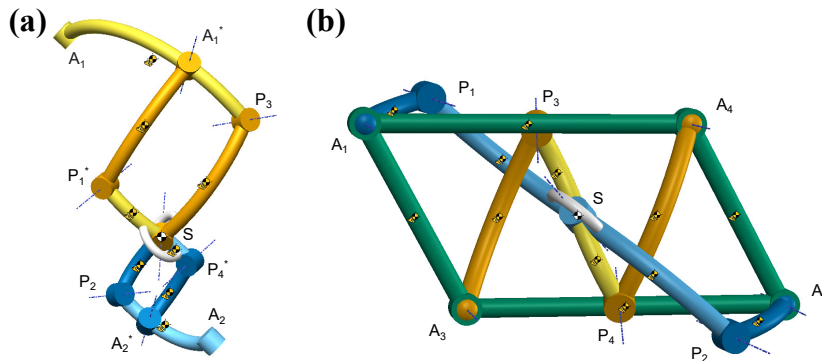
Similar to the planar pantograph, it is also possible to shift links to another location as illustrated in Fig. 7a, such that they remain parallel and thereby retain force balance. Compared to the Fig. 5a, links  $A_1P_1$  and links  $A_2P_4$  have been shifted along their connecting links to  $A_1^*P_1^*$  and  $A_2^*P_4^*$  respectively. This results in a shorter link  $P_1^*P_4^*$  through point  $S$ .

**Fig. 6** Balanced double spherical pantograph variation with four times altering curvature and ball joints in  $A_1$  and  $A_2$ .



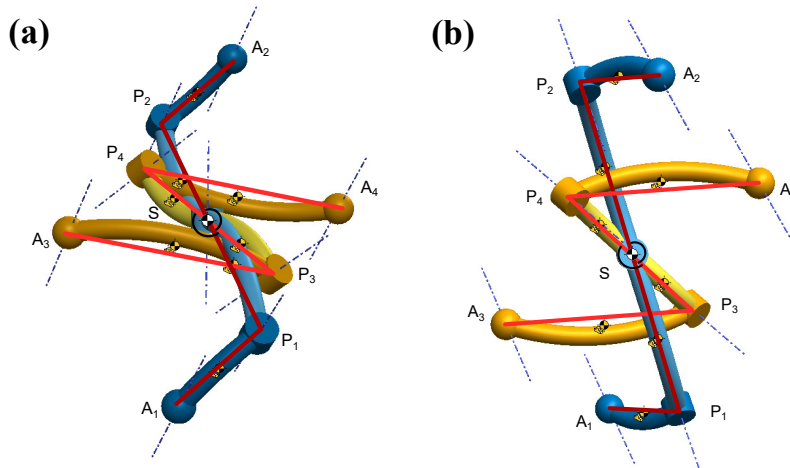
### 3.3 Double S shaped mechanism with connecting 4R four-bar linkage

Figure 7b presents a complex example of a balanced spherical mechanism, namely a double S shaped spherical mechanism with a surrounding 4R four-bar linkage. This mechanism is derived from a planar solution of the grand 4R four-bar based linkage



**Fig. 7** a) Variation of balance double spherical pantograph with shifted links; b) Double S shaped mechanism with external 4R four-bar linkage and common CoM in point  $S$

architecture, which is an advanced combination of multiple balanced pantographs[9]. Here linkage  $A_1P_1SP_2A_2$  with solely revolute joints can be seen as a S shape geometry, with linkage  $A_3P_3SP_4A_4$  forming a secondary S shaped geometry. Links  $P_1SP_2$  and  $P_3SP_4$  have midway a shared revolute joint in point  $S$ , where the common CoM is located for any pose. The surrounding planar 4R four-bar parallelogram is connected using ball joints in revolute joints  $A_i$ . Force balance is retained for link lengths of equal length, different lengths for near and distant links or symmetrical link lengths around point  $S$ . Figure 8 shows two projections of the S-geometries of the mechanism.



**Fig. 8** Balanced geometries within Double S variation: a) Out of plane Z shape (XY); b) Out of plane Z shape (XZ)

## 4 Conclusion

A spherical shaking force balanced pantograph was presented, derived from the planar balanced pantograph. Based on this spherical pantograph, five variants of for balanced designs were shown, namely an alternative configuration on the spherical pantograph, three variations of a double spherical pantograph and a double S shaped mechanism with external 4R four-bar linkage. The projections of the spherical mechanisms onto the orthogonal planes were shown to result into known planar geometries for force balance, mostly planar pantographs. This makes it possible to calculate the mass parameters for balance with the equations known for the planar case. The feasible variations of link lengths and link curvature radii for which force balance is possible have been discussed. Using the presented spherical pantograph, it is possible to design a wide variety of new inherently balanced spherical or non-spherical mechanisms, following the approach in this paper and in [1, 9].

## References

1. Van der Wijk, V.: Methodology for analysis and synthesis of inherently force and moment-balanced mechanisms - theory and applications (dissertation). University of Twente, Enschede (2014) doi: 10.3990/1.9789036536301
2. De Silva, C. W.: Vibration: fundamentals and practice. 2nd edn. CRC press, Boca Raton (2006)
3. Altarac, S., Berlioz-Arthaud, P., Thiébaud, E., Foy, R., Balega, Y.Y., Dainty, J.C., Fuensalida, J.J.: Effect of telescope vibrations upon high angular resolution imaging. *Monthly Notices of the R. Astronomical Society* **322**(1) 141-148 (2001) doi: 10.1046/j.1365-8711.2001.04111.x
4. Arakelian, V.: Inertia forces and moments balancing in robot manipulators: a review, *Advanced Robotics*, 31:14, 717-726 (2017) doi: 10.1080/01691864.2017.1348984
5. Gosselin, C.M.: Static Balancing of Spherical 3-DOF Parallel Mechanisms and Manipulators. *The International J. of Robotics Research* 18(8):819-829 (1999) doi: 10.1177/02783649922066583
6. Moore, B., Schicho, J., Schröcker, HP: Dynamic balancing of linkages by algebraic methods (dissertation). Johannes-Kepler University Linz, Linz (2009)
7. Borugadda, A.: Extending the Adjusting Kinematic Parameter approach to spatial robotic mechanisms (graduate thesis). University of Saskatchewan, Saskatoon (2019)
8. Gill, G.S., Freudenstein, F.: Minimization of Inertia-Induced Forces in Spherical Four-bar Mechanisms. Part 1: The General Spherical Four-Bar Linkage. *ASME. J. Mech., Trans., and Automation* 105(3):471-477 (1983) doi: 10.1115/1.3267384
9. Van der Wijk, V.: The Grand 4R Four-Bar Based Inherently Balanced Linkage Architecture for synthesis of shaking force balanced and gravity force balanced mechanisms. *Mech. Mach. Theory* **150**, 103815 (2020) doi: 10.1016/j.mechmachtheory.2020.103815
10. Van der Wijk, V.: The Spatial Pantograph and Its Mass Balance. *Advances in Robot Kinemat. 2022. ARK 2022. Springer Proceedings in Advanced Robotics*, vol 24. Springer, Cham. (2022) doi: 10.1007/978-3-031-08140-8\_46



# 4

## Inherently Balanced Remote Center Mechanisms

# Inherently Balanced Remote Center Mechanisms

**Abstract** This paper investigates the possibilities for designing shaking force balanced remote center mechanisms, using inherently shaking force balanced spherical pantographs. First three types of force balanced spherical pantographs are introduced, followed by the balance conditions for the double spherical pantograph. Next, ten variations of inherently shaking force balanced remote center mechanisms are presented using the force balanced spherical pantographs. Their potential benefits, drawbacks, design freedom and constraints are explained. Lastly, a realistic force balanced remote center mechanism is presented suitable for a beam-steering application, which uses three scaled shifted double spherical pantographs as legs of a parallel manipulator. A mirror is positioned such that the reflective surface aligns with the remote center of rotation, allowing for tip-tilt motion.

## 1 Introduction

Remote Center Mechanisms (RCMs) and by extension spherical mechanisms are used in applications such as tele-surgery, gimbals, grippers or contour machining [1]–[4], where high precision and/or high frequency movements are required. The precision of these movements can be negatively influenced by shaking forces and shaking moments generated due to the inertia of the moving parts [5]. Dynamic balancing aims to reduce the resulting shaking forces and moments, by specific movement and distribution of mass.

Dynamic balancing receives significant academic interest for planar or spatial mechanisms, but spherical and even more specific remote center mechanisms receives less. Noteworthy are Yaşır [6] which shows the design process of a statically balanced remote center mechanism for medical applications. Here the configuration for the parallel Remote Center Mechanism (RCM) is partly chosen on ease of (static) balance, which is achieved using counterweights.

Hayward [7] presents a seven Degree of Freedom (DoF) force balanced haptic device. This achieves force balance of its remote center serial manipulator using counterweights. Kim [8] shows gravity compensation for a three DoF RCM, which is achieved by a moving mass attached to gears and wires located on a parallelogram structure. Suh [9] splits a serial gravity compensated tool handler into a spring balanced translational part and a serial spherical/ remote center balanced part. This remote center part is statically balanced using counterweights, springs and translational adjustment. Lastly, Jamshidifar [10] presents a five DoF parallel manipulator which is used for haptic simulation of large-organ laparoscopic surgery. Here the manipulator is gravity balanced for yaw and pitch motion using counterweights, resulting in a partially force balanced manipulator.

Many dynamic balancing methods such as using counterweights, active control or Assur groups [11]–[13] result in an increase in mass and complexity. Inherent balancing, on the contrary, is known for resulting in balanced solutions with relatively low complexity, mass and inertia [14].

The goal of this paper is to design inherently shaking force balanced remote center mechanisms using inherently shaking force balanced spherical pantographs. First, three types of spherical inherently balanced pantographs are introduced, and balance conditions are deduced for the double spherical pantograph. Next, ten possible combinations of inherently balanced spherical pantographs are shown which form force balanced remote center mechanisms. Lastly, a realistic inherently shaking force balanced remote center mechanism is presented for a beam steering use case.

## 2 Shaking force balanced spherical pantographs

In the previous chapter, several shaking force balanced pantographs were derived based on inherent balancing theory [14]. Fig. 1 shows the three main types of mechanisms, from left to right: the spherical pantograph, the double spherical pantograph and the double S shaped mechanism with surrounding 4R four-bar linkage. These mechanisms show arc-based trajectories with the end effector points  $A_i$  whilst retaining shaking force balance. Variations, constraints and more details of these pantographs are described in the previous chapter.

### 2.1 Balance conditions of double spherical pantograph

Balance of these spherical pantographs can be proven using principal vectors [14] and projections. As an example, the balance conditions for the double spherical pantograph visible in Fig. 1b are presented below. First, the double spherical pantograph is projected on a plane intersecting  $A_1^*$ ,  $S$  and  $A_2^*$  as visible in Fig. 1b. This in-plane projection can be simplified to Center of Mass (CoM) locations along links normalized to their link lengths.

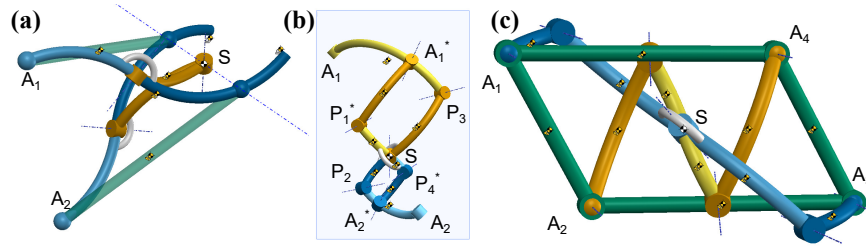


**Fig. 1** a) Spherical pantograph; b) Double spherical pantograph; c) Double S shaped mechanism with connecting 4R four-bar

Additionally, masses  $m_4$ ,  $m_3$ ,  $m_5$  and  $m_6$  of distant links  $P1^*A1^*$ ,  $P3A1^*$ ,  $P2A2^*$  and  $P4^*A2^*$  respectively can be split into eight equivalent masses ( $m_4 = m_4^{(1)} + m_4^{(2)}$ , etc.), which is visible in Fig. 2.

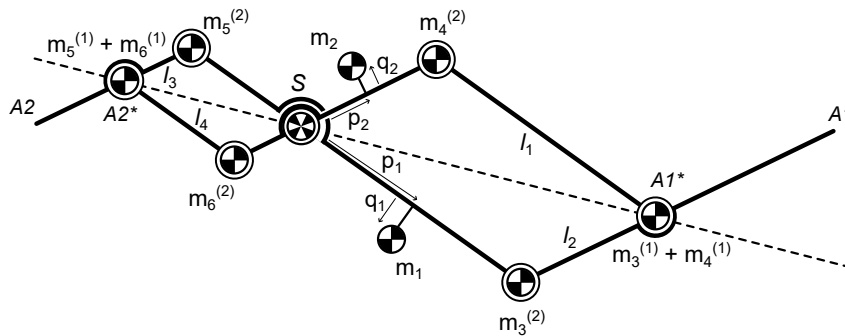


**Fig. 2** Double pantograph in-plane projection

The in-plane geometry can be split into two Equivalent Linear Momentum Systems (ELMS) [14] and a geometry for equivalent masses of the distant links, shown in Fig. 3a and Fig. 3b respectively. Solving the ELMS for constant linear momentum leads to the following balance conditions:

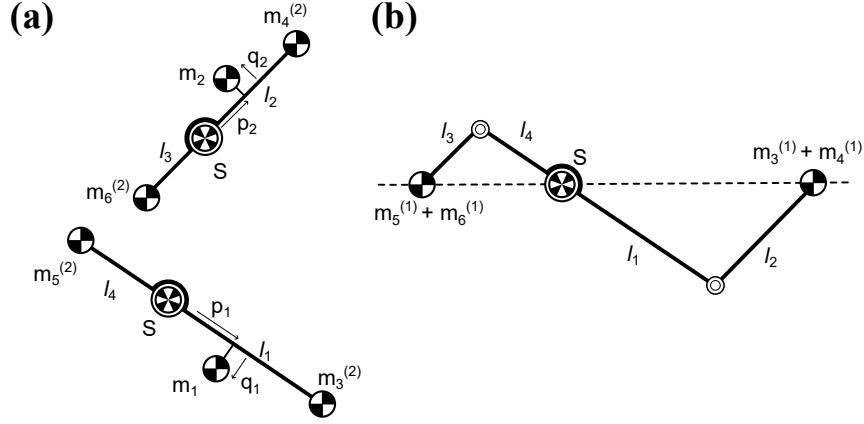


**Fig. 3** a) ELMS; b) Distant link equation

$$m_3^{(2)}l_1 = m_5^{(2)}l_4 - m_1p_1 \quad (1)$$

$$m_4^{(2)}l_2 = m_6^{(2)}l_3 - m_2p_2 \quad (2)$$

$$m_1q_1 = 0 \quad (3)$$

$$m_2q_2 = 0 \quad (4)$$

And solving the geometry for equivalent masses of the distant links for a stationary CoM provide the following two additional balance conditions:

$$(m_3^{(1)} + m_4^{(1)})l_1 = (m_5^{(1)} + m_6^{(1)})l_4 \quad (5)$$

$$(m_3^{(1)} + m_4^{(1)})l_2 = (m_5^{(1)} + m_6^{(1)})l_3 \quad (6)$$

Relevant to note is the required mapping from distances  $p_n$  and  $q_n$  in the planar projection to positions related to an arc shaped link. Figure 4a shows  $p_n$  is the normalized distance along a straight line through both joints  $P_i$  of the link, and  $q_n$  normal to this line and located on the plane describing the arc of the link.

This means  $q_n$  of different links within the spherical mechanism do not point in similar directions, therefore inner and distant link  $q_n$  cannot be used interchangeably for balancing contrary to planar mechanisms [14]. Distant link  $q_3$  and  $q_6$  as well as  $q_4$  and  $q_5$  can be balanced according to their mass ratio, visible in equations (7) and (8):

$$m_3q_3 = m_5q_5 \quad (7)$$

$$m_4q_4 = m_6q_6 \quad (8)$$

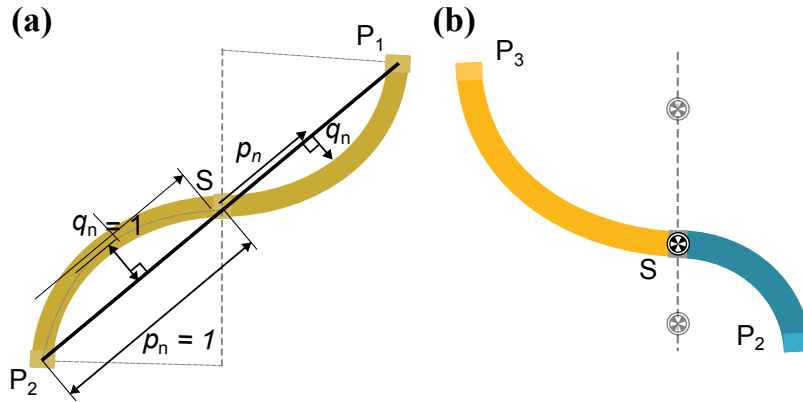


**Fig. 4** a) Normalized distances  $p_n$  and  $q_n$  based on the straight line distance between joints  $P_1$  and  $P_2$ ; b) Found balance conditions place CoM of inner links  $P_3SP_2$  and  $P_1SP_4$  in point  $S$ , but are probably able to be positioned anywhere along the axis through point  $S$

Inner links  $q_1$  and  $q_2$  can be balanced according to the equations (3) and (4). However, this is a limited balance case, due the projection ignoring the spherical nature of these links. A more complete solution, such as a fully spatial description would most likely include a relation between  $q$  and  $p$  to place the combined CoM not just in the point  $S$ , but along the rotation axis through point  $S$  as is shown in Fig. 4b. Since the inner links only rotate around this axis, a combined CoM anywhere along this axis would still result in a fully force balanced spherical mechanism.

### 3 Inherently shaking force balanced remote center mechanisms

An interesting aspect of dynamic balancing is the ability to directly combine multiple balanced components and retain force and moment balance [15]. This means multi-DoF mechanisms can be made using combination of single DoF balanced mechanisms, which allows for the design of RCMs using the balanced spherical pantographs. This section will present (in order) shaking force balanced remote center mechanisms using spherical pantographs, double spherical pantographs and double S shaped mechanisms respectively as well as design constraints and feasible variations. All concepts shown are based on equal radii and arc lengths, allowing for visual comparison in workspace and possible collisions.

### 3.1 Remote center mechanisms using spherical pantograph

The end effector of the spherical pantograph makes an arc-based trajectory with points  $A_1$  and  $A_2$  (see Fig. 1a), which can be used to create two spherical motion concepts.

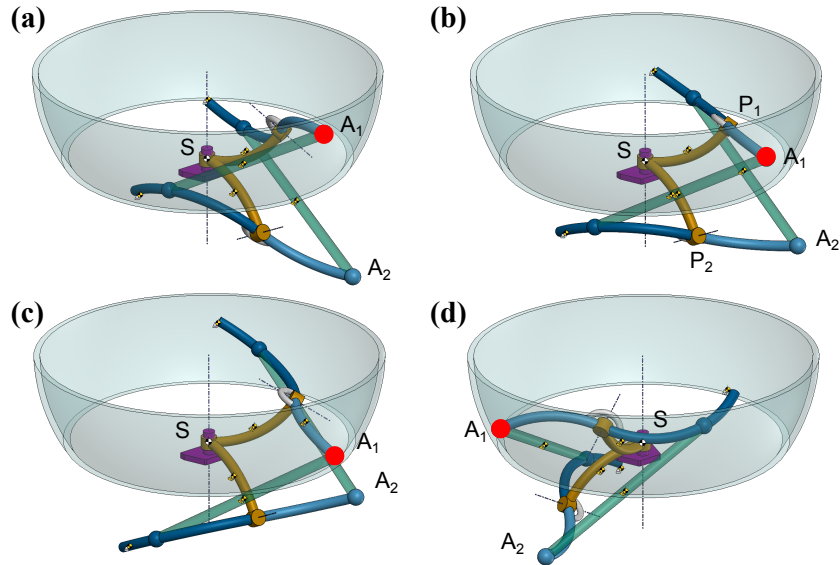


**Fig. 5** RCM by placing a spherical pantograph on a swivel with a band shaped workspace: a,b,c) show movement of  $A_1$  when  $SP_1$  and  $SP_2$  are moved in opposite directions; and d) shows rotation around axis through point  $S$

Fig. 5 shows the first concept which constrains the balanced spherical pantograph in point  $S$  such that revolute joint aligns with the axis of the base. This allows for full rotation of the pantograph (as visible in Fig. 5d), which combined with the spherical motion of the internal DoF (shown in Fig. 5a,b&c) creates a curved band workspace around a remote center. A drawback of this design is the requirement to drive both DoF around the same rotation axis through point  $S$ , which means drive location is more difficult. Another negative of this concept are the ball joints in points  $A_i$ , which means no joint or link is present that always directly points at the Center of Rotation (CoR). Furthermore, the trajectory of points  $A_i$  due to the internal DoF are not straight lines across the curvature of the band, making control more challenging.

Fig. 6 shows the second concept which connects multiple spherical pantograph end effectors ( $A_1$  and  $A_3$ ) in a single ball joint ( $A_{13}$ ). Depending on the number of legs, various shapes and sizes of workspace are feasible. The movement when individual legs are actuated is shown in Fig. 6a,b&c as well as Fig. 6d,e&f.

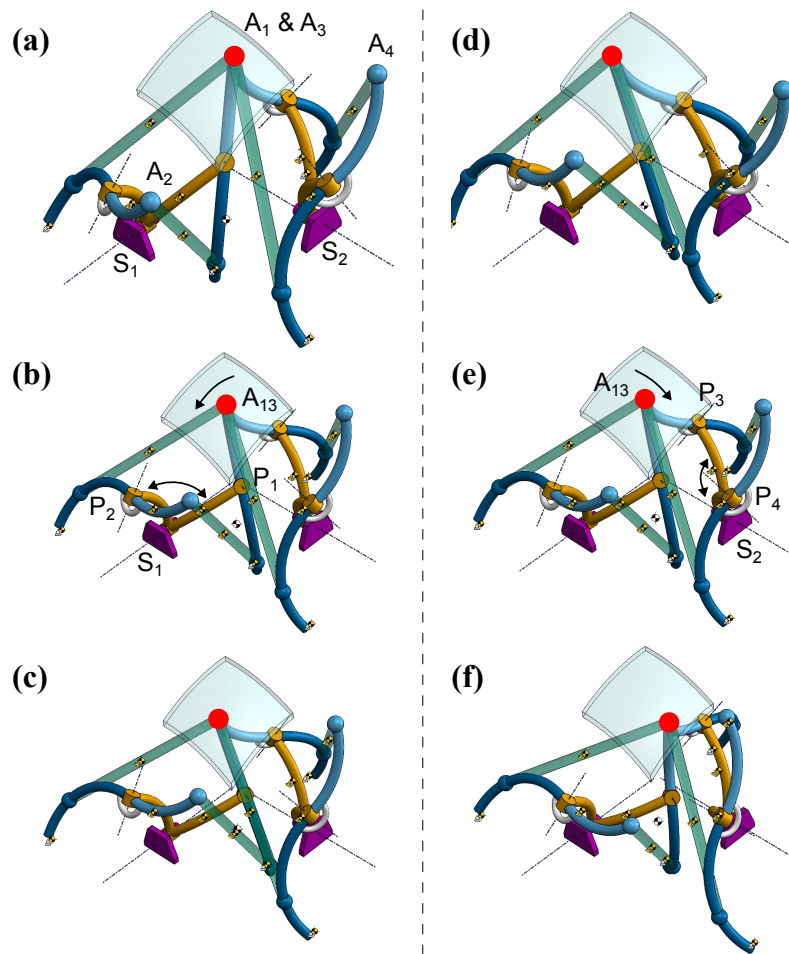


**Fig. 6** RCM consisting of two spherical pantograph legs, where movement of legs is shown in square workspace: a,b,c) Movement of  $A_{13}$  when  $S_1P_1$  and  $S_1P_2$  are moved oppositely; and d,e,f) Movement of  $A_{13}$  when  $S_2P_3$  and  $S_2P_4$  are moved oppositely.

Benefits of this concept are a larger stiffness from the use of multiple legs as well as easier actuation for the full workspace, due to the ability to use both internal DoFs for remote center motion. Driving two internal DoFs means the location of drives can be separated and placed in individual bases  $S_1$  and  $S_2$ . Drawbacks are the reduced workspace compared to the first concept together with the practical difficulties such as potential internal collisions due to the multitude of links as well as the required multi link ball joint.

Also, creating a parallel mechanism means the inclusion of singularities where DoFs are gained or lost for certain configurations of the mechanisms and should therefore be avoided and taken into account during control.

The variation of the spherical pantograph can also be used to create RCMs, using the same swivel or combined leg setup, as visible in Fig. 7. Benefits compared to the first two concepts are a larger but similar shaped workspace. However, similar negatives are still present such as potential collisions, four-way ball joints, actuation and/or singularities.

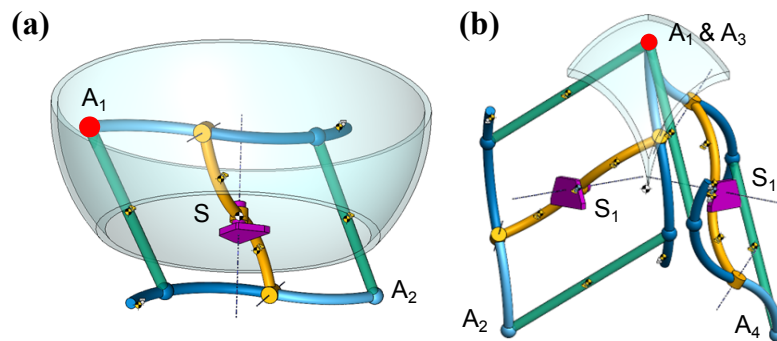
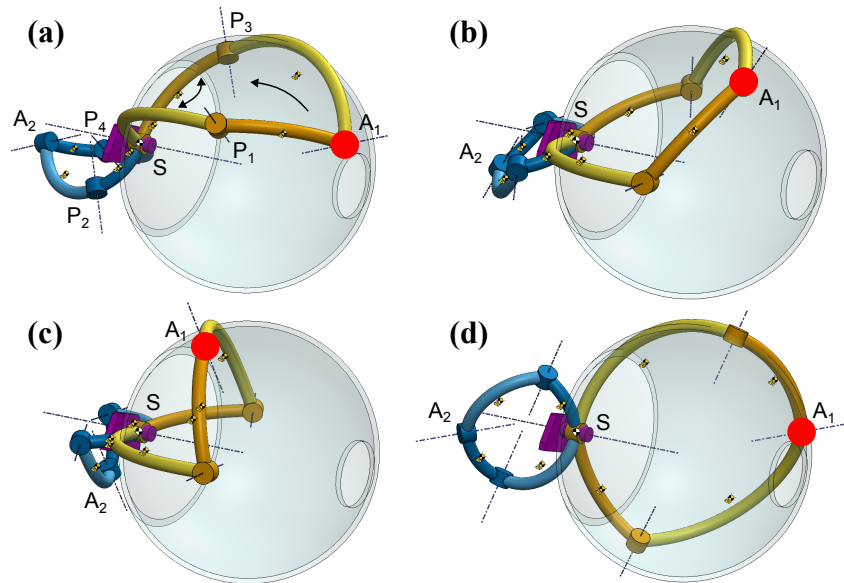


**Fig. 7** RCM using a variation of the spherical pantograph: a) RCM consisting of a spherical pantograph variation on a swivel with band shaped workspace; b) RCM consisting of two spherical pantograph variations, with square workspace

### 3.2 Remote center mechanisms using double spherical pantograph

The double spherical pantograph has the points  $A_1$  and  $A_2$  making arc-based movement, allowing for the following concepts.

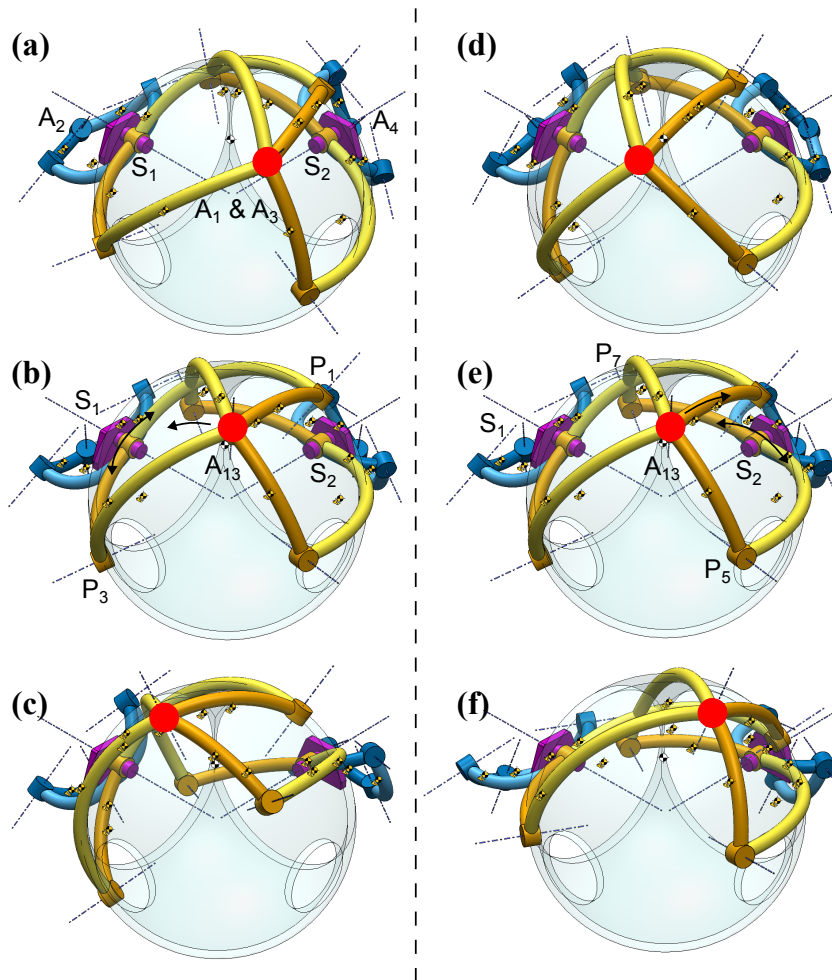
Fig. 8 shows a double spherical pantograph constrained using a fixed swivel, which is aligned with the rotation axis of the mechanism in point  $S$ . This allows for an almost completely spherical workspace, with areas near and far from the base unreachable. The size of the achievable workspace is fully determined by internal collisions of links, thus a different ratio between  $AP_1$  and  $AP_2$  can allow for more compact folding and therefore a larger workspace. Depending on the ratio of link lengths between  $SP_1A_1P_2$  and  $SP_3A_2P_4$  the mechanism can also be a compact balanced solution, since a large movement of  $A_1$  is feasible with a small but heavy  $A_2$  side. Another benefit is the intersection of the revolute joints in points  $A_i$  with the CoR making pointing easier as well as both points  $A_1$  and  $A_2$  showing opposite mirrored trajectory. A negative is the requirement to both drive the internal DoF and external rotation around point  $S$  in the same point, which is more difficult.



**Fig. 8** RCM by placing a double spherical pantograph on a swivel: a,b,c) Arc shaped trajectory of  $A_1$  is shown when  $SP_1$  and  $SP_2$  move oppositely; d) Rotation around axis through point  $S$  allows for spherical workspace of point  $A_1$

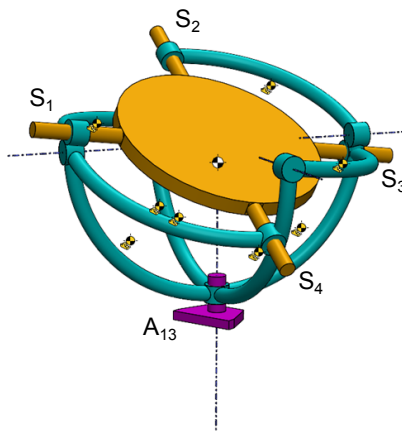
The second concept visible in Fig. 9 is a combination of double spherical pantographs, connecting points  $A_1$  and  $A_3$  in a single revolute joint  $A_{13}$ . This concept is stiffer and easier to actuate than the first concept, since only internal DoFs have to be actuated. Collision of links becomes a larger potential problem, but contrary to the shared ball joint of the spherical pantograph combination concept is the simple shared revolute joint. Workspace is however smaller compared to the swivel concept and singularities are present.

Fig. 10 shows an interesting concept where a simplified but specific version of the second concept is fixed in point  $A_{13}$  and uses a platform between points  $S_i$ . This platform acts as a tip-tilt end effector, with its CoM central and above the rotation axis through point  $A_{13}$  to achieve full force balance. Actuation of the internal DoFs is enough to achieve full rotational range of motion. However, the weight of the actuators would need to be included within the balance if they are not all placed in the single shared revolute joint point  $A_{13}$ . Additionally, the arc length of each link must be  $\frac{1}{2}\pi$  \* radii for the mechanism to function.



**Fig. 9** RCM consisting of two double spherical pantographs: a,b,c) Movement of end effector  $A_{13}$  is shown when  $S_1P_1$  and  $S_1P_3$  move oppositely; and d,e,f) Movement of end effector  $A_{13}$  is shown when  $S_2P_5$  and  $S_2P_7$  move oppositely

Equally to the spherical pantograph based RCM, the double pantograph variation as mentioned in chapter 2 can also be applied with a swivel or combination of multiple legs as shown in Fig. 11a and 11b respectively. The addition of the ball joint in points  $A_1$  and  $A_3$  makes for a more difficult connection when multiple legs are combined. Also, pointing of the end effector towards to the CoR is difficult based on the links. The feasible workspaces are however larger than spherical pantograph variations.



**Fig. 10** RCM consisting of two double spherical pantographs in an inverted position, allowing for tip-tilt movement around CoR.

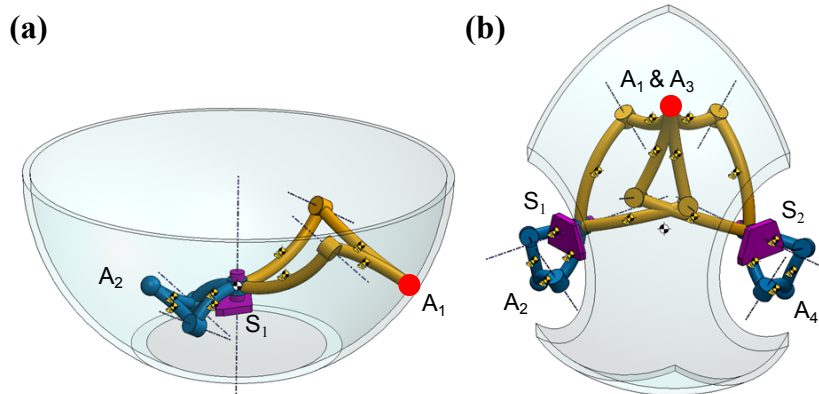


**Fig. 11** RCM using a variation of the double spherical pantograph: a) RCM consisting of a double spherical pantograph variation on a swivel; b) RCM consisting of two double spherical pantograph variations

### 3.3 Remote center mechanisms using double S mechanism

The last concept is the double S shaped mechanism with surrounding 4R four-bar linkage on a swivel, visible in Fig. 12. This mechanism shows a similar but smaller workspace to the spherical pantograph, but a large disadvantage is the multitude of links which increases the chance of internal collisions. Additionally, the ball joint and revolute joint both present in points  $A_i$  is also disadvantage.

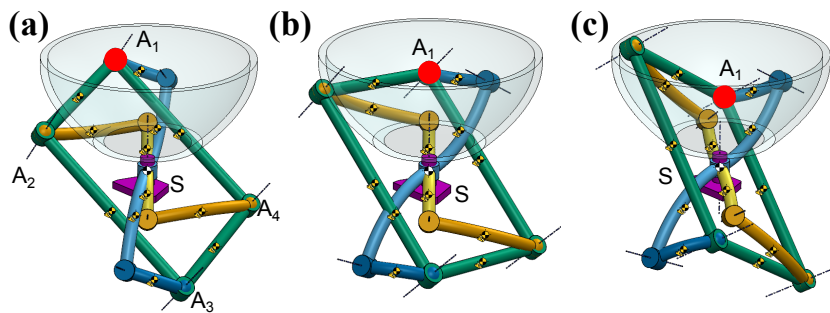


**Fig. 12** RCM by placing a double S shaped mechanism with 4R four-bar constraining linkage on a swivel, where end effector  $A_1$  forms a cone shaped workspace

### 3.4 Design constraints

Achieving remote center motion is feasible with the presented types of spherical pantographs either by specific constraints or combining multiple pantographs. Here the combined pantographs are required to have a matching end effector as well as a similar CoR, which either requires similar link lengths and radii or has to be attached to the axis of the end effector in case of a revolute joint. Also relevant is the requirement for revolute joints to be intersecting [16], except when also ball joints are used. If the revolute joints do not intersect, then the combined motion of the links either does not form a spherical motion trajectory or does not allow for any motion at all.

### 3.5 Variations

Feasible adjustments to the spherical pantographs according to chapter 2 also apply in these remote center mechanism combinations, if the above-mentioned design constraints are preserved/ maintained.

Adding more links or parts to the RCM, as is done with the concept shown in Fig. 10, does require additional balancing to retain a fully balanced mechanism. The addition of an interlink in between end effectors is feasible, as shown between end effectors  $A_1$  and  $A_3$  in Fig. 13, which could allow for an additional controllable DoF. This interlink could be modelled as equivalent masses at the connecting end effectors  $A_i$  and then be taken into account when balancing the legs.

Combining multiple double S shaped mechanisms and attaching their end effectors in a single ball joint would most likely lead to many internal collisions and is therefore not considered. Combinations of multiple types of spherical pantographs are also feasible, if the CoR of the end effectors match in location as well as end effectors aligning in a single point or along similar axis.

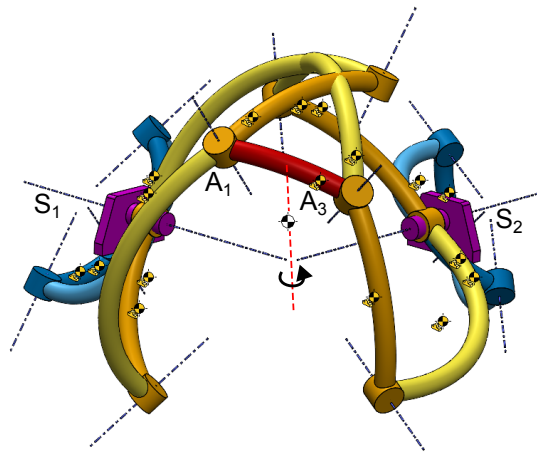


**Fig. 13** RCM with interlink  $A_1A_3$ , which has translation along the sphere as well as rotation around an axis through the CoR

#### 4 Possible use-case

Remote center mechanisms are used in several applications, such as surgery robots [17] or haptic control for tele-surgery [1]. These applications however have small mass and small accelerations, making dynamic balancing less beneficial. An interesting possibility for RCMs is to attach a part to the end effector which intersects with CoR, to create a tip/tilt motion in this point. This could make RCMs useful for applications with larger accelerations such as antenna pointing [18] or tip-tilt stages [19]. Pure rotational motion could however also be achieved by serial or parallel manipulators, of which an overview of interesting high speed parallel spherical manipulators is provided in Appendix C.

Beam steering is another application where high frequency tip-tilt motion of a mirroring surface allows for fast positioning of light or sound at desired places [20]. Here literature states a gap in performance of desired range of motion and frequency, which is limited due to vibrations. Using a force balanced mechanism with tip-tilt motion could potentially reduce this negative effect from vibrations. More information about other beam steering methods can be found in Appendix D.

#### 4.1 Remote center based beam steering mechanism

Figure 14 shows an inherently balanced remote center mechanism, which has a mirrored surface positioned in the CoR allowing for tip-tilt movement of the mirror. The legs are connected to the base using round pins and are connected together in the end effector by a pin to which the mirror is also connected. The pin is connected to one of the legs to ensure the orientation of the symmetrical mirror design remains constant, while still allowing the other legs to rotate around the pin. This pin is also constrained in translation, to ensure the center of the mirror surface remains at the CoR.

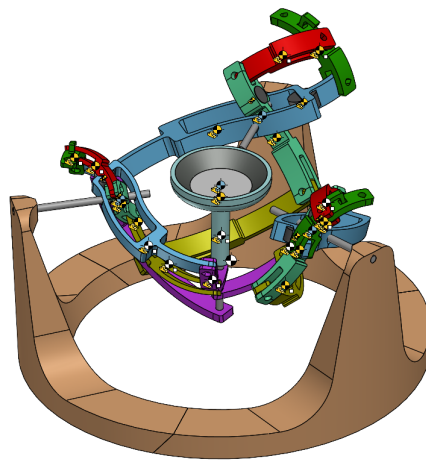


**Fig. 14** A realistic example of a beam steering tip-tilt mechanism, where mirror (center part) rotates around the remote CoR due to the three double spherical shifted pantographs as legs

The design uses three legs forming a parallel manipulator which increases the stiffness, rigidity, load carrying capacity as well as the ability to place an additional drive to improve performance and additional actuated stability [21]. The increased stiffness also means a higher eigenfrequency which allows for higher frequency actuation [22]. The legs are balanced according to the balance conditions mentioned in section 2.1 but are scaled individually (80%, 100% and 120% of a balanced double spherical pantograph mechanisms) to have different radii. This ensures the movement of a leg is along a unique sphere thereby preventing collisions between legs. The legs are positioned at 120° degrees apart, which ensures the stiffness is homogeneously distributed as well as providing optimal space per leg to reduce the possibility of collisions. An additional benefit of a parallel manipulator is the location of the drives, which in this case can easily be positioned near the bases. A drawback is the inclusion of singularities which makes control more difficult, although the design of the legs currently physically limits the movement from reaching a singularity.



**Fig. 15** Demonstration model from side and top view

Current specifications are a range of motion of  $\sim 21^\circ$  degrees to a single side, thus  $42^\circ$  degrees in total. Redesigning the connections to be single sided between linkages can reduce the possibility of collisions, which can increase the range of motion. This comes at the loss of producibility and joint stiffness. The current materials used are PLA (FDM printable), Titanium (Ti) as well as Lead weights. The reason for choosing PLA and Ti is a ratio of 3.6 in density (PLA is  $1250 \text{ kg/m}^3$  [23] and Ti is  $4500 \text{ kg/m}^3$  [24]), which is required due to the scaling present in the legs. Different material combinations with the same ratio are feasible (for example PTFE & Brass, FEP & Stainless steel, Zinc & PPS [24], [25]). The overall dimensions of the RCM are a disc shaped space with a diameter of 340 mm and a height of 150 mm. Mass of the total mechanism (excluding spacers, nuts and bolts) is roughly 900 grams. The demonstration model is shown in Fig. 15 and a full overview of the moving parts used is visible in table 1, excluding spacers and bolts/nuts/pins.

Possible variations are different lengths ratio of linkages, inclusion of more legs for more stiffness and performance potential or the interesting inclusion of an additional drive positioned at the end effector which can rotate the mirror along an axis through the CoR. This addition would introduce a twist DoF which can be use together with a tilted mirror for more adjustment of the incoming beam. On the other hand, the addition of a drive at the end effector means more moving mass which will have to be balanced either by the legs or the mirror as well as reduced performance due to the increased inertia.

Part:	Radius1(mm)	Arc length(deg)	Arc length2(mm)	Radius2 (mm) (opposite direction)	Arc length2(deg)	Arc length2(mm)	Cross-section(mm)	Material	Mass(g)	CoM (x,y,z) (mm)	
Pant1_Link1	70	70	85.52113335	35	70	42.76056667	10x10	PLA	12.06	6.47,0,-17.35	
Pant1_Link2	70	35	42.76056667	35	35	21.38028334	10x10	PLA	5.02	2.54,-0.01,-12.17	
Pant1_Link3	70	70	85.52113335	-	-	-	10x10	PLA	6.2	13.70,33.85,-0.01	
Pant1_Link4	35	70	42.76056667	-	-	-	10x10	TI	13.45	2.21,16.84,-0.01	
Pant1_Link5	70	35	42.76056667	-	-	-	10x10	PLA	5.28	13.93,32.52,-0.01	
Pant1_Link6	35	35	21.38028334	-	-	-	10x10	TI	11.06	6.77,16.36,-0.01	
Pant1_Lead1	-	-	-	-	-	-	r6.75x7	Lead	11.02	-	0.5,5.0
Pant1_Lead2	-	-	-	-	-	-	r4.5x10.2	Lead	7.14	-	0.5,10.0
<i>(Scaled 80% of Pant1)</i>											
Pant2_Link1	56	70	68.41690668	28	70	34.20845334	8.32x8	PLA	6.42	4.97,-0.01,-13.59	
Pant2_Link2	56	35	34.20845334	28	35	17.10422667	8.32x8	PLA	2.54	2.14,-0.02,10.14	
Pant2_Link3	56	70	68.41690668	-	-	-	8.32x8	PLA	3.25	10.91,27.19,-0.01	
Pant2_Link4	28	70	34.20845334	-	-	-	8.32x8	TI	6.98	5.74,13.87,-0.02	
Pant2_Link5	56	35	34.20845334	-	-	-	8.32x8	PLA	2.75	11.08,26.07,-0.02	
Pant2_Link6	28	35	17.10422667	-	-	-	8.32x8	TI	5.69	5.36,13.11,-0.03	
Pant2_Lead1	-	-	-	-	-	-	r5.4x5.68	Lead	5.72	-	0.2,8.0
Pant2_Lead2	-	-	-	-	-	-	r3.6x8.4	Lead	3.76	-	0.4,2.0
<i>(Scaled 120% of Pant1)</i>											
Pant3_Link1	84	70	102.62536	42	70	51.31268001	12x12	PLA	21.16	7.63,0,-20.38	
Pant3_Link2	84	35	51.31268001	42	35	25.65634	12x12	PLA	8.69	3.16,-0.01,-14.81	
Pant3_Link3	84	70	102.62536	-	-	-	12x12	PLA	10.81	16.49,40.52,0.01	
Pant3_Link4	42	70	51.31268001	-	-	-	12x12	TI	23.63	8.69,20.13,-0.01	
Pant3_Link5	84	35	51.31268001	-	-	-	12x12	PLA	9.26	16.76,38.97,-0.01	
Pant3_Link6	42	35	25.65634	-	-	-	12x12	TI	10.79	8.17,19.86,-0.01	
Pant3_Lead1	-	-	-	-	-	-	r8.1x8.58	Lead	19.45	-	0.4,29.0
Pant3_Lead2	-	-	-	-	-	-	r5.4x12.6	Lead	12.7	-	0.6,30.0
<b>Radius(mm) Height(mm)</b>											
Mirror_base	27.5	8	-	-	-	-	-	PLA	12.38	-	0.7,34.0
Mirror_Lead	25	8.1	-	-	-	-	-	Lead	50.56	-	0.5,32.0

**Table 1** Dimensions of all moving parts, excluding bolts/nuts, spacers

A noteworthy discussion is the number of constraints, which has positive and negative attributes. Over constraining a mechanism can increase load carrying capacity, increase stiffness, simplify design and lower stress concentrations [16], [26]. Drawbacks however are sensitivity to assembly and fabrication errors thereby reducing precision as well potential asymmetric thermal expansion. The current double spherical pantograph uses revolute joints throughout and is therefore over constrained. A spherical mechanism where all joints move along a sphere (which is a constraint itself) does not require additional constraints in translations. To ensure the movement is along a sphere in practice a single revolute joint is required, while the other joints can be cylindrical of type. This would result in a perfectly constrained spherical mechanism. The combination of three legs with three cylindrical joints at the base and one revolute joint at the end effector is three times under constrained. However, the design is such that the angle between the legs is  $120^\circ$  degree, which causes the translation of the cylindrical joints to be cancelled by each other when the legs have equal length. This causes the cylindrical joints to function as revolute joints, making the combination of legs perfectly constrained. However, when the legs are not equal length, then translation can occur of a single leg when the other legs change length. Therefore this design uses three revolute joints at the base. Redesigning the double spherical pantograph to use six cylindrical joints could improve the precision of the model.

## 5 Conclusion

This chapter/paper shortly introduces the three main types of spherical inherently shaking force balanced pantographs and present the balance conditions for the double spherical pantograph, based on principal vectors and projections. The use of projections provides a full shaking force balance, but limited design freedom due to the information loss from using projections. Based on these spherical pantographs, ten possible shaking force balanced remote center mechanisms were shown, each with their benefits and drawbacks described. Required design constraints and possible variations of these RCMs are discussed. To demonstrate the usability of the found RCMs, a remote center mechanism was designed using three shifted double spherical pantographs of various radii forming a parallel manipulator. This can be used for beam steering applications, where high frequency, large range of motion and low vibrations are relevant. The design choices and possible improvements have been mentioned.

## References

- [1] M. A. Laribi, T. Riviere, M. Arsicault, and S. Zegloul, "A new teleoperated robotic system for minimally invasive surgery: Modeling and identification," in *2013 International Conference on Control, Decision and Information Technologies (CoDIT)*, IEEE, May 2013. doi: 10.1109/codit.2013.6689621.
- [2] G. Chen, Y. Lou, and Y. Shen, "A hybrid and compact spherical mechanism of large workspace and output torque with unlimited torsion for hand-held gimbal," in *2017 IEEE International Conference on Robotics and Biomimetics (ROBIO)*, IEEE, Dec. 2017. doi: 10.1109/robio.2017.8324699.
- [3] P. V. Chanekar, M. A. A. Fenelon, and A. Ghosal, "Synthesis of adjustable spherical four-link mechanisms for approximate multi-path generation," *Mechanism and Machine Theory*, vol. 70, pp. 538–552, Dec. 2013, ISSN: 0094-114X. doi: 10.1016/j.mechmachtheory.2013.08.009.
- [4] G. Gogu, *Structural Synthesis of Parallel Robots: Part 4: Other Topologies with Two and Three Degrees of Freedom*. Springer Netherlands, 2012, ISBN: 9789400726758. doi: 10.1007/978-94-007-2675-8.
- [5] V. Arakelian, "Inertia forces and moments balancing in robot manipulators: A review," *Advanced Robotics*, vol. 31, no. 14, pp. 717–726, Jul. 2017, ISSN: 1568-5535. doi: 10.1080/01691864.2017.1348984.
- [6] A. Yaşır, "Design of a 2r1t mechanism with remote center of motion for minimally invasive transnasal surgery applications," Ph.D. dissertation, Izmir Institute of Technology (Turkey), 2018.
- [7] V. Hayward, P. Gregorio, O. Astley, *et al.*, "Freedom-7: A high fidelity seven axis haptic device with application to surgical training," in *Lecture Notes in Control and Information Sciences*. Springer Berlin Heidelberg, 1998, pp. 443–456, ISBN: 9783540409205. doi: 10.1007/bfb0112983.

- [8] C.-K. Kim, D. G. Chung, M. Hwang, *et al.*, “Three-degrees-of-freedom passive gravity compensation mechanism applicable to robotic arm with remote center of motion for minimally invasive surgery,” *IEEE Robotics and Automation Letters*, vol. 4, no. 4, pp. 3473–3480, Oct. 2019, issn: 2377-3774. doi: 10.1109/lra.2019.2926953.
- [9] J.-w. Suh and E.-c. Choi, “Design and verification of a gravity-compensated tool handler for supporting an automatic hair-implanting device,” *IEEE Robotics and Automation Letters*, vol. 4, no. 4, pp. 4410–4417, Oct. 2019, issn: 2377-3774. doi: 10.1109/lra.2019.2928763.
- [10] H. Jamshidifar, F. Farahmand, S. Behzadipour, and A. Mirbagheri, “Mechanical design of a 5-dof robotic interface for application in haptic simulation systems of large-organ laparoscopic surgery,” *Scientia Iranica*, vol. 0, no. 0, Apr. 2023, issn: 2345-3605. doi: 10.24200/sci.2023.58723.5866.
- [11] I. Kochev, “General theory of complete shaking moment balancing of planar linkages: A critical review,” *Mechanism and Machine Theory*, vol. 35, no. 11, pp. 1501–1514, Nov. 2000, issn: 0094-114X. doi: 10.1016/s0094-114x(00)00015-x.
- [12] V. van der Wijk and J. L. Herder, “Active dynamic balancing unit for controlled shaking force and shaking moment balancing,” in *Volume 2: 34th Annual Mechanisms and Robotics Conference, Parts A and B*, ser. IDETC-CIE2010, ASME/ED, Jan. 2010. doi: 10.1115/detc2010-28423.
- [13] S. Briot and V. Arakelian, “Complete shaking force and shaking moment balancing of in-line four-bar linkages by adding a class-two rrr or rrp assur group,” *Mechanism and Machine Theory*, vol. 57, pp. 13–26, Nov. 2012, issn: 0094-114X. doi: 10.1016/j.mechmachtheory.2012.06.004.
- [14] V. van der Wijk, “Methodology for analysis and synthesis of inherently force and moment-balanced mechanisms: Theory and applications,” Ph.D. dissertation, University Library/University of Twente, isbn: 9789036536301. doi: 10.3990/1.9789036536301.
- [15] V. van der Wijk, “Methodology for analysis and synthesis of inherently force and moment-balanced mechanisms: Theory and applications,” Ph.D. dissertation, University Library/University of Twente, isbn: 9789036536301. doi: 10.3990/1.9789036536301.
- [16] H. M. J. Soemers, *Design principles: For precision mechanisms*, en. 2011, isbn: 9789036531030.
- [17] F. Pugin, P. Bucher, and P. Morel, “History of robotic surgery : From aesop® and zeus® to da vinci®,” *Journal of Visceral Surgery*, vol. 148, no. 5, e3–e8, Oct. 2011, issn: 1878-7886. doi: 10.1016/j.jviscsurg.2011.04.007.
- [18] T. Itul and D. Pisla, “Dynamics of a 3-dof parallel mechanism used for orientation applications,” in *2008 IEEE International Conference on Automation, Quality and Testing, Robotics*, IEEE, 2008. doi: 10.1109/aqtr.2008.4588862.
- [19] G. Chen, Y. Ding, X. Zhu, P. Liu, and H. Ding, “Design and modeling of a compliant tip-tilt-piston micropositioning stage with a large rotation range,” *Proceedings of the Institution of Mechanical Engineers, Part C: Journal of*

- Mechanical Engineering Science*, vol. 233, no. 6, pp. 2001–2014, Jul. 2018, ISSN: 2041-2983. DOI: 10.1177/0954406218781401.
- [20] G. Römer and P. Bechtold, “Electro-optic and acousto-optic laser beam scanners,” *Physics Procedia*, vol. 56, pp. 29–39, 2014, ISSN: 1875-3892. DOI: 10.1016/j.phpro.2014.08.092.
- [21] R. Ricard and C. M. Gosselin, “On the development of reactionless parallel manipulators,” in *Volume 7A: 26th Biennial Mechanisms and Robotics Conference*, ser. IDETC-CIE2000, American Society of Mechanical Engineers, Sep. 2000. DOI: 10.1115/detc2000/mech-14098.
- [22] A. Lecours and C. Gosselin, “Reactionless two-degree-of-freedom planar parallel mechanism with variable payload,” *Journal of Mechanisms and Robotics*, vol. 2, no. 4, Sep. 2010, ISSN: 1942-4310. DOI: 10.1115/1.4002388.
- [23] *Polyfluor.nl*, <https://www.polyfluor.nl/assets/files/datasheet-pla-filament-uk.pdf>, [Accessed 06-05-2024].
- [24] E. Edge, *Densities of Metals and Elements Table* — *engineersedge.com*, [https://www.engineersedge.com/materials/densities\\_of\\_metals\\_and\\_elements\\_table\\_13976.htm](https://www.engineersedge.com/materials/densities_of_metals_and_elements_table_13976.htm), [Accessed 06-05-2024].
- [25] *Density of Plastics Material: Technical Properties Table* — *omnexus.specialchem.com*, <https://omnexus.specialchem.com/polymer-property/density>, [Accessed 13-05-2024].
- [26] Z. Ying, Y. Yan-An, and C. Jian-Zhong, “An independent active balancer for planar mechanisms,” *Transactions of the Canadian Society for Mechanical Engineering*, vol. 31, no. 2, pp. 167–190, Jun. 2007, ISSN: 0315-8977. DOI: 10.1139/tcsme-2007-0011.

# 5

## Discussion

Following the methods and results related to the sub-goals, several points will be discussed in this chapter.

### 5.1. Literature research

The literature research into micro-precision applications has a very broad scope which reveals many interesting precision influencing factors. This however lacks a specific focus on spherical/ remote center mechanisms. Extending the research to include remote center mechanisms more specifically could result into new insight concerning precision influencing factors as well as determining the dynamic balancing relevance for spherical mechanisms. Research for the beam-steering use-case and into dynamically balanced Remote Center Mechanisms (RCMs) filled this void and showed most RCMs are used for medical surgery related applications. Here balance is relevant to keep a tool in a fixed orientation without force, which is where shaking force balancing could provide a significant benefit. Converting these RCMs to provide only rotational DoFs means they can be applied in applications such as pointing or tip-tilt stages. Here larger accelerations occur making force balancing even more relevant.

### 5.2. Projections

Balance of the novel inherently balanced spherical pantographs is currently proven using balanced shapes within projections. If all Cartesian projections are force balanced for a spatial mechanism, then the entire spatial mechanism must be balanced. The drawback of using projections is a loss of information from 3d to 2d. This results in more simplified or specific conditions, limiting the design freedom. Describing the spherical pantographs spatially could provide a more general solution, where curvatures and radii of links would be included as design options to achieve balance. However, the algebraic spatial descriptions of these spherical pantographs are quite complex and were therefore not feasible within the allotted time frame for this thesis.

### 5.3. Reflection on state of the art

Within the graduation time frame, some new relevant publications were made. Reyes [16] shows the use of spherical mechanisms for exoskeletons, in aiding the user by reducing loads. Here loads are currently transferred to different parts of the user, which could potentially lead to new medical problems. Gravity balancing or balancing moments to reduce these loads are stated as potential future requirements, which is where dynamic balancing could provide significant benefit. Christensen [17] shows several upper body exoskeletons currently apply gravity balancing for loads, but this could potentially also be solved by force balancing with the added benefit of remaining force balanced during movement.

## 5.4. Future work

Some potential future work for this research is relevant to note. First off, determining balance conditions of the spherical pantograph based on an spatial algebraic model would allow for more general solutions compared to using projections. Also, producing and evaluating the spherical mechanisms can validate the achievable balance as well as determine other characteristics such as kinematics, singularities and stiffness. Moreover, validating the spherical designs for moment balance as well as incorporating constant inertia design [18] could potentially lead to fully dynamically balanced spherical mechanisms. Lastly, similar shapes within planar mechanisms can be balanced using inherent balance theory, and extending this to spherical mechanisms could potentially lead to additional interesting new balanced spherical mechanisms.

# 6

## Conclusion

The goal of this thesis is to present new inherently force balanced spherical mechanisms for micro precision applications, which has been achieved using multiple sub-goals.

First off, the use-case of dynamic balancing for high speed and high-precision applications with motion was researched, through a qualitative analysis. This showed potentially significant benefits for five of the six chosen high speed precise application with motion, namely (space) telescopes, space manipulation, additive manufacturing, motion stages and beam steering. Engines/drives require new balancing methods to receive further benefit.

Following a gap found in the literature research related to dynamic balancing of spherical mechanisms, three new types of inherently shaking force balanced spherical pantograph-based mechanisms were developed. These are the spherical pantograph, the double spherical pantograph and the double S shaped mechanism with surrounding 4R four-bar linkage. Also, two variations of the spherical pantograph and the double spherical pantograph are presented, resulting in a total of five novel force balanced mechanisms. These mechanisms have been designed using inherent balance theory as well as projections, and have their movements and constraints explained. The feasible design freedom per type to retain balance, such as varying radii, unequal link lengths, scaled sides and shifting links have also been presented. Also, the balance conditions for the double spherical pantograph have been determined.

Lastly, the balanced spherical pantographs are used to create ten inherently shaking force balanced remote center mechanisms, which are either based on the use of a swivel or combining multiple pantographs to form a parallel manipulator. This allows all end effectors to show spherical movement, around a fixed Center of Rotation. Each mechanism has its pros and cons described as well as design freedom and movement. Additionally, to show the potential of the remote center mechanisms, an exemplary use-case was chosen which is beam steering. For this, a realistic remote center mechanism was designed where three scaled shifted double spherical pantographs act as legs for a parallel manipulator. A mirror is attached to the end effectors and is positioned such that it performs tip-tilt movement around the shared center of rotation, while retaining force balance.

# Bibliography

- [1] R. Willis, *Principles of Mechanism: Designed for the Use of Students in the Universities, and for Engineering Students Generally*. Cambridge University Press, Nov. 2010, ISBN: 9780511782657. DOI: 10.1017/cbo9780511782657. [Online]. Available: <http://dx.doi.org/10.1017/CB09780511782657>.
- [2] G. Singh and V. Banga, “Robots and its types for industrial applications,” *Materials Today: Proceedings*, vol. 60, pp. 1779–1786, 2022, ISSN: 2214-7853. DOI: 10.1016/j.matpr.2021.12.426. [Online]. Available: <http://dx.doi.org/10.1016/j.matpr.2021.12.426>.
- [3] *21st Century Kinematics: The 2012 NSF Workshop*. Springer London, 2013, ISBN: 9781447145103. DOI: 10.1007/978-1-4471-4510-3. [Online]. Available: <http://dx.doi.org/10.1007/978-1-4471-4510-3>.
- [4] D.-O. Lee, G. Park, and J.-H. Han, “Hybrid isolation of micro vibrations induced by reaction wheels,” *Journal of Sound and Vibration*, vol. 363, pp. 1–17, Feb. 2016, ISSN: 0022-460X. DOI: 10.1016/j.jsv.2015.10.023. [Online]. Available: <http://dx.doi.org/10.1016/j.jsv.2015.10.023>.
- [5] *Conveyor Belts: What Is It? How Does It Work? Types, Parts — iqsdirectory.com*, <https://www.iqsdirectory.com/articles/conveyor-belts.html>, [Accessed 06-05-2024].
- [6] Z. Wu, X. Jing, B. Sun, and F. Li, “A 6dof passive vibration isolator using x-shape supporting structures,” *Journal of Sound and Vibration*, vol. 380, pp. 90–111, Oct. 2016, ISSN: 0022-460X. DOI: 10.1016/j.jsv.2016.06.004. [Online]. Available: <http://dx.doi.org/10.1016/j.jsv.2016.06.004>.
- [7] G. Wu, J. Li, R. Fei, X. Wang, and D. Liu, “Analysis and design of a novel micro-dissection manipulator based on ultrasonic vibration,” in *Proceedings of the 2005 IEEE International Conference on Robotics and Automation*, IEEE. DOI: 10.1109/robot.2005.1570162. [Online]. Available: <http://dx.doi.org/10.1109/ROBOT.2005.1570162>.
- [8] Y. Li and G. Bone, “Are parallel manipulators more energy efficient?” In *Proceedings 2001 IEEE International Symposium on Computational Intelligence in Robotics and Automation (Cat. No.01EX515)*, ser. CIRA-01, IEEE. DOI: 10.1109/cira.2001.1013170. [Online]. Available: <http://dx.doi.org/10.1109/CIRA.2001.1013170>.
- [9] S. B. Yi Zhang Susan Finger, *Chapter 3. More on Machines and Mechanisms — cs.cmu.edu*, <https://www.cs.cmu.edu/~rapidproto/mechanisms/chpt3.html>, [Accessed 06-05-2024].
- [10] *Me.iastate.edu*, <https://www.me.iastate.edu/jmvance/conceptual-design-spherical-mechanism-synthesis/>, [Accessed 06-05-2024].
- [11] V. van der Wijk, “Methodology for analysis and synthesis of inherently force and moment-balanced mechanisms: Theory and applications,” Ph.D. dissertation, University Library/University of Twente, ISBN: 9789036536301. DOI: 10.3990/1.9789036536301. [Online]. Available: <http://dx.doi.org/10.3990/1.9789036536301>.
- [12] B. Wei and D. Zhang, “A review of dynamic balancing for robotic mechanisms,” *Robotica*, vol. 39, no. 1, pp. 55–71, Mar. 2020, ISSN: 1469-8668. DOI: 10.1017/S0263574720000168. [Online]. Available: <http://dx.doi.org/10.1017/S0263574720000168>.
- [13] G. Lowen, F. Tepper, and R. Berkof, “Balancing of linkages—an update,” *Mechanism and Machine Theory*, vol. 18, no. 3, pp. 213–220, Jan. 1983, ISSN: 0094-114X. DOI: 10.1016/0094-114x(83)90092-7. [Online]. Available: [http://dx.doi.org/10.1016/0094-114x\(83\)90092-7](http://dx.doi.org/10.1016/0094-114x(83)90092-7).
- [14] D. Nenchev, K. Yoshida, P. Vichitkulsawat, and M. Uchiyama, “Reaction null-space control of flexible structure mounted manipulator systems,” *IEEE Transactions on Robotics and Automation*, vol. 15, no. 6, pp. 1011–1023, 1999, ISSN: 1042-296X. DOI: 10.1109/70.817666. [Online]. Available: <http://dx.doi.org/10.1109/70.817666>.
- [15] V. ARAKELIAN, *Gravity compensation in robotics—a review*, 2019.

- [16] F. A. Reyes, D. Shuo, and H. Yu, "Shoulder-support exoskeletons for overhead work: Current state, challenges and future directions," *IEEE Transactions on Medical Robotics and Bionics*, vol. 5, no. 3, pp. 516–527, Aug. 2023, ISSN: 2576-3202. DOI: 10.1109/tmrb.2023.3275761. [Online]. Available: <http://dx.doi.org/10.1109/TMRB.2023.3275761>.
- [17] S. S. Christensen, "User-centered modelling and design of assistive exoskeletons," 2023.
- [18] D. Boere, *The constant inertia mechanism and its use in a high-speed 2-DoF inherently dynamically balanced parallel manipulator* | TU Delft Repositories — repository.tudelft.nl, <https://repository.tudelft.nl/islandora/object/uuid:77e59bb6-87db-49cc-b482-456125663bcd?collection=education>, [Accessed 06-05-2024], 2022.
- [19] G. Wu and S. Bai, "Design and kinematic analysis of a 3-rrr spherical parallel manipulator reconfigured with four-bar linkages," *Robotics and Computer-Integrated Manufacturing*, vol. 56, pp. 55–65, Apr. 2019, ISSN: 0736-5845. DOI: 10.1016/j.rcim.2018.08.006. [Online]. Available: <http://dx.doi.org/10.1016/J.RCIM.2018.08.006>.
- [20] "Spherical parallel manipulator (spm) 2 dof inverse kinematics simulations." (), [Online]. Available: <https://www.youtube.com/watch?v=I1CILK-h0UM>.
- [21] I. Tursynbek, A. Niyetkaliye, and A. Shintemirov, "Computation of unique kinematic solutions of a spherical parallel manipulator with coaxial input shafts," in *2019 IEEE 15th International Conference on Automation Science and Engineering (CASE)*, IEEE, Aug. 2019. DOI: 10.1109/coase.2019.8843090. [Online]. Available: <http://dx.doi.org/10.1109/COASE.2019.8843090>.
- [22] L. Wang, S. Cui, C. Ma, and L. Zhang, "Compound impedance control of a hydraulic driven parallel 3ups/s manipulator," *Chinese Journal of Mechanical Engineering*, vol. 33, no. 1, Aug. 2020, ISSN: 2192-8258. DOI: 10.1186/s10033-020-00470-2. [Online]. Available: <http://dx.doi.org/10.1186/s10033-020-00470-2>.
- [23] X. Duan, Y. Yang, and B. Cheng, "Modeling and analysis of a 2-dof spherical parallel manipulator," *Sensors*, vol. 16, no. 9, p. 1485, Sep. 2016, ISSN: 1424-8220. DOI: 10.3390/s16091485. [Online]. Available: <http://dx.doi.org/10.3390/s16091485>.
- [24] M. Callegari, "Design and prototyping of a spherical parallel machine based on 3-cpu kinematics," in *Parallel Manipulators, New Developments*. I-Tech Education and Publishing, Apr. 2008, ISBN: 9783902613202. DOI: 10.5772/5368. [Online]. Available: <http://dx.doi.org/10.5772/5368>.
- [25] S. Zarkandi, "Kinematic analysis and optimal design of a novel 3-p<u>r</u>r spherical parallel manipulator," *Proceedings of the Institution of Mechanical Engineers, Part C: Journal of Mechanical Engineering Science*, vol. 235, no. 4, pp. 693–712, Jul. 2020, ISSN: 2041-2983. DOI: 10.1177/0954406220938806. [Online]. Available: <http://dx.doi.org/10.1177/0954406220938806>.
- [26] H. El Jjouaoui, G. Cruz-Martinez, J.-C. Avila Vilchis, A. Vilchis González, S. Abdelaziz, and P. Poignet, "Modeling of a remote center of motion spherical parallel tensegrity mechanism for percutaneous interventions," in *Springer Proceedings in Advanced Robotics*. Springer International Publishing, 2022, pp. 332–339, ISBN: 9783031081408. DOI: 10.1007/978-3-031-08140-8\_36. [Online]. Available: [http://dx.doi.org/10.1007/978-3-031-08140-8\\_36](http://dx.doi.org/10.1007/978-3-031-08140-8_36).
- [27] "The agile eye." (), [Online]. Available: <https://robot.gmc.ulaval.ca/en/research/research-thrusts/parallel-mechanisms/the-agile-eye/>.
- [28] E. Gezgin, S. Özbek, D. Güzin, O. E. Ağbaş, and E. B. Gezer, "Structural design of a positioning spherical parallel manipulator to be utilized in brain biopsy," *The International Journal of Medical Robotics and Computer Assisted Surgery*, vol. 15, no. 5, Jun. 2019, ISSN: 1478-596X. DOI: 10.1002/rcs.2011. [Online]. Available: <http://dx.doi.org/10.1002/rcs.2011>.
- [29] A. Ruiz, F. J. Campa, O. Altuzarra, S. Herrero, and M. Diez, "Mechatronic model of a compliant 3prs parallel manipulator," *Robotics*, vol. 11, no. 1, p. 4, Dec. 2021, ISSN: 2218-6581. DOI: 10.3390/robotics11010004. [Online]. Available: <http://dx.doi.org/10.3390/robotics11010004>.
- [30] J. Enferadi and V. Saffar, "A virtual power algorithm for dynamics analysis of a 3-rrcp spherical parallel robot using the screw theory," *Australian Journal of Mechanical Engineering*, vol. 18, no. 3, pp. 351–363, Oct. 2018, ISSN: 2204-2253. DOI: 10.1080/14484846.2018.1526439. [Online]. Available: <http://dx.doi.org/10.1080/14484846.2018.1526439>.

- [31] F. Ahmed, K. Singh, and K. P. Esselle, "State-of-the-art passive beam-steering antenna technologies: Challenges and capabilities," *IEEE Access*, vol. 11, pp. 69 101–69 116, 2023. DOI: 10.1109/ACCESS.2023.3278570.
- [32] G. Römer and P. Bechtold, "Electro-optic and acousto-optic laser beam scanners," *Physics Procedia*, vol. 56, pp. 29–39, 2014, ISSN: 1875-3892. DOI: 10.1016/j.phpro.2014.08.092. [Online]. Available: <http://dx.doi.org/10.1016/j.phpro.2014.08.092>.
- [33] P. Bechtold, R. Hohenstein, and M. Schmidt, "Evaluation of disparate laser beam deflection technologies by means of number and rate of resolvable spots," *Optics Letters*, vol. 38, no. 16, p. 2934, Aug. 2013, ISSN: 1539-4794. DOI: 10.1364/ol.38.002934. [Online]. Available: <http://dx.doi.org/10.1364/OL.38.002934>.
- [34] J. Lee, J. Lee, and Y. H. Won, "Beam steering and forming in compact electrowetting prism array with separate electrode control," *OSA Continuum*, vol. 4, no. 9, p. 2400, Aug. 2021, ISSN: 2578-7519. DOI: 10.1364/osac.430925. [Online]. Available: <http://dx.doi.org/10.1364/OSAC.430925>.
- [35] P. F. McManamon and A. Ataei, "Progress and opportunities in optical beam steering," in *Quantum Sensing and Nano Electronics and Photonics XVI*, M. Razeghi, J. S. Lewis, G. A. Khodaparast, and E. Tournié, Eds., SPIE, May 2019. DOI: 10.1117/12.2511987. [Online]. Available: <http://dx.doi.org/10.1117/12.2511987>.
- [36] Y. Monnai, X. Lu, and K. Sengupta, "Terahertz beam steering: From fundamentals to applications," *Journal of Infrared, Millimeter, and Terahertz Waves*, vol. 44, no. 3–4, pp. 169–211, Feb. 2023, ISSN: 1866-6906. DOI: 10.1007/s10762-022-00902-1. [Online]. Available: <http://dx.doi.org/10.1007/s10762-022-00902-1>.
- [37] L. F. DeSandre, "Agile beam-steering technologies for laser radar transceivers," in *Design, Modeling, and Control of Laser Beam Optics*, Y. Kohanzadeh, G. N. Lawrence, J. G. McCoy, and H. Weichel, Eds., SPIE, Jun. 1992. DOI: 10.1117/12.58935. [Online]. Available: <http://dx.doi.org/10.1117/12.58935>.
- [38] "Active optics." (), [Online]. Available: [https://en.wikipedia.org/wiki/Active\\_optics](https://en.wikipedia.org/wiki/Active_optics).
- [39] "What is active and adaptive optics?" (), [Online]. Available: [https://www.eso.org/sci/facilities/develop/ao/what\\_ao.html](https://www.eso.org/sci/facilities/develop/ao/what_ao.html).
- [40] "Active optics." (), [Online]. Available: [https://www.eso.org/public/teles-instr/technology/active\\_optics/](https://www.eso.org/public/teles-instr/technology/active_optics/).
- [41] A. Arecchi, T. Messadi, and R. J. Koshel, *Field Guide to Illumination* (Field Guides). Bellingham, WA, Aug. 2007.
- [42] A. Akatay, C. Ataman, and H. Urey, "High-resolution beam steering using microlens arrays," *Optics Letters*, vol. 31, no. 19, p. 2861, Sep. 2006, ISSN: 1539-4794. DOI: 10.1364/ol.31.002861. [Online]. Available: <http://dx.doi.org/10.1364/OL.31.002861>.
- [43] "Adaptive optics." (), [Online]. Available: [https://en.wikipedia.org/wiki/Adaptive\\_optics](https://en.wikipedia.org/wiki/Adaptive_optics).
- [44] B.-S. Kim, S. Gibson, and T.-C. Tsao, "Adaptive control of a tilt mirror for laser beam steering," in *Proceedings of the 2004 American Control Conference*, IEEE, 2004. DOI: 10.23919/acc.2004.1384437. [Online]. Available: <http://dx.doi.org/10.23919/ACC.2004.1384437>.
- [45] "Adaptive optics." (), [Online]. Available: [https://www.atnf.csiro.au/outreach/education/senior/astrophysics/adaptive\\_optics.html](https://www.atnf.csiro.au/outreach/education/senior/astrophysics/adaptive_optics.html).
- [46] "Owl concept design report," in May 2004, ch. 8. Adaptive Optics.
- [47] "Technologies." (), [Online]. Available: <http://www.eso.org/sci/facilities/develop/ao/tecno.html>.
- [48] "Piezoelectric gimbal mount." (), [Online]. Available: [https://www.thorlabs.com/newgrouppage9.cfm?objectgroup\\_id=12199](https://www.thorlabs.com/newgrouppage9.cfm?objectgroup_id=12199).
- [49] S. T. S. Holmstrom, U. Baran, and H. Urey, "Mems laser scanners: A review," *Journal of Microelectromechanical Systems*, vol. 23, no. 2, pp. 259–275, Apr. 2014, ISSN: 1941-0158. DOI: 10.1109/JMEMS.2013.2295470. [Online]. Available: <http://dx.doi.org/10.1109/JMEMS.2013.2295470>.
- [50] "Silicon light machines glv and plv spatial light modulators." (), [Online]. Available: <https://www.youtube.com/watch?v=yahKy7toJSk>.

- [51] A. Yalcinkaya, H. Urey, D. Brown, T. Montague, and R. Sprague, "Two-axis electromagnetic microscanner for high resolution displays," *Journal of Microelectromechanical Systems*, vol. 15, no. 4, pp. 786–794, Aug. 2006, ISSN: 1057-7157. DOI: 10.1109/jmems.2006.879380. [Online]. Available: <http://dx.doi.org/10.1109/JMEMS.2006.879380>.
- [52] J. I. Montagu and H. DeWeerd, "Optomechanical scanning applications, techniques, and devices," in *The Infrared and Electro-Optical Systems Handbook, Vol. 3: Electro-Optical Components*. SPIE, Jul. 1993, ISBN: 9781510631342. DOI: 10.1117/3.2543822.ch3. [Online]. Available: <http://dx.doi.org/10.1117/3.2543822.ch3>.
- [53] W. Piyawattanametha, P. Patterson, D. Hah, H. Toshiyoshi, and M. Wu, "Surface- and bulk- micromachined two-dimensional scanner driven by angular vertical comb actuators," *Journal of Microelectromechanical Systems*, vol. 14, no. 6, pp. 1329–1338, Dec. 2005, ISSN: 1057-7157. DOI: 10.1109/jmems.2005.859073. [Online]. Available: <http://dx.doi.org/10.1109/JMEMS.2005.859073>.
- [54] C. Errando-Herranz, N. Le Thomas, and K. B. Gylfason, "Low-power optical beam steering by microelectromechanical waveguide gratings," *Optics Letters*, vol. 44, no. 4, p. 855, Feb. 2019, ISSN: 1539-4794. DOI: 10.1364/ol.44.000855. [Online]. Available: <http://dx.doi.org/10.1364/OL.44.000855>.
- [55] "Fine steering mirror." (), [Online]. Available: <https://demcon.com/fine-steering-mirror/>.
- [56] "Galvo-resonant scanners and controllers." (), [Online]. Available: [https://www.thorlabs.com/newgrouppage9.cfm?objectgroup\\_id=11579](https://www.thorlabs.com/newgrouppage9.cfm?objectgroup_id=11579).
- [57] "Kinematic mirror mounts with piezoelectric adjusters." (), [Online]. Available: [https://www.thorlabs.com/newgrouppage9.cfm?objectgroup\\_id=231](https://www.thorlabs.com/newgrouppage9.cfm?objectgroup_id=231).
- [58] V.-F. Duma, G. Dobre, D. Demian, *et al.*, "Handheld probes and galvanometer scanning for optical coherence tomography," in *Optical Systems Design 2015: Optical Design and Engineering VI*, L. Mazuray, R. Wartmann, and A. P. Wood, Eds., SPIE, Sep. 2015. DOI: 10.1117/12.2191130. [Online]. Available: <http://dx.doi.org/10.1117/12.2191130>.
- [59] A. Wehr and U. Lohr, "Airborne laser scanning—an introduction and overview," *ISPRS Journal of Photogrammetry and Remote Sensing*, vol. 54, no. 2–3, pp. 68–82, Jul. 1999, ISSN: 0924-2716. DOI: 10.1016/S0924-2716(99)00011-8. [Online]. Available: [http://dx.doi.org/10.1016/S0924-2716\(99\)00011-8](http://dx.doi.org/10.1016/S0924-2716(99)00011-8).
- [60] "Galvo-galvo scan head and controller." (), [Online]. Available: [https://www.thorlabs.com/newgrouppage9.cfm?objectgroup\\_id=10674](https://www.thorlabs.com/newgrouppage9.cfm?objectgroup_id=10674).
- [61] "Two-axis vantagepro® galvanometer system scan heads." (), [Online]. Available: [https://www.thorlabs.com/newgrouppage9.cfm?objectgroup\\_id=14124](https://www.thorlabs.com/newgrouppage9.cfm?objectgroup_id=14124).
- [62] "Dual-axis vantagepro® galvanometer scan head systems, ±22.5° scan angle." (), [Online]. Available: [https://www.thorlabs.com/newgrouppage9.cfm?objectgroup\\_id=14132](https://www.thorlabs.com/newgrouppage9.cfm?objectgroup_id=14132).
- [63] "Fast steering mirror." (), [Online]. Available: [https://www.thorlabs.com/newgrouppage9.cfm?objectgroup\\_id=15347](https://www.thorlabs.com/newgrouppage9.cfm?objectgroup_id=15347).
- [64] "Laser applications: Galvo scanners reach megahertz-scale range repetition rates for laser micromachining." (), [Online]. Available: <https://www.laserfocusworld.com/lasers-sources/article/16546979/laser-applications-galvo-scanners-reach-megahertzscale-range-repetition-rates-for-laser-micromachining>.
- [65] F. M. Tapos, D. J. Edinger, T. R. Hilby, M. S. Ni, B. C. Holmes, and D. M. Stubbs, "High bandwidth fast steering mirror," in *Optomechanics 2005*, A. E. Hatheway, Ed., SPIE, Aug. 2005. DOI: 10.1117/12.617960. [Online]. Available: <http://dx.doi.org/10.1117/12.617960>.
- [66] G. Garcia-Torales, "Risley prisms applications: An overview," in *Advances in 3OM: Opto-Mechatronics, Opto-Mechanics, and Optical Metrology*, J. P. Rolland, V.-F. Duma, and A. G. H. Podoleanu, Eds., SPIE, May 2022. DOI: 10.1117/12.2616071. [Online]. Available: <http://dx.doi.org/10.1117/12.2616071>.
- [67] "Mechanical scanners: Risley prism scanners improve on gimbal/galvo alternatives." (), [Online]. Available: <https://www.laserfocusworld.com/optics/article/16550223/mechanical-scanners-risley-prism-scanners-improve-on-gimbal-galvo-alternatives>.

- [68] H. D. Tholl, "Novel laser beam steering techniques," in *Technologies for Optical Countermeasures III*, D. H. Titterton, Ed., SPIE, Sep. 2006. DOI: 10.1117/12.689900. [Online]. Available: <http://dx.doi.org/10.1117/12.689900>.
- [69] P. Church, J. Matheson, X. Cao, and G. Roy, "Evaluation of a steerable 3d laser scanner using a double risley prism pair," in *Degraded Environments: Sensing, Processing, and Display 2017*, J. ( N. Sanders-Reed and J. ( J. Arthur, Eds., SPIE, May 2017. DOI: 10.1117/12.2262198. [Online]. Available: <http://dx.doi.org/10.1117/12.2262198>.
- [70] V. Vuthea and H. Toshiyoshi, "A design of risley scanner for lidar applications," in *2018 International Conference on Optical MEMS and Nanophotonics (OMN)*, IEEE, Jul. 2018. DOI: 10.1109/omn.2018.8454641. [Online]. Available: <http://dx.doi.org/10.1109/OMN.2018.8454641>.
- [71] K. Tyszka, M. Dobosz, and T. Bilaszewski, "Double wedge prism based beam deflector for precise laser beam steering," *Review of Scientific Instruments*, vol. 89, no. 2, Feb. 2018, ISSN: 1089-7623. DOI: 10.1063/1.5011979. [Online]. Available: <http://dx.doi.org/10.1063/1.5011979>.
- [72] A. Li, W. Sun, W. Yi, and Q. Zuo, "Investigation of beam steering performances in rotation risley-prism scanner," *Optics Express*, vol. 24, no. 12, p. 12 840, Jun. 2016, ISSN: 1094-4087. DOI: 10.1364/oe.24.012840. [Online]. Available: <http://dx.doi.org/10.1364/OE.24.012840>.
- [73] W. C. Warger II and C. A. DiMarzio, "Dual-wedge scanning confocal reflectance microscope," *Optics Letters*, vol. 32, no. 15, p. 2140, Jul. 2007, ISSN: 1539-4794. DOI: 10.1364/ol.32.002140. [Online]. Available: <http://dx.doi.org/10.1364/OL.32.002140>.
- [74] "Spatiotemporal control of light." (), [Online]. Available: <https://www.wavefrontshaping.net/post/id/77>.
- [75] Z. He, F. Gou, R. Chen, K. Yin, T. Zhan, and S.-T. Wu, "Liquid crystal beam steering devices: Principles, recent advances, and future developments," *Crystals*, vol. 9, no. 6, p. 292, Jun. 2019, ISSN: 2073-4352. DOI: 10.3390/cryst9060292. [Online]. Available: <http://dx.doi.org/10.3390/cryst9060292>.
- [76] "Deflectors." (), [Online]. Available: <https://www.polytec.com/eu/optical-systems/products/laser-accessories/electro-optic-components/deflectors>.
- [77] "Acousto-optic deflectors." (), [Online]. Available: <https://www.youtube.com/watch?v=qrljXkC9t9Q>.

# A

## Precision factors and effects

This appendix contains an overview of all factors and/or effects per high precision application discussed in chapter 2. A classification, visible in Table A.1, was used to signify the traits of each application and what aspect of the application the effect/cause is related to. All findings from research into literature are visible per application in tables A.2, A.3 and A.4. The sources can be referenced to chapter 2.

Task	Base	Movement	Related to:
M = Manipulation	F = Fixed	S = Spatial	Environmental
O = Orientation	FF = Free floating	P = Planar	Process
T = Transferring		R = Rotating SP = Both possible	Machine

Table A.1: Explanation of traits and types of effects

Space telescope	Telescopes	Sources	Space manipulation	Sources
<i>FF, S, O</i>	<i>F, SP, O</i>		<i>FF, SP, M</i>	
Micro-vibrations		[36]	Micro-vibrations	[36]
Sensors		[36]	Sensors	[36], [56]
Coolers (piston)	Cooler fans/ system/ motors	[36], [40], [45]	Coolers	[36], [129]
RWA		[36]	RWA	[36], [124]
CMG		[36]	CMG	[36], [166]
Solar array drives		[36]	Solar array drives	[36], [60]
Unaccounted transmission paths		[167]	Interaction with object	[60]
Frame/ appendage flexibility		[32]	Assembly planning order	[60]
Scanning mechanism		[32]	Identification payload	[60]
Adaptive or active optics	Adaptive optics (finite sampling, limited DoFs, measurement noise, light brightness, anisoplanatism)	[168]	Contact effects on payload	[60]
Jitter in LOS control		[169]	Control	[60]
Thrusters/ despin		[33]	Motion planning	[60]
Aerodynamics	Wind loading	[33], [45], [56]	1 G test validation	[60]
Uneven gravity		[33]	Collisions with environment	[60]
Solar radiation pressure		[33], [56]	Controller inaccuracies	[60]
Lubrication problems		[126]	Joint flexibility	[60]
Pointing Mechanism (PM)		[36]	Model of system during testing	[60]
Thermal induced disturbances		[33]	Frame/ appendage flexibility	[60]
Fretting from launch		[126]	Teleoperation	[60]
	Optics production	[170]	Thrusters	[33]
	Optics verification	[170]	Aerodynamics	[33]
	Air turbulences	[170]	Uneven gravity	[33]
	Aberations	[142]	Solar radiation pressure	[33]
	Ground vibrations	[45]	Fretting from launch	[67]
	Shutters	[45]		
	Telescope orientation	[45]		
	Tracking errors	[45]		
	Actuator imperfections	[45]		

Table A.2: Effects and causes on (space) telescopes and space manipulation

Engines/drives <i>F, R, T</i>	Sources	3d printing (FDM) <i>F, S, M</i>	3d printing (SLA/SLS) <i>F, P, O</i>	Sources
Vibrations due to dynamic balance	[69], [71], [77], [78]	Nozzle diameter/ pressure	Nozzle diameter/ shape	[86], [99], [108], [171], [173]
Thermal deformations	[71], [78]		Fluid properties (IJ, DW)	[86], [108], [173]
Bearings (pneumatic hammer/ stiffness/ thermal expansion/ control stability)	[78]	Melting dynamics filament	Thermal conductivity of material	[86], [171]
Thermal isolation	[71]	Layer height	Minimum thickness (surface tension & viscosity (SLM))	[102], [171]
Axial force	[174]	Heating		[86]
Tip leakage	[71]	Filament consistency	Mixing (IJ)	[99], [171], [173]
Thermal measuring/ modelling error	[78]	Cooling (shrinkage)	Shrinkage due to cooling	[99], [171], [173]
Frame/ appendage flexibility	[70]	Feedstock shape and resolution		[171]
Chemical reaction	[71]	Travel speed		[89]
Manufacturing defects (etching, machining, forging, assembly, casting)	[69], [84]	Consistency/ repeatability printer parts	Spot size consistency	[86], [99], [175]
Shock wave losses	[71]	Software/ control		[88]
Creep & oxidation	[71]	Mathematical error		[98]
Control	[69], [71]	Vibrations	Wiper induced vibrations (SLA)	[86], [88]-[90]
Inhomogeneous & anisotropic material	[69]	Print speed/ acceleration	Scanning speed	[100], [102]-[104]
Cavitation	[71]	First layer/ bed levelling		[99]
Eigenmodes	[79]	Model dimension mismatch (distortion)		[99], [175]
External forces (noise, environmental changes)	[79]	Arc shape causing over extrusion		[99]
Fluid leakage (tolerances)	[71]	Slicer/motion planning (retraction, jerk)		[89], [98], [99]
Whirling of shaft	[69]	Gravity		[176]
Viscous forces	[71]	Air gap		[177], [178]
Gas pressure pulses	[70]	Raster shape/ orientation		[179]
Wear & aging	[69]	Building direction		[172]
Calibration	[79]		Laser source quality	[86]
Centrifugal growth	[71]		Hatch spacing	[104]
			Curing dynamics (MJ)	[86]
			Laser optics/ scanning mechanism	[86]
			Layer compaction/ recoating (SLS)	[95], [96]
			Printhead resolution (MJ)	[86]
			Droplet properties (MJ) (overspreading)	[86]
			Reactive small particles	[94]
			Splatter (High velocity) (IJ)	[173]
			Droplet evaporation (AJP)	[173]
			Jetting to stage speed relation (IJ)	[108]
			Material process parameter	[171]
		Motion stage related error, see Motion stage	Motion stage related error, see Motion stage	

Table A.3: Effects and causes on engines/drives and FDM and SLA/SLS 3d printing

Motion stage	Sources	Beam steering	Sources
<i>F, SPR, M</i>		<i>F, SP, O</i>	
Frame/ appendage flexibility	[106], [118], [122]	Setup/ assembly (beam diameter, bearing, preload, lubricant, mounting)	[141], [142]
Noise motion stage	[121]	Inertia	[142]
Abbe error (z-wobble due to runout/straightness)	[98], [99], [121], [142]	Jitter (External vibrations, bearing wobble, friction, torque ripple)	[142], [147]
Backlash (clearances, deformation, belt)	[99], [121], [122], [180]	Control (settling time, bias error, noise magnification)	[142], [147]
<b>External forces</b>	[121]	Reaction torque (limits acceleration)	[142]
Friction/stiction	[87], [121], [142], [180]	Drift (actuator, control & thermal)	[141], [142], [147], [174]
Controller (integer rounding)	[87], [121]	Thermals	[141], [142]
System dynamics/ modelling	[118], [121]	Linearity (responsivity)	[142], [147]
Transmission stiffness	[87]	<b>External vibrations</b>	[142]
<b>Vibrations (environment, motor driver)</b>	[88], [117], [119], [121]	Adaptive optics (finite sampling, limited DoFs, Measurement noise, light brightness, anisoplanatism)	[168]
Voltage slamming (instant max volt) (backlash stepper)	[122]	Frame/ mechanism flexibility (resonance)	[142], [147]
<b>Environmental conditions</b>	[121]	Smooth continuous rotation (scanning)	[142]
Production/ assembly error	[115], [182]	<b>Atmospheric conditions (convection, turbulence, varying index of refraction, air flow)</b>	[142]
Cosine error (misalignment sensor)	[121]	Creep (ferroelectric material)	[42]
Tracking error (friction)	[181]	Hysteresis (PZT)	[153]
Coupling	[87], [121], [123]	Cross coupling / wobble	[147], [152]
Inertia	Any dyn. Bal. Sources, [87]	Feedback sensor/ tracking error	[142], [147]
Thermal expansion (stage & different parts)	[121]		
Calibration	[115]		
Drift (lubricant migration, thermal variations)	[121]		
Hysteresis (elastic forces)	[121]		
Torque ripple	[122]		
Load (dynamic and <b>static forces</b> )	[121]		
Actuator error	[118]		
PZT hysteresis	[153]		
Joint sensors	[115]		

Table A.4: Effects and causes on motion stages and beam steering

# B

## Overview researched force balanced spherical mechanisms

This appendix contains an overview of all functioning and non-functioning spherical pantograph based mechanisms. For the non-functioning mechanisms, possible reasons are provided for why the mechanism either does not function or retain its balance. Since not all mechanisms were relevant (not generic/ simplified), mechanisms displayed here will vary in refinement. This means designs can vary as well as be more conceptual/simplified compared to mechanisms presented in Chapter 3 and 4.

### B.1. Functioning mechanisms

These are all functioning spherical pantographs of which certain versions have also been presented in Chapter 3 or Chapter 4.

#### Equal length spherical pantograph

As shown in Chapter 3, Fig. 2b, an equal link length spherical pantograph is visible in Fig. B.1.

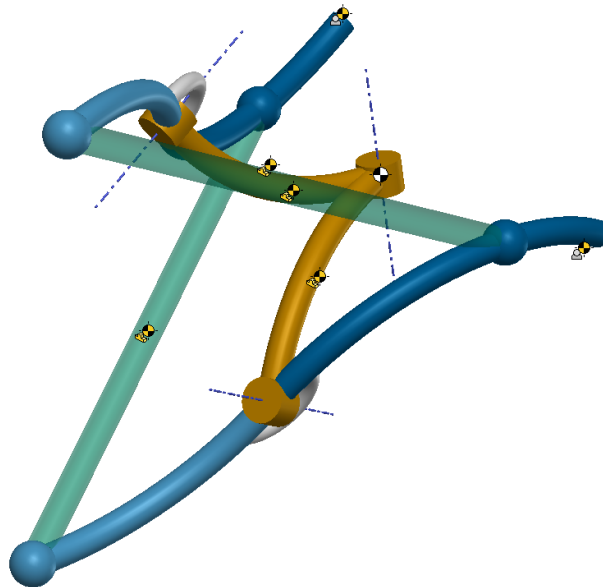


Figure B.1: Equal length spherical pantograph

### Kite shaped spherical pantograph

A feasible variation is the kite shaped pantograph (also viable in planar form), where the distant linkages with end-effectors (green) have a longer link length compared to the near links and compensating part (blue) (see Fig. B.2).

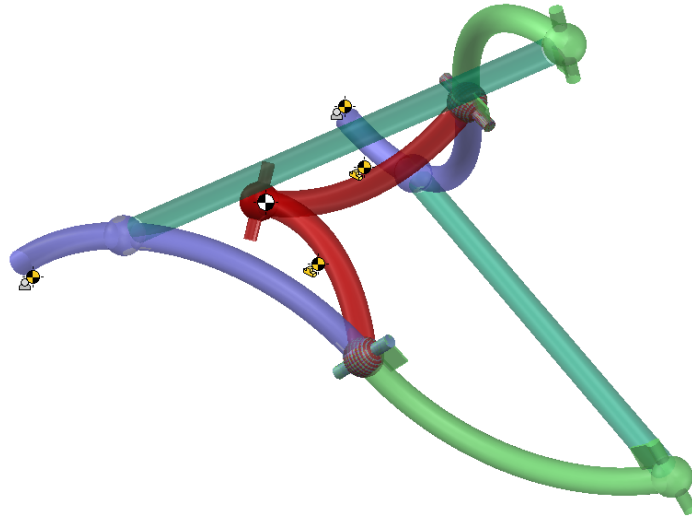


Figure B.2: Spherical pantograph where distant links (green) are longer compared to near link (red) or secondary link (blue)

### Variation equal length spherical pantograph

As shown in Chapter 3, Fig. 4, an equal link length spherical pantograph is visible in Fig. B.3.

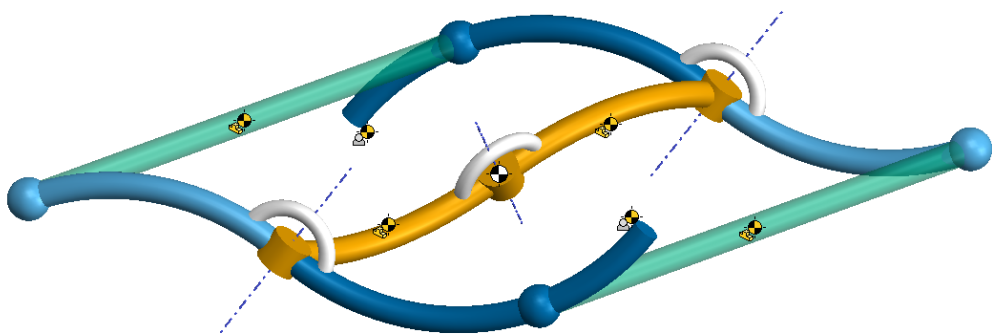


Figure B.3: Variation of equal length spherical pantograph

### Variation kite shaped spherical pantograph

This is a variation on the kite shaped spherical pantograph visible in Fig. B.2, which retains its mass balance as well as functionality. Distant link (light green) has a longer link length compared to inner links (red) or compensating links (blue) are visible in Fig. B.4. The inner links (red) are co-linear.

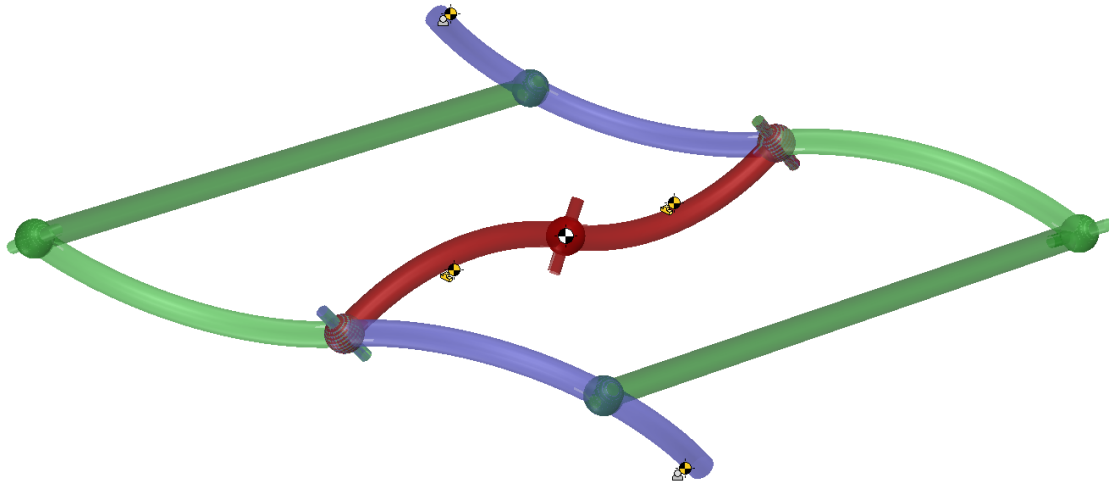


Figure B.4: Spherical pantograph where distant links (green) are longer compared to near link (red) or secondary link (blue)

### Equal length double spherical pantograph

Equal length links are used to create the most simple version of a double spherical pantograph, as visible in Fig. B.5.

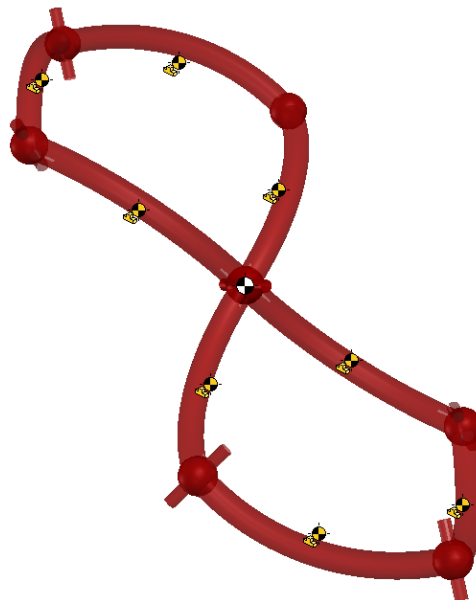


Figure B.5: Double spherical pantograph with equal link length

### Scaled double spherical pantograph

The scaled double spherical pantograph has 2 sides, which are scaled in length as well as inversely in mass, shown in Fig. B.6.

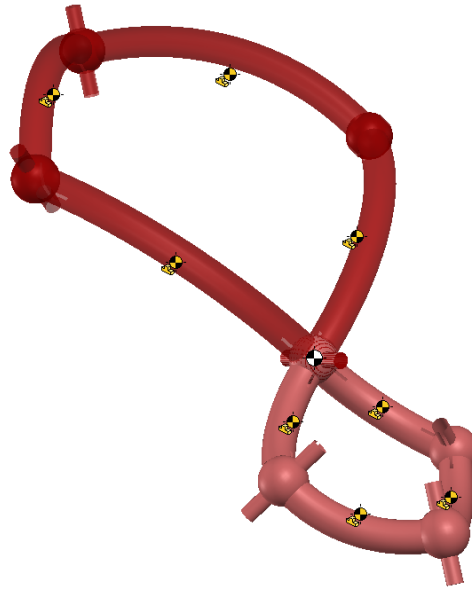


Figure B.6: Double spherical pantograph which is scaled around center point

### Parallelogram shaped scaled double spherical pantograph

The double spherical pantograph can also be parallelogram shaped (1 pair of long links and 1 pair of short links), as seen in Fig. B.7. This is also visible in Chapter 2, Fig. 5.

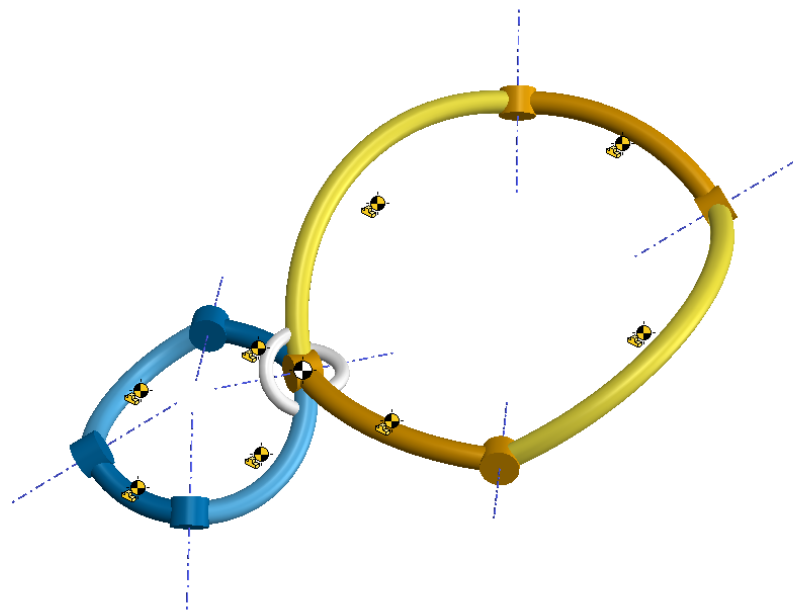


Figure B.7: Double spherical pantograph with a parallelogram shape (long and short link pairs) as well as scaled around center point

### Kite shaped scaled double spherical pantograph

A different version of the scaled double spherical pantograph is kite shaped, where distant links are longer than near links, as visible in Fig. B.2.

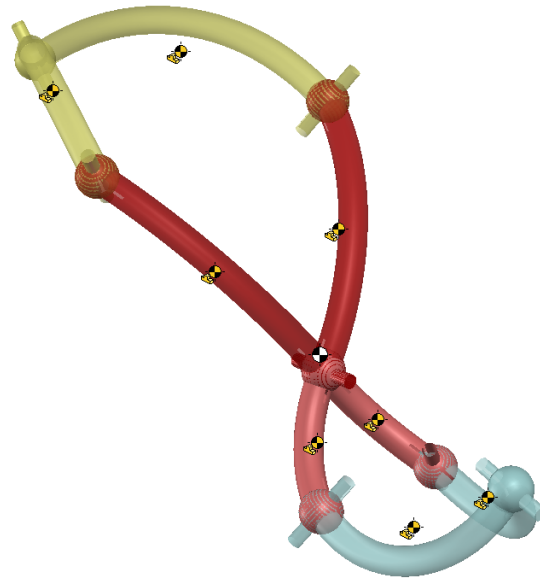


Figure B.8: Double spherical pantograph with a kite shape (distant links (yellow and blue) longer than near links (red)) and scaled around center point

### Shifted double spherical pantograph

Shifting distant links is also feasible, where a smaller parallelogram or rhombus will be formed (see Fig. B.9). The remaining sections can be removed which would simply result in a smaller double spherical pantograph.

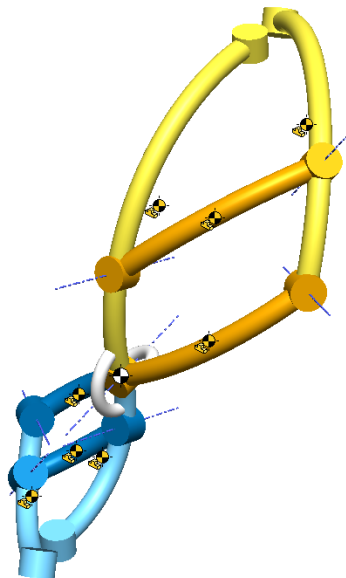


Figure B.9: Double spherical pantograph with parallelogram shape where distant links (1 dark blue and 1 orange) are shifted along to form a smaller parallelogram

### Variation equal length double spherical pantograph

The variation of the double spherical pantograph uses ball joints at the end effectors, which is visible in Fig. B.10. The links here have equal lengths. A drawback is the presence of a singularity, causing this mechanism to potentially lose its mirrored motion and thus balance.

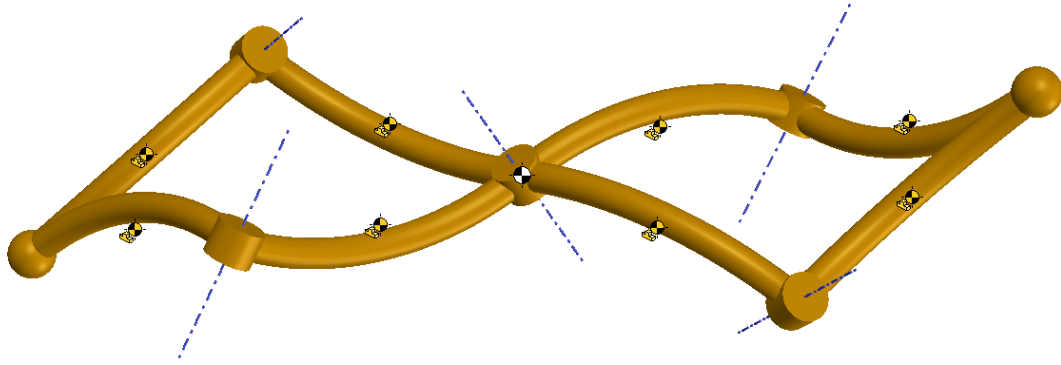


Figure B.10: Variation of double spherical pantograph with equal link lengths

### Variation scaled double spherical pantograph

Similarly to the double spherical pantograph visible in Fig. B.6, a scaled version around the center is also feasible as seen in Fig. B.11. This is also visible in Chapter 2 Fig. 6.

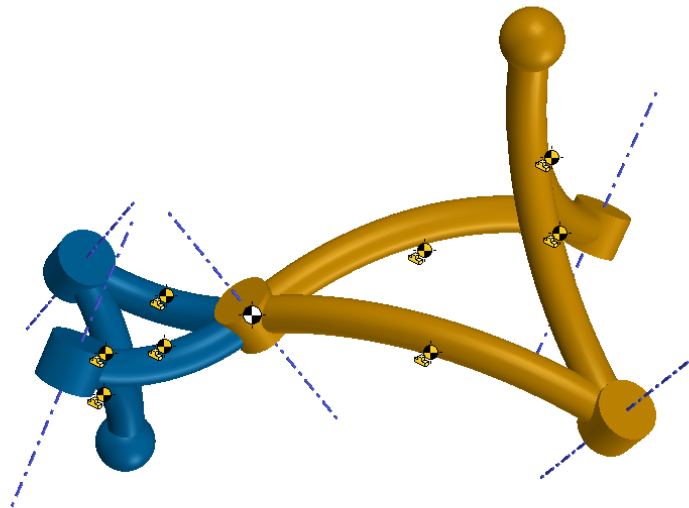


Figure B.11: Variation of double spherical pantograph which is scaled around the center

**Variation Kite shaped non scaled double spherical pantograph**

A kite can be drawn in 2 ways, either long near links or long distant links. Both versions are balanced, but the short distant/long near links version works without collisions, shown in Fig. B.12. Short/long requires redesigning since distant links collide, as visible in Fig. B.13.

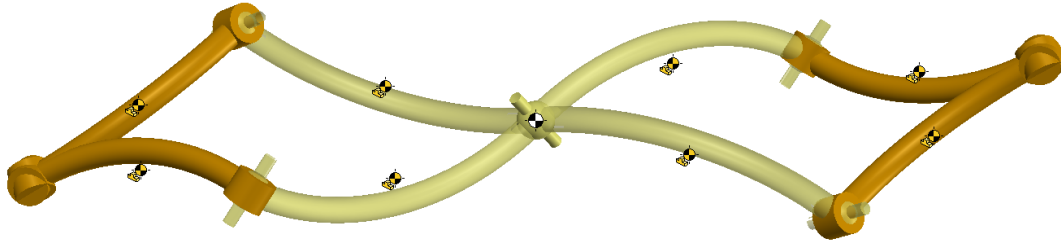


Figure B.12: Variation of kite shaped double spherical pantograph, with short distant links (dark) and long near links (light)

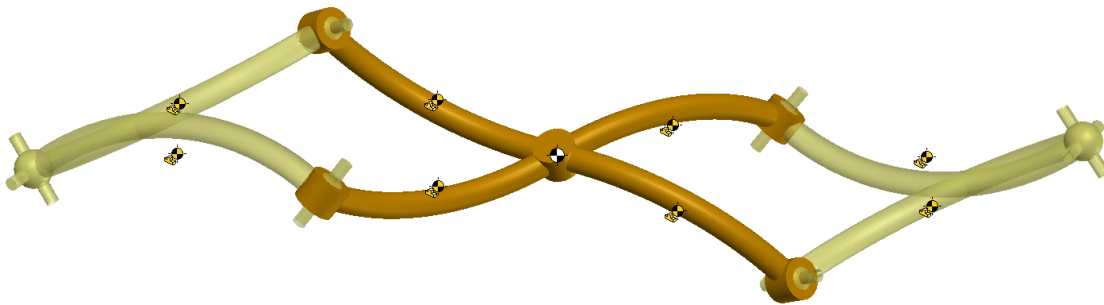


Figure B.13: Variation of kite shaped double spherical pantograph, with long distant links (light) and short near links (dark). Here long links visible collide, thus requiring redesigning

### Equal length double S shaped mechanism with surrounding 4R four-bar

The double S shaped mechanism with surrounding 4R four-bar is based on a planar version. The spherical version is shown in Fig. B.14, where equal link lengths (red and blue) can be constrained using an equal length 4R four-bar (green). Inner links (red and blue) are co-linear and ball joints are used between four-bar (green) and S shaped links (red and blue).

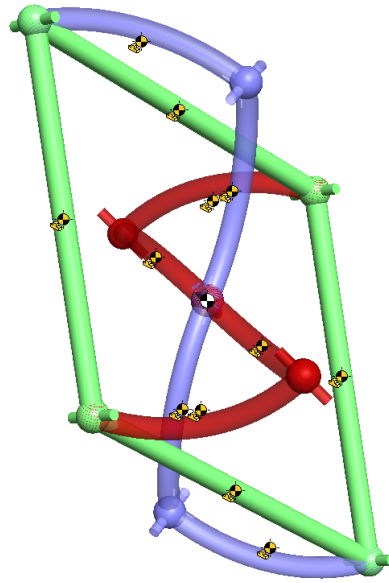


Figure B.14: Equal length double S shaped mechanism with surrounding equal length 4R four-bar

### Unequal length double S shaped mechanism with surrounding 4R four-bar

A feasible variation is unequal length links, visible in Fig. B.15, where the inner links are either shorter or longer than distant links. This requires a different surrounding 4R four-bar to constrain the desired movement.

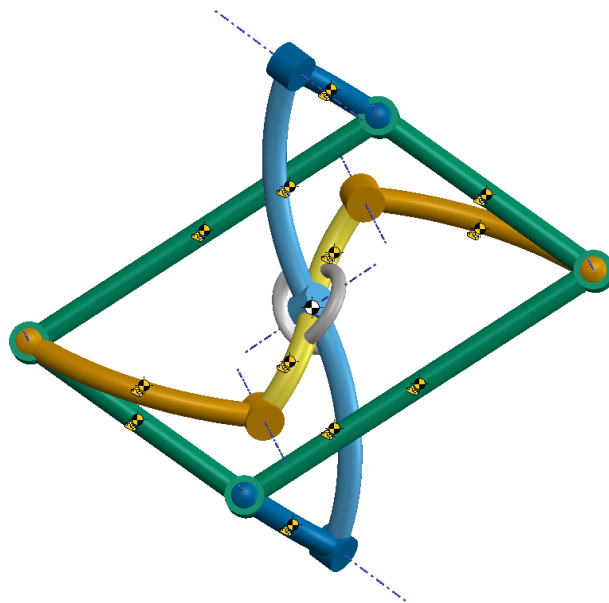


Figure B.15: Double S shaped mechanisms with unequal length links and parallelogram 4R four-bar

**Kite shaped double S shaped mechanism with surrounding 4R four-bar**

A kite shaped double S mechanism is also feasible, in both orientations (i.e. short inner/ long distant links or long inner/ short distant links). Figure B.16 shows long inner links and short distant links, with a equal link length surrounding 4R four-bar.

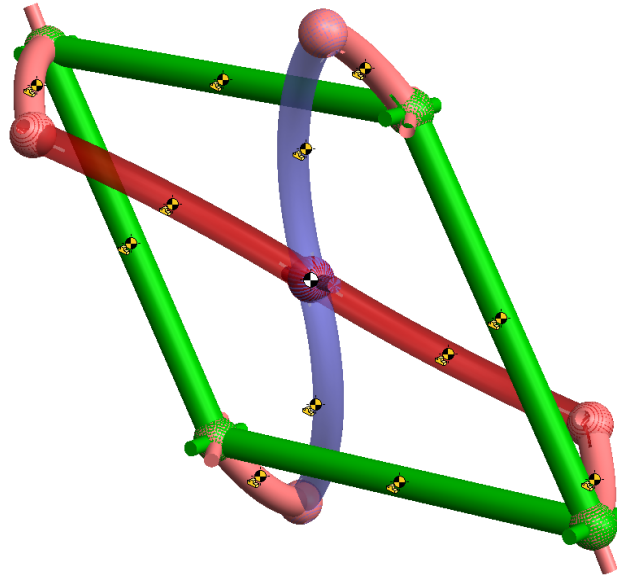


Figure B.16: Kite shaped double S shaped mechanisms with long inner links and short outer links

## B.2. Non-functioning mechanisms

Non-functioning of mechanisms can have many reasons, either kinematics or balance related. Here are several non-functioning mechanisms displayed as well as reasoning why combined alterations are not working. Mechanisms with similar shapes are not discussed, since they are not fully researched within this thesis. Equally, unbalanced shapes such as a similar radius spherical pantograph will be shown, but where not further researched due to clear initial unbalance.

### Parallelogram shaped spherical pantograph

The functioning spherical pantograph (shown in Fig. B.2 and B.1) relies equal length or symmetrical links for balance. The parallelogram shaped mechanism with longer links (visible in Fig. B.17) places the masses not only further away from the joint, but also out of plane due to the curved nature. This causes an unbalance in this out of plane direction.

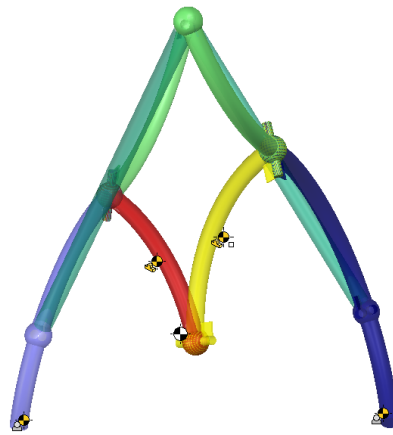


Figure B.17: Parallelogram shaped spherical pantograph, where the link length of yellow is 125% of red, causing an unbalanced movement.

### Scaled spherical pantograph

The mechanism shown in Fig. B.18 functions similarly to the spherical pantograph visible in Fig. B.1 concerning types of joints, but requires a variable length constraining linkage (dark green), making the current constraining method not feasible. If a different type of constraining can be applied, then the mechanism can be force balanced, although with a relatively small range of motion.

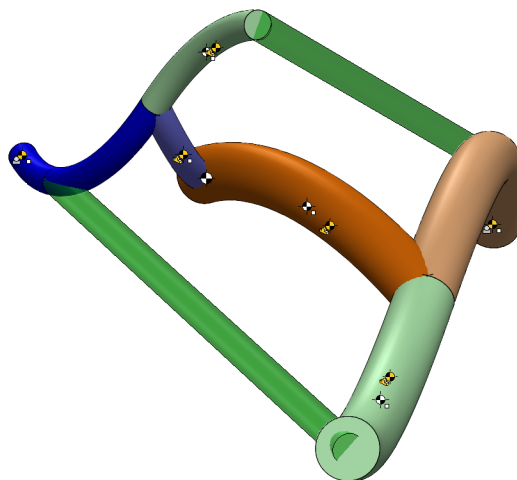


Figure B.18: Scaled spherical pantograph, in a fixed orientation due to the fixed length constraint links (dark green)

### Variation parallelogram shaped spherical pantograph

The variation of the parallelogram shaped spherical pantograph shares the same problem as the normal pantograph, with out of plane unbalance due to the longer links (yellow) as can be seen in Fig. B.19. Here it is clearly visible that both sides of the spherical pantograph are not parallel, and thus include an unbalanced motion when driven.

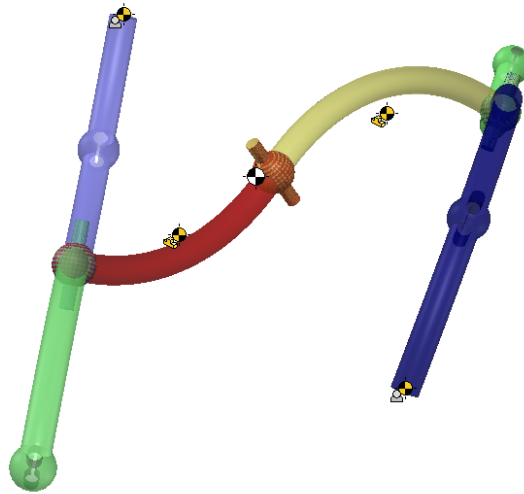


Figure B.19: Variation of parallelogram shaped spherical pantograph, where out of plane unbalance is visible by non-parallel planes of left (light) and right (dark) sides of the mechanism

### Variation scaled spherical pantograph

The variation of the scaled spherical pantograph mechanism shown in Fig. B.20 can also be balanced, but similarly to the scaled spherical pantograph requires variable length constraint links, making it unfeasible with the current design.

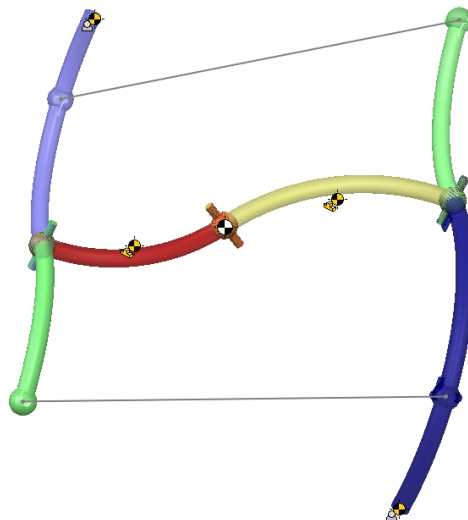


Figure B.20: Variation of spherical pantograph which is scaled around center, where different radii are used but requires variable length constraint links

### Variation parallelogram shaped double spherical pantograph

The parallelogram shaped variant of the double spherical pantograph variation (shown in scaled version in Fig. B.21) cannot function, due to the end-effector points not aligning and therefore not allowing for a ball joint connection.

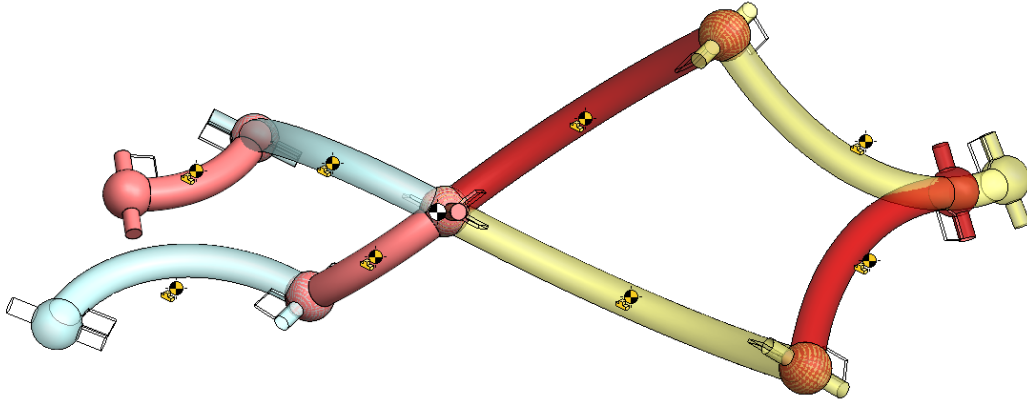


Figure B.21: Parallelogram shaped version of double spherical pantograph variation, where end-effector points do not align and can therefore not be connected.

### Variation scaled double spherical pantograph

The scaled version of the double spherical pantograph variation (visible is scaled and kite variant in Fig. B.22) has besides the collision problem due to the kite shape, also a non symmetrical motion of both sides. The smaller side will fold faster, thereby not allowing for mirrored motion of the larger side as well as limit the movement of the larger side. This creates an unbalanced mechanism.

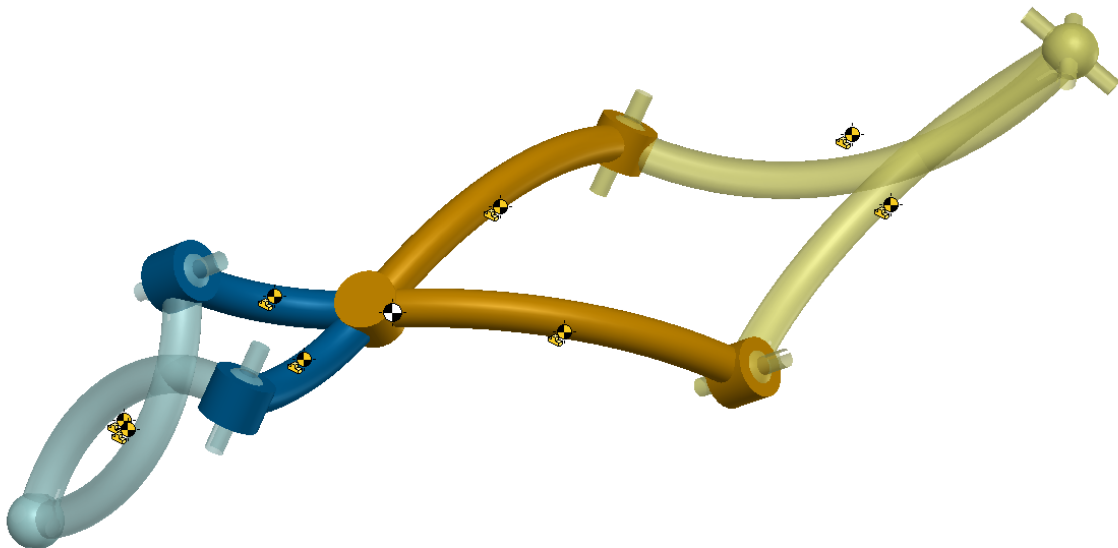


Figure B.22: Scaled variant of the double spherical pantograph variation, where collision is visible as well as a non symmetrical motion and therefore no force balance

### Scaled Double S mechanism

The scaled double S mechanism has a trapezium shaped 4R four-bar constraining linkage, which requires variable link lengths to allow for balanced motion. The current constraining design therefore doesn't allow for movement.

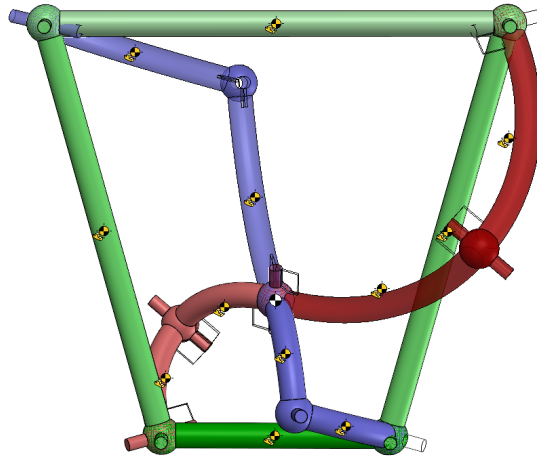


Figure B.23: Scaled Double S mechanism, where a variable link length trapezium shaped four-bar constraining linkage would be required, which isn't feasible with the current design

### Shifting of linkages

Shifting is possible if the original shape is preserved and the required constraints are not altered. The spherical pantograph and variation will change from an equal and symmetrical version to an unequal parallelogram shaped version when links are shifted. Since these, as shown in Fig. B.17 and B.19, are not balanced, shifting is therefore not feasible. Similarly for the double spherical pantograph variation, where shifting would also create a parallelogram shape as visible in Fig. B.21 which doesn't function. Shifting within the double S shaped mechanism, visible in Fig. B.24, could be made to function by redesigning the planar 4R four-bar linkage, but the shifted linkages would still result in an unbalanced mechanism due to a lack of symmetry.

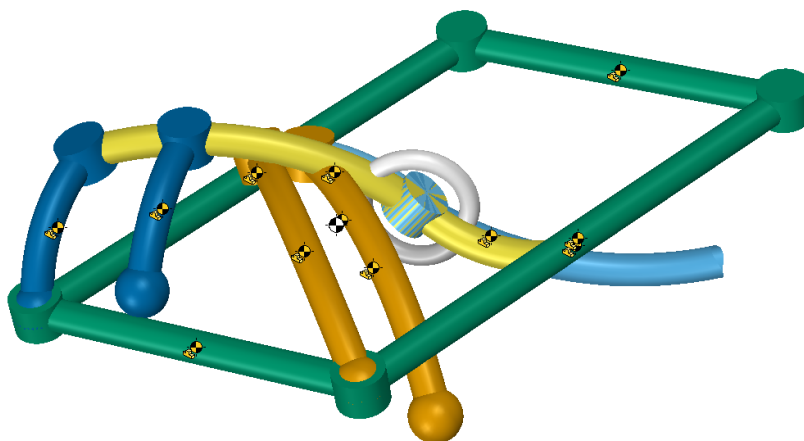


Figure B.24: Shifted double S shaped mechanism, where planar 4R four-bar would need to be redesigned to allow for functionality. However, balance would still not be present, due to a lack of symmetry.

### Variations of scaled mechanism

Kite or parallelogram shaped mechanism can be combined with scaling around the center point, if both variations are possible (such as the double pantograph variants visible in Fig. B.7, B.8 and B.28). This means only the double spherical pantograph retains its functionality and balance when both scaled around the center point and kite or parallelogram shaped. This is most likely due to the symmetric nature of this design, allowing for more variations.

### Non balanced shapes

The following shapes (Fig. B.25, B.26 and B.27) are also not balanced, due to out of plane unbalance.

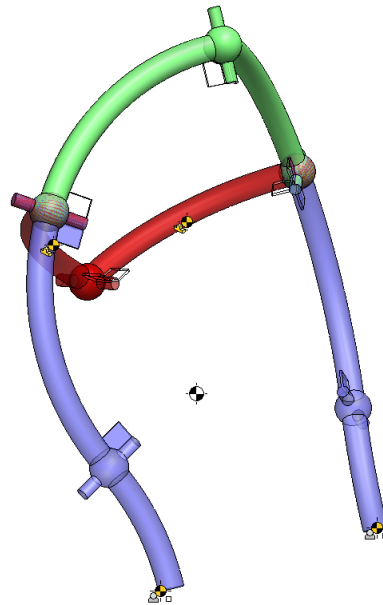


Figure B.25: Same radius spherical pantograph, with unbalance out of plane

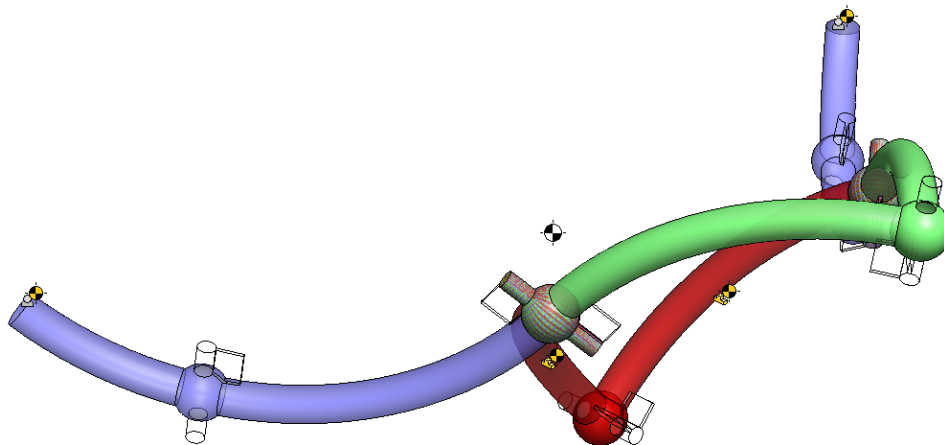


Figure B.26: Same radius spherical pantograph, with counter masses (blue) in opposite direction remains unbalanced out of plane.

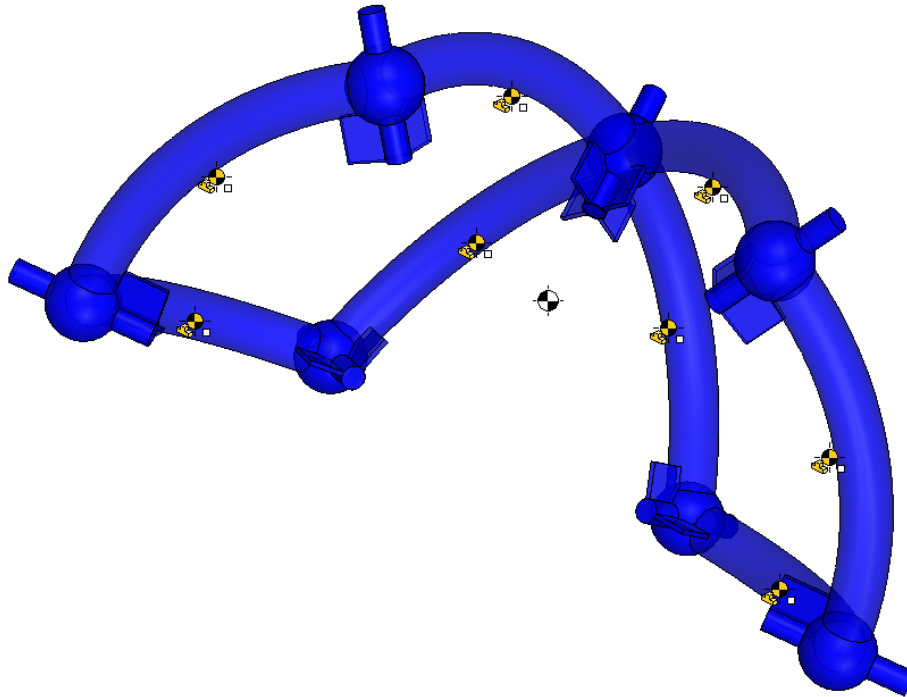


Figure B.27: Same radius double spherical pantograph is also unbalanced out of plane

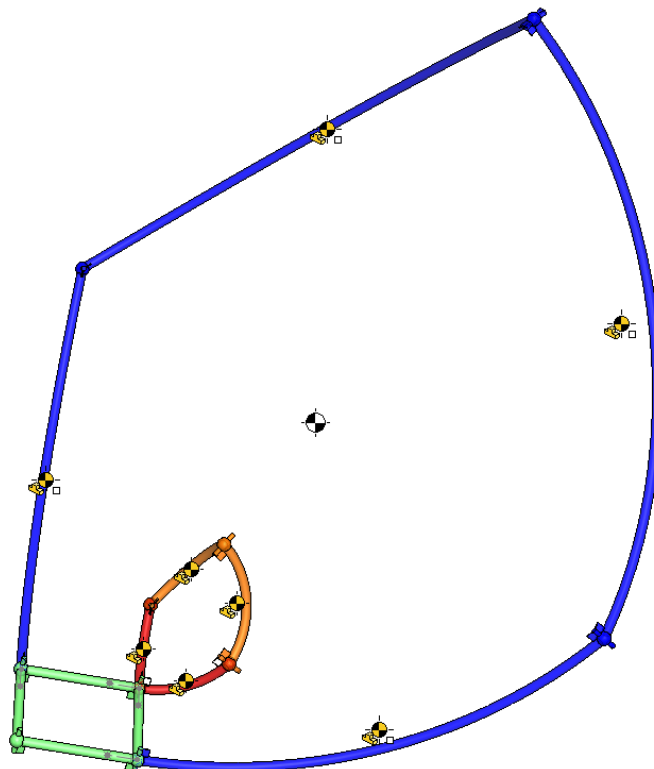


Figure B.28: Similar Shapes, which functions like a Bennett linkage, is unbalanced. Unclear what the balance conditions are.

# C

## Overview of spherical mechanisms

Several Spherical Parallel Manipulators (SPMs) are presented, including their sources. This is by no means a conclusive overview of all SPM, but a small relevant section which functioned as inspiration.

### A 3-RRR Spherical Parallel Manipulator Reconfigured with Four-bar Linkages

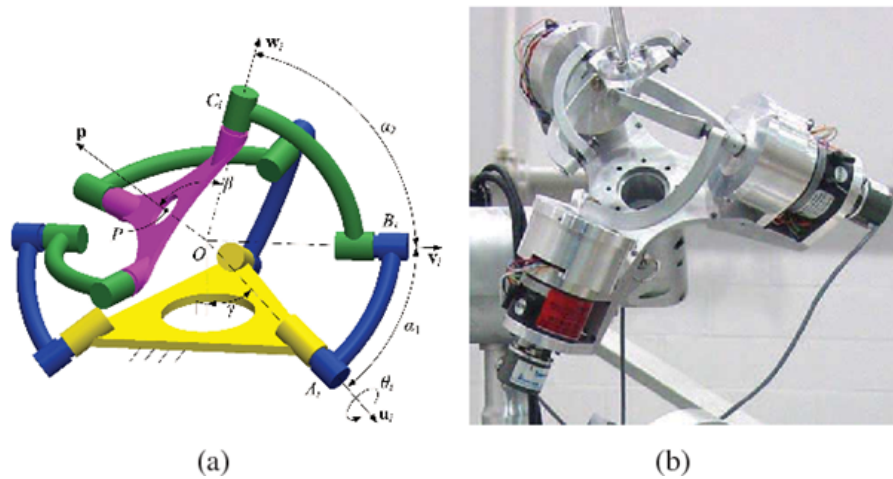


Figure C.1: Standard RRR [19]

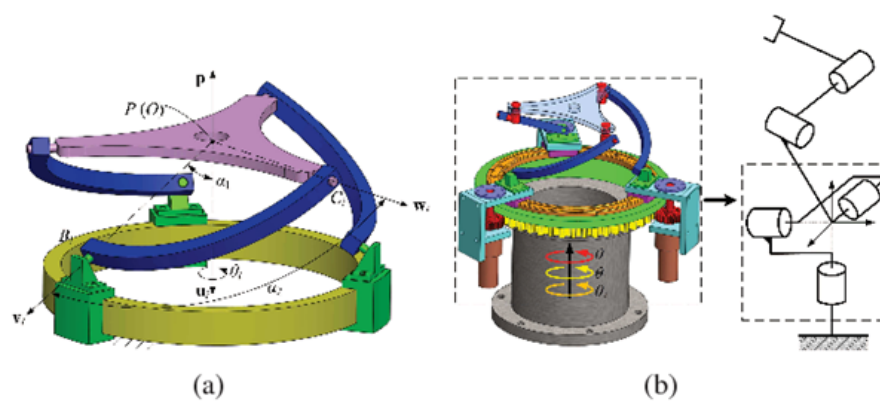


Figure C.2: RRR with bottom R being a prism sliding along a single circular ring (yellow and green) [19]

## Spherical Parallel Manipulator (SPM) 2 DOF Inverse Kinematics Simulation

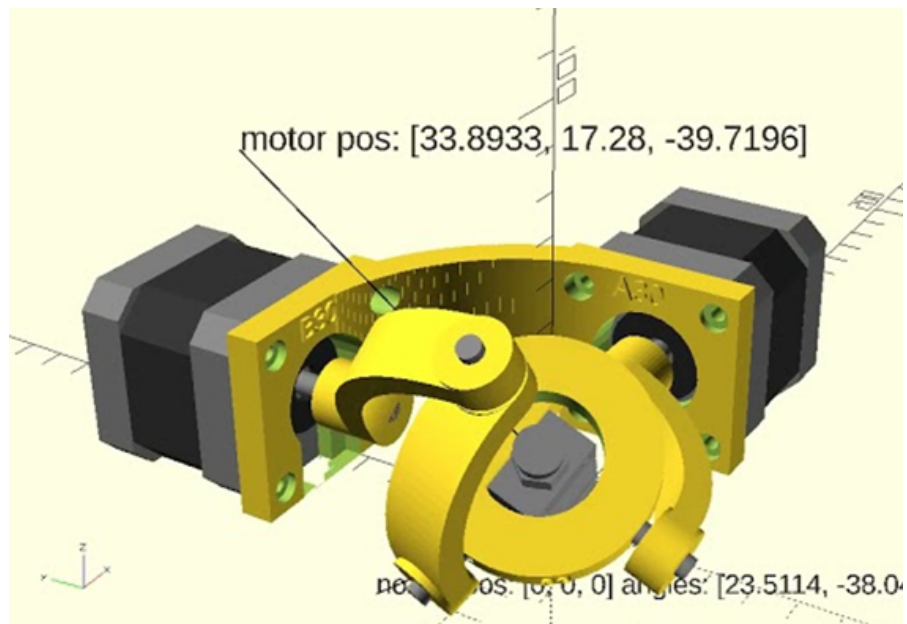


Figure C.3: RRR & RR SPM [20]

## Computation of Unique Kinematic Solutions of a Spherical Parallel Manipulator with Coaxial Input Shafts

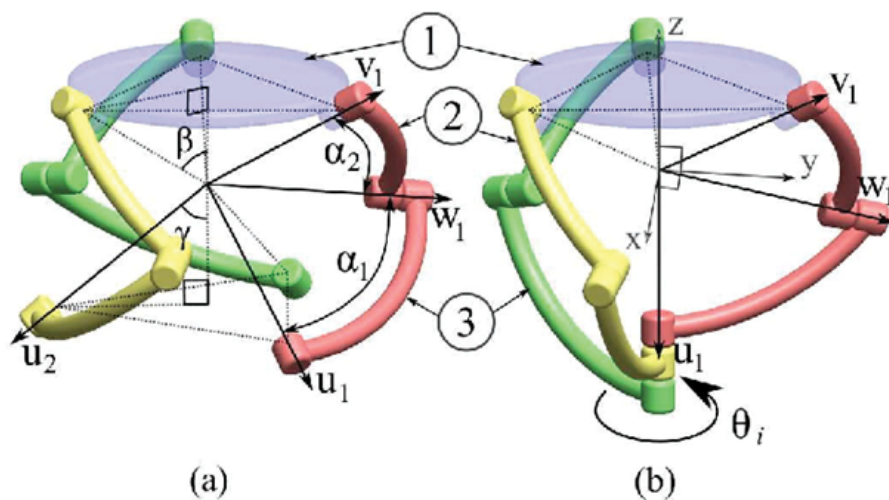


Figure C.4: Spherical Parallel Manipulators (SPM) with 2 Inputs and 2 links (RR and RRR) [21]

### Compound Impedance Control of a Hydraulic Driven Parallel 3UPS/S Manipulator

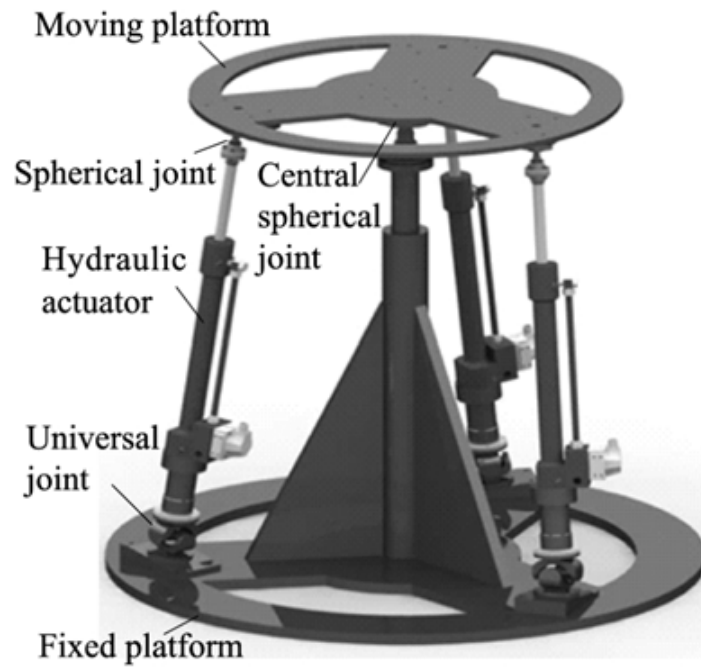


Figure C.5: 3 UPS/S manipulator, using linear actuators [22]

### Modelling and Analysis of a 2-DOF Spherical Parallel Manipulator

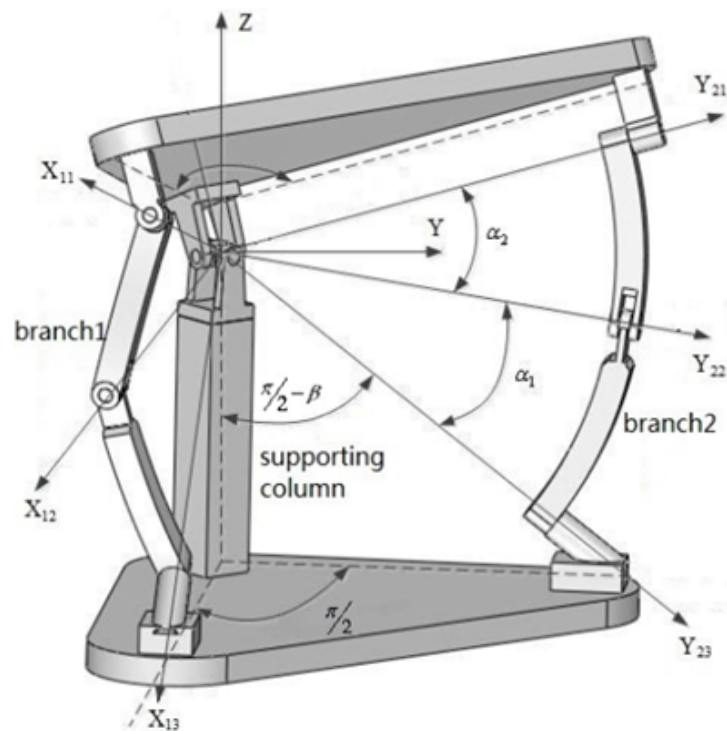


Figure C.6: RR & 2RRR SPM, rotating around RR joint at the supporting column [23]

## Design and Prototyping of a Spherical Parallel Machine Based on 3-CPU Kinematics

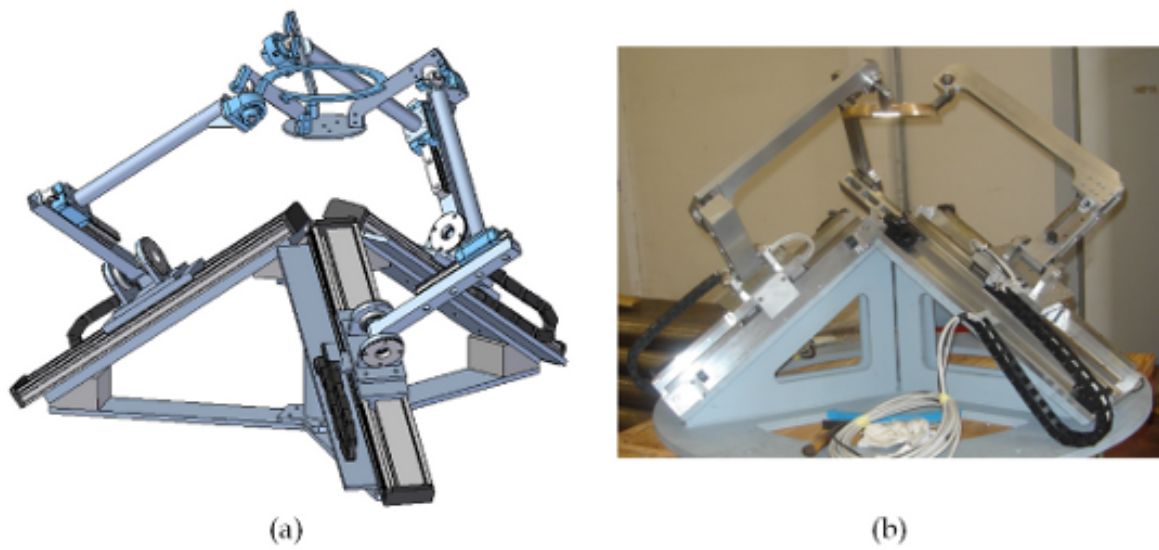


Figure C.7: 3PRRR SPM where linear actuators are used [24]

## Kinematic analysis and optimal design of a novel 3-PRR spherical parallel manipulator

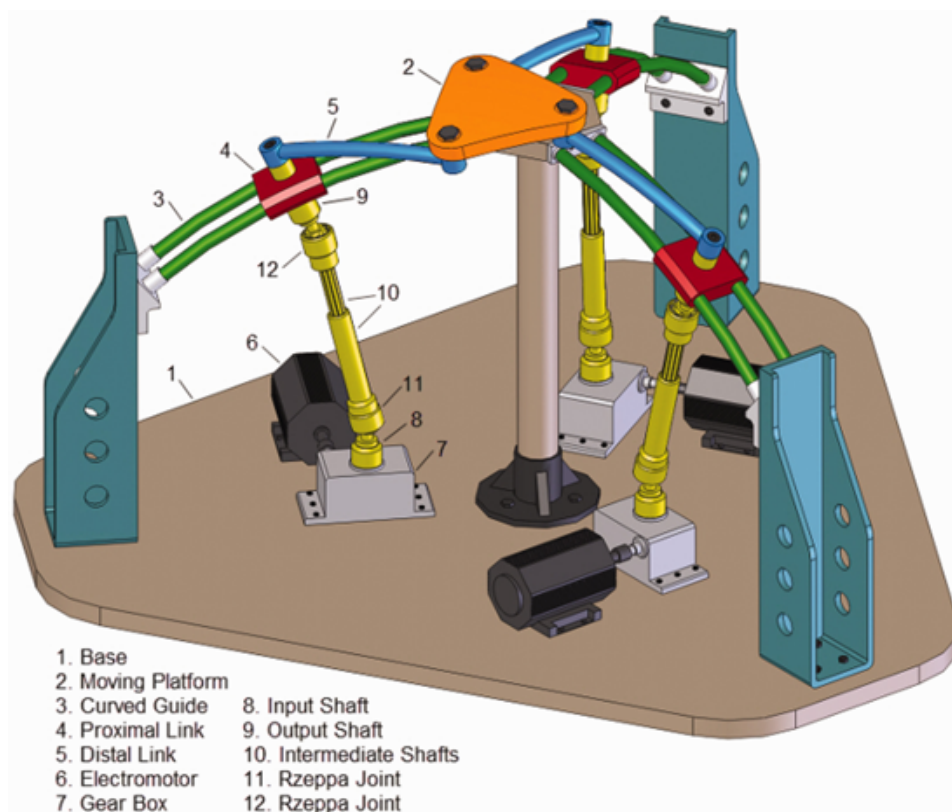


Figure C.8: 3-PRR with sliding across rails [25]

### Modelling of a Remote Center of Motion Spherical Parallel Tensegrity Mechanism for Percutaneous Interventions

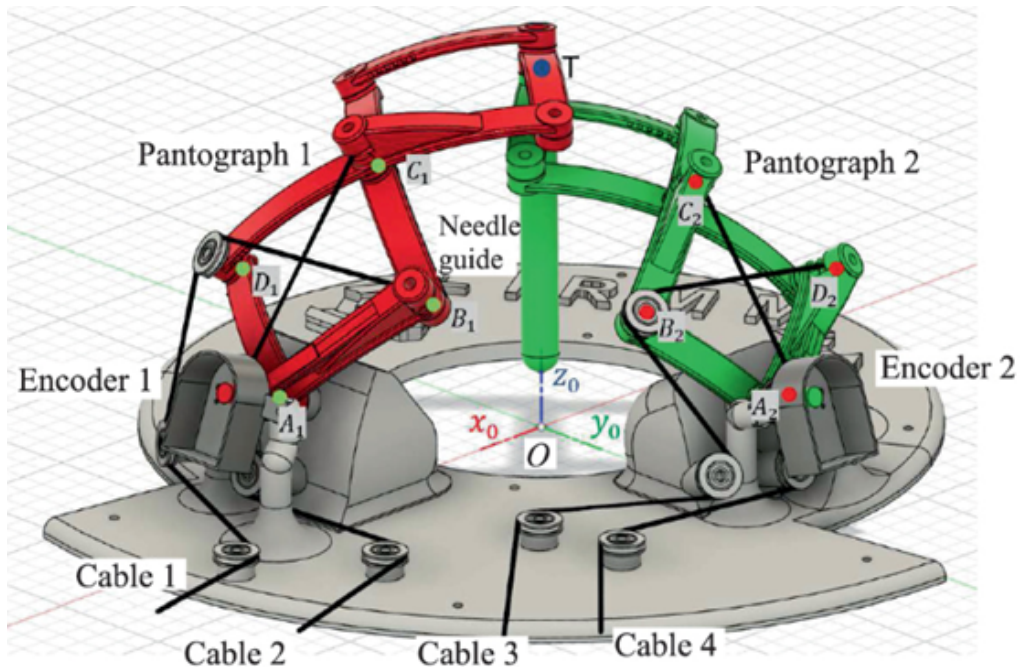


Figure C.9: Design using 2 curved pantographs to have a rotation around a single point O (remote center) [26]

### THE AGILE EYE

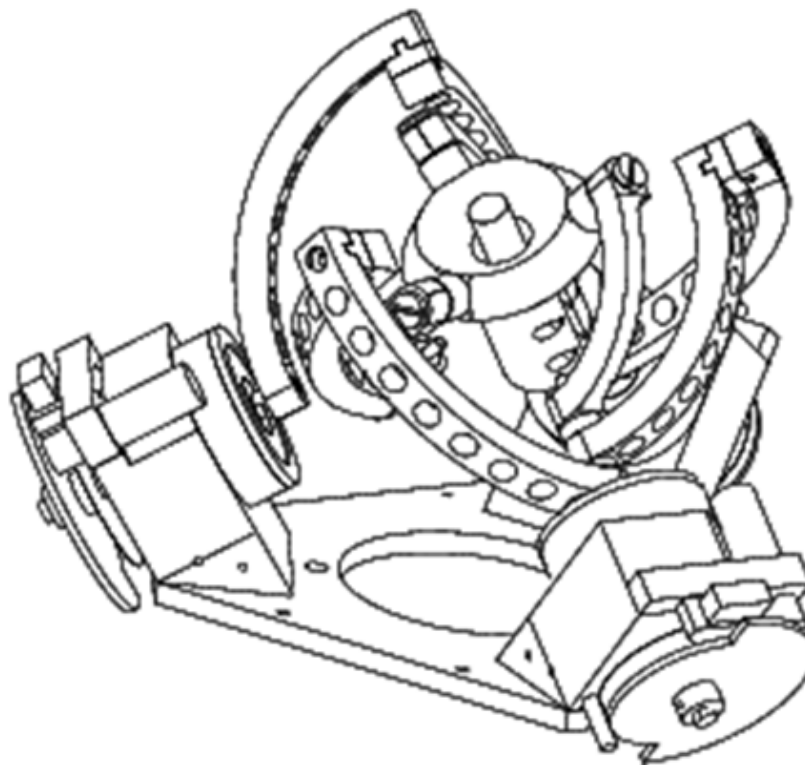


Figure C.10: Agile eye, using 3RRR links for very high speeds [27]

## Structural design of a positioning spherical parallel manipulator to be utilized in brain biopsy

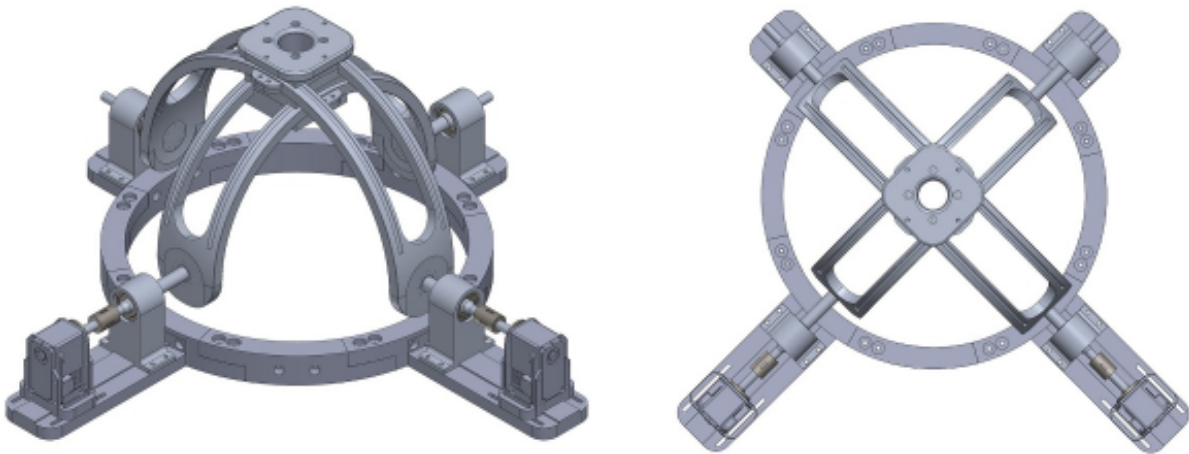


Figure C.11: A sliding puck in between rails that rotate [28]

## Mechatronic Model of a Compliant 3PRS Parallel Manipulator

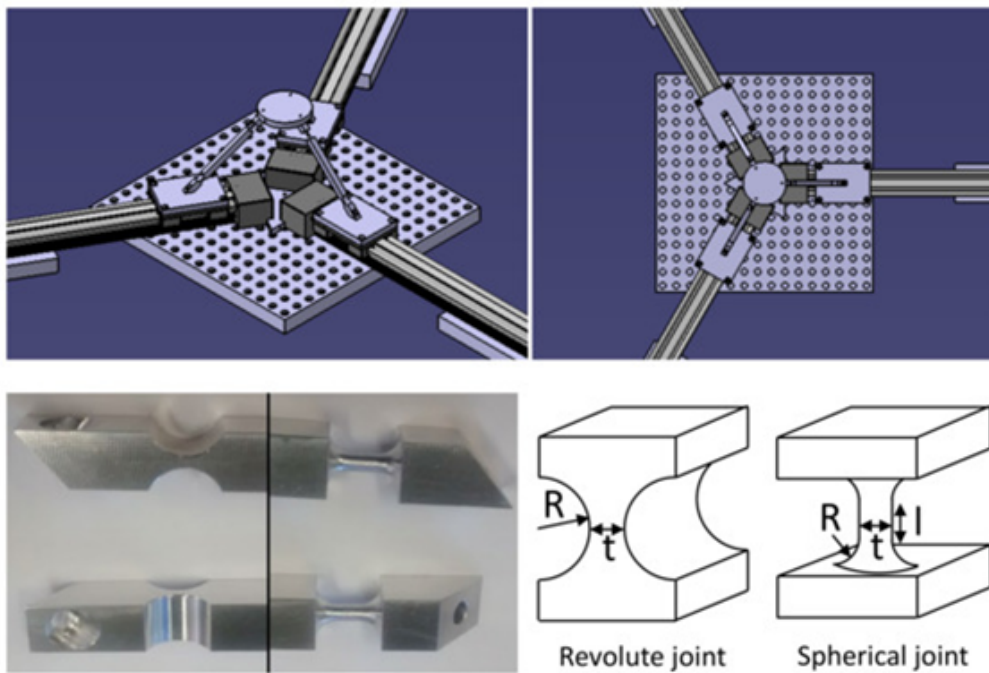


Figure C.12: 3PRS manipulator, which uses linear actuators to change the angle of legs and uses compliant joints [29]

### A virtual power algorithm for dynamics analysis of a 3-RRcP spherical parallel robot using the screw theory



Figure C.13: A 3RRcP (circular track for prism), allowing for rotational movement [30]

# D

## Mini review Beam steering application

Beam steering is used to alter the path light takes, by adjusting a lens or mirror. Here tip/tilt is required to steer and piston motion (up and down) to compensate phase difference when an array of mirrors or lenses is used.

Beam steering can be split into mechanical and non-mechanical, as well as active and passive. Passive systems are inexpensive, less losses, easily scalable, reproducible and thermally stable [31]. However, these 'passive' systems have a steering antenna to achieve a difference in input angle (not really passive thus!). Ranges of motion are between  $\pm 20$  to  $60^\circ$  degrees and only limited in frequency by the laser source angling. Solutions described are for microwaves.

Beam steering can be split into multiple methods:

- Active optics
- Lenslet arrays
- Adaptive optics
- Gimbals
- MEMS
- Rotating polygons/ mirror
- Fast steering mirror/ scanning mirror
- Risley prism
- Resonant scanner
- Optical deflectors (EOD & OAD)

Number of resolvable spots can be deemed as the resolution of the deflector, as it defines the number of independent spots or pixels that can be addressed across the maximum deflection angle [32]. Aka small maximum deflection angle means low number of independent spots.

Performance overview

Scan type	Deflection speed	
	Low	High
Raster scanning		Polygon wheel & resonant scanners
Random-access scanning	Galvano-, piezo- & MEMS scanners	Optical deflectors (EODs & OADs)

Fig. 1. Categories of laser beam scanner technologies.

Table 1. Properties\* (typical values) and comparison of laser beam scanners for a near-infrared wavelength.

Scanning technology	Aperture [mm]	Max. deflection angle $\theta$ [rad]	Max. velocity $\dot{\theta}$ [ $10^3$ rad/s]	Accuracy $\Delta\theta$ [ $\mu$ rad]	Response time $\tau$ [ $\mu$ s]	Efficiency or Transparency
		(Number of resolvable spots $N$ )	(Rate of resolvable spots $\dot{N}$ [ $10^6$ ])	(Accuracy per resolvable spot [%])		
Galvo scanner	7 ... 30	0.5 ... 1 (3000 ... 18000)	$\sim 0.1$ (0.5 ... 1)	$< 2$ ( $< 5$ )	$\sim 10^3$	$> 95\%$
Polygon scanner	2 ... 12	0.6 ... 1 (2000 ... 7000)	1 ... 10 (5 ... 40)	$\sim 200$ ( $\sim 120$ )	$\geq 10^3$	$> 90\%$
Piezo scanner	10 ... 25	0.01 ... 0.1 (100 ... 1000)	0.01 ... 0.1 (0.1 ... 1)	$\sim 1$ ( $\sim 1$ )	$\sim 10^3$	$> 95\%$
MEMS scanner – static	1 ... 2.5	$\sim 0.5$ (200 ... 1000)	0.1 ... 1 (0.1 ... 1)	n.a.	$\sim 10^3$	$> 90\%$
MEMS scanner – resonant	$\sim 1$	0.5 ... 1 (500 ... 1000)	10 ... 30 (5 ... 20)	n.a.	$\geq 10^3$	$> 90\%$
EOD (Pockels effect)	2	$\sim 0.001$ (2)	2 ... 20 (3 ... 30)	$\sim 1$ ( $\sim 0.2$ )	0.04 ... 1	$> 85\%$
EOD (Kerr effect, KTN)	0.5	$\sim 0.2$ (50)	$\sim 40$ (15)	n.a.	$\sim 10$	$> 90\%$
AOD	1 ... 10	0.01 ... 0.05 (10 ... 500)	5 ... 250 (20 ... 80)	$\ll 0.1$ ( $\ll 0.1$ )	0.5 ... 15	60% ... 80%

\*Data according to official information by Cambridge Technology Inc., Scanlab AG, Raylase AG, Piezosystem Jena GmbH, Physik Instrumente (PI) GmbH & Co. KG, Fraunhofer-Institut IPMS, Lemoptix SA, Adriatic Research Institute, Hamamatsu Photonics K.K., AA Opto-Electronic Company, Gooch & Housego, Brimrose Corp., Isomet Corp., IntraAction Corp., NTT Advanced Technology Corp. and Conoptics Inc.

(a) Performance table [32]

(b) Overview of properties of various beam steering methods [32]

Figure D.1: Performance of beam steering methods

“Performance of random-access mirror based scanners, in terms of maximum deflection angle velocity, is physically limited by the inertia associated with the rotating mirror and other moving parts of these scanners.” (visible in Fig. D.2) [32]. Inertia gap determines accuracy and frequency combination where no current random-access solution exists [33].

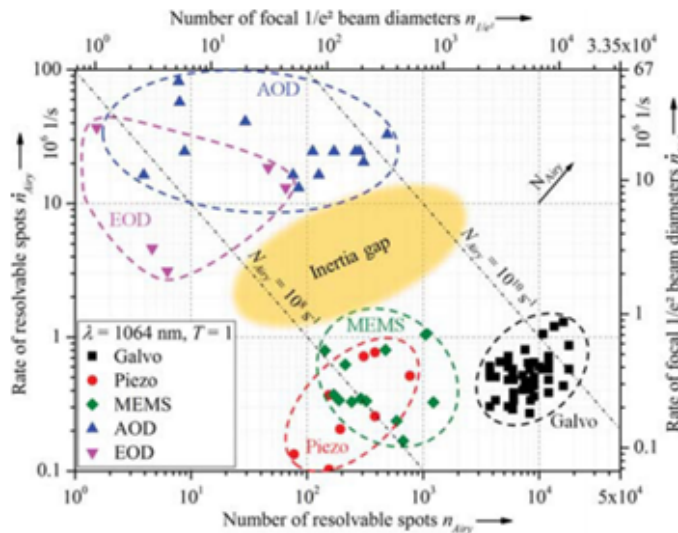
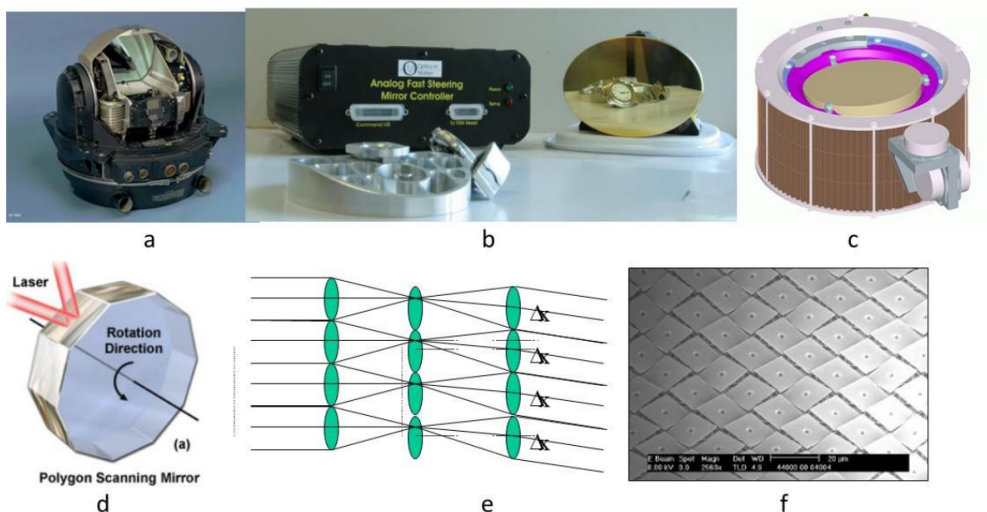


Fig. 5. Number and rate of resolvable spots and focal beam diameters  $1/e^2$  for  $\lambda = 1064$  nm and  $T = 1$ . Reproduced from Bechtold et al. (2013b).

Figure D.2: Inertia Gap visible in frequency (vertical axis) and resolution (horizontal axis) [32]

### Mechanical beam steering

Mechanical movement has the advantage of providing accurate and reliable performance, at the cost of increased size & weight as well as high cost and large amounts of power [34].



**Figure 1 : Mechanical Approaches to Beam Steering, a) Gimbal, b) Fast Steering Mirror (FSM), c) Risley prism, d) Rotating Polygon, e) Lenslet Array, and f) MEMS array.**

Figure D.3: Overview Mechanical solutions for beam steering [35]

Mechanical solutions, such as Galvo-scanners, MEMS or piezo scanners are fundamentally limited by the inertia associated with the mass of the rotating mirror and other moving parts [32]. Also influenced negatively by drift and temperature dependencies, but larger range in possible wavelengths to handle compared to EOD/AOD. Solutions for beam steering of IR spectra wave (THz order) exist, allowing for more than ± 120° degrees of steering angle at 200 Hz bandwidth [36]. These angles are however in a preferential direction, with less angle in a secondary direction. Also, the high angles tend to be oscillating systems again. Additionally, frequency is often limited in range to certain bandwidths.

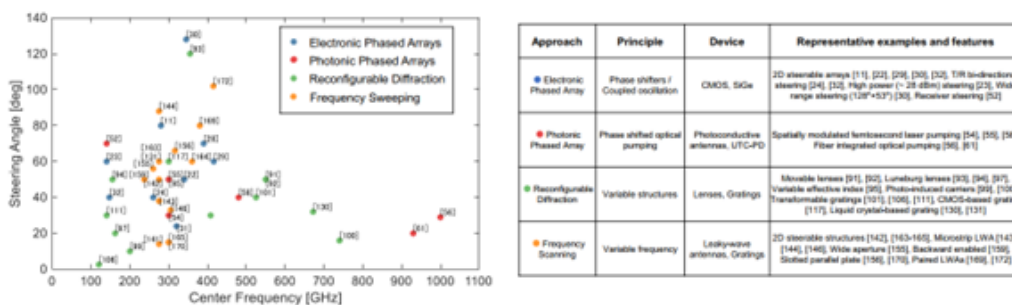


**Fig. 26 Summary of the demonstrated beam steering ranges for the representative approaches reviewed in this article**

Figure D.4: Performance of beam steering with steering angle vs frequency[36]

Trivia: Lenses can also be used to adjust radio waves. Mechanical monolithic solutions for beam steering are eventually limited by mass ( $D^3$ ) and power ( $D^5$ ), which is why array based set-ups are a better solutions ( $D^2$  scaling for both) [37]. However, influence of vibrations in an array can create array-element positional errors which result in image blur. Up to 1.6th wave can be adjusted for in 1992, but structure required to make a coherent array would be very heavy and still influenced by thermal effects. A feedback loop or post detection to adjust for the positional errors. Reaction forces reduce pointing performance in mechanical beam steering [37].

### Active optics

Active optics is similar to adaptive optics, but at lower frequencies. It focuses on low frequency (1Hz) movement for disturbance control (from wind, temperature and mechanical stress), stabilization (vibrations, air turbulence and acoustic noise) [38]. These are used in interferometers as well as laser set ups. (0.05 Hz or less [39])

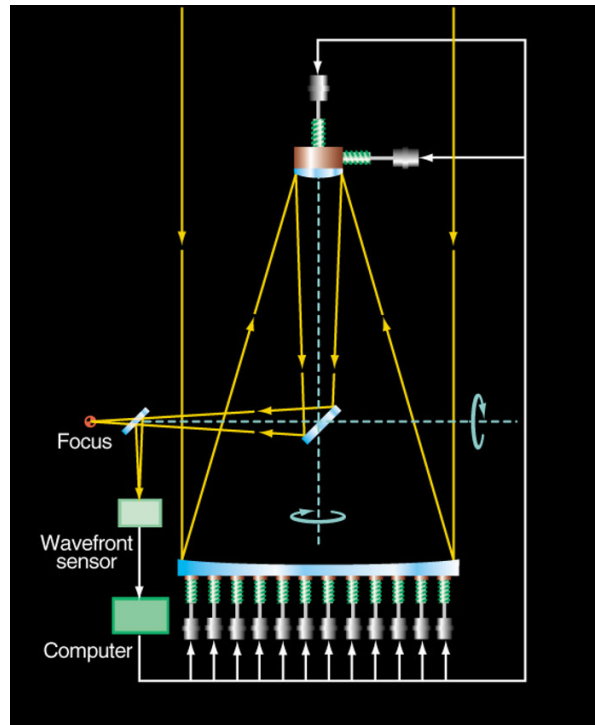


Figure D.5: Active optics [40]

### Lenslet array

Lenslet array is an array of many smaller lenses, which when moved up and down parallel to the each other allows for steering of image. The lens is split into multiple smaller concave lens faces, where superposition causes a single image at the focal plane [41]. This solution has large steering angles, but is very sensitive and thus hard to control. Compact and can be optimized to substantially reduce off-axis aberrations [37].(0.25 rad at 25kHz [42])

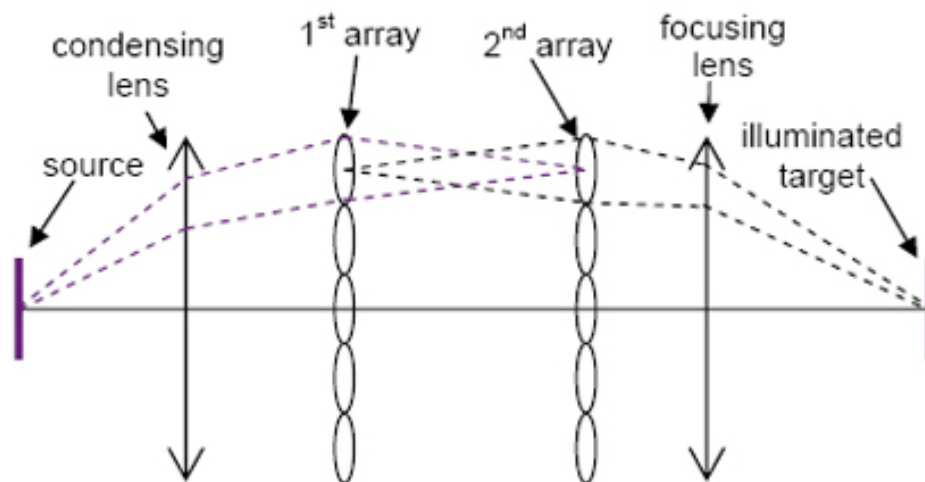


Figure D.6: Lenslet array

## Adaptive optics

Adaptive optics is used to do wavefront correction and static aberration correction, which is used in ground-based telescopes, retinal imaging, microscopy, free-space optical communication, optical trapping or beam stabilization [43]. This is high frequency adjustment (100-1000Hz), at smaller amplitude. Frequencies range from several hundred Hz [44] to 1000 Hz [45] ( $\pm 75^\circ$  degrees at  $< 0.1\text{Hz}$  and  $\pm 0.1^\circ$  degree at  $> 10\text{Hz}$  [46]) Movement within adaptive optics of 9, 30 or 100 micron [47] at above frequencies, visible in Fig. D.7.

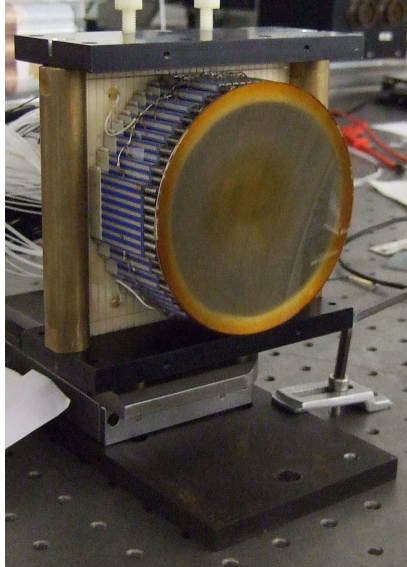


Figure D.7: Adaptive Optics [47]

## Gimbals

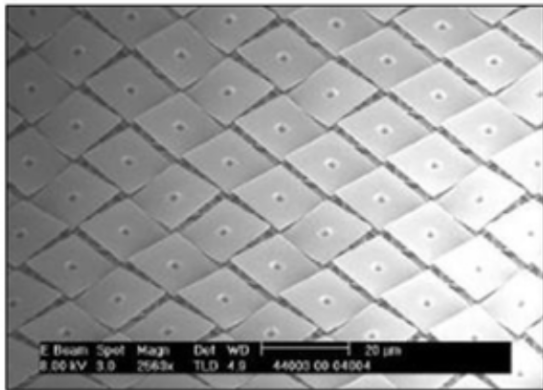
Inertially stabilized platforms have many applications, such as surveillance, target tracking, missile guidance, gun-turret control, communications, astronomical telescope and handheld cameras. The gimbal visible in Fig. D.8 can have an optic placed in the center and have up to 30mrad at 360Hz tip/tilt rotation [48]).



Figure D.8: Gimbal mount [48]

## MEMS

MEMS laser scanners (visible in Fig. D.9a) are used for applications such as confocal microscope, bar code reading, finger print sensing, Optical coherence spectroscopy (OCT), Retinal Scanning Display (RSD), printing, head-up displays and LIDAR [49]. Requirements are more demanding for display applications, since scanning is limited by optics and signals. MEMS can be split into 3 types for displaying, namely 2-dimensional arrays (I.e. DLP beamer (folding mirror array)), 1-dimensional arrays (GLV (ribbon bending array)) and 2-dimensional laser scanning devices (100-350kHz [50]). Resonant MEMS have a range between 17-76° degrees, with resonant frequencies of 17.4 - 40 kHz, resulting in resolution between 17-79.5° degrees mm. 65° and 53° degrees at 60Hz and 21.3 kHz frequency, by vibration of a mirror around 2 axis. The axis rotate with compliant joints using a single actuator at 45° degrees to the joints. Each vibration mode allows for a different scanning direction, based on design of compliant joint. A resonant scanner is therefore never vibrationless [51].



(a) Optical MEMS devices, where small plate are rotated to reflect the incoming ray [35]

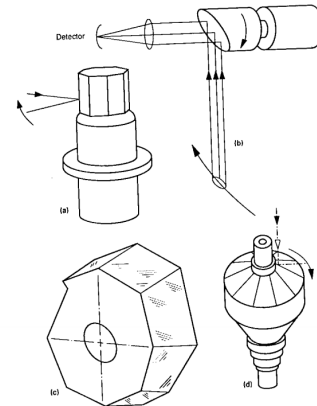


Fig. 3.6 Polygon scanners. [Parts (a), (b), and (d) from Ref. 1, © 1991 Marcel Dekker; part (c) from Ref. 2, © 1991 Marcel Dekker.]

(b) Rotating polygon scanner workings[52]

Non-resonant MEMS have a resolution between 36° and 120° degrees mm, with a range of deflection between 10-29° and 65° degrees (1D scanner) [49]. (6.2° degrees with 315Hz and 144 Hz max freq. (MEMS) [53], 5.6° degrees with 200kHz max frequency (MEMS) [54]). 2d mems scanner have angles ranging between 10-43° degrees, but can be improved using a magnification lens (120° at 4kHz). This however does mean the light beam becomes smaller to achieve a larger steering angle [35], [49]. Hybrids also exist, which can achieve more angle when driven at resonance frequencies (39° (11.2 kHz) to 7.25° (60Hz)).

## Rotating polygons/ mirrors

These mirrors are used to scan an object, by moving across a pre-defined path, shown in Fig. D.9b. This can be done at very slow or fast rates (8 to 50kHz) and small to large angles (up to 180° degrees) [52]. They are negatively effected by mirror distortion, bearing wear, vibration, noise and gyroscopic effects as well as having a lower scan efficiency of the polygon shape. Benefits are high speed, angle and velocity stability.

## Fast steering mirror

Fast steering mirrors (also called galvanometers) move a single mirror face fast (mainly) in tip and tilt directions, visible in Fig. D.10. They do have a certain amount of settling time (6msec), but allow for high frequencies [35]. Bandwidth is influenced by the lowest uncontrollable resonance of the scanners armature, occurring commonly between 2.6 and 5 kHz i.e. 10Hz or lower [52].

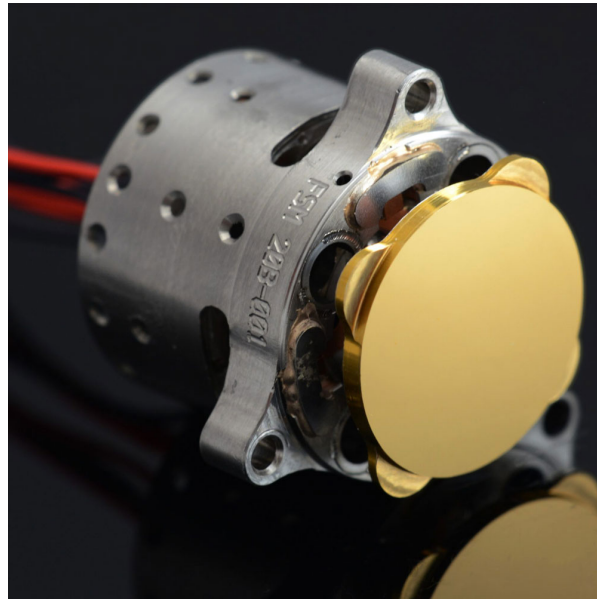


Figure D.10: Fast steering mirror [55]

Resonant scanners are a type of steering mirror, where the mirror is oscillated at the resonance frequency of the entire system. This will give, based on the mode that is excited, a fixed pattern of movement at a fixed frequency [52]. Resonant frequency are commonly between 10 and 18000 Hz with a range of motion between 2 and 30° degrees ( $\pm 7.5^\circ$  at 8-12kHz [56]). Piezoelectric versions also exist, which can have high frequencies (45kHz or more) but only very small steering angles ( $<0.05^\circ$  degrees) [52] at high voltages ( $\pm 2^\circ$  degrees & 125 kHz [57]). Combination of variants are also possible for more range or more DoFs, such as polygon-galvo, disk-galvo, resonant scanner-galvo, polygon-polygon or a cam drive scanner. Range of Galvanometers are limited to  $\pm 6^\circ$  degrees (6.6° degrees total at 400Hz [58]) ( $\pm 7^\circ$  degrees at 630Hz[59]) (bandwidth 2axis 20Hz [44]) ( $\pm 7.5^\circ$  degrees at 500Hz (array) [60]) (+-22.5° & 2.8kHz (small angle) (2-axis) [61]) (+- 0.2° degrees at 2.5kHz [62]) (+-0.4° degrees at 4kHz (2-axis) (22.5° degrees max) [62]) (+-1.2° at 333 Hz (2-axis) [63]) Very fast Galvo scanners have developed, capable of 275 kHz to 2MHz, but range has to be limited [64]. (10  $\mu\text{m}$  at 2.7 kHz (3-axis) [65])

## Risley prism

Risley prisms are an array of multiple prisms (2 or more) (visible in D.11, which steer a beam by rotating the individual prisms [31], [66]. This can be a single direction rotation, thus less accelerations. Common problems are a blind spot around the optical axis (thus limited shallow angle) as well as non linearity introducing distortion. Also, the relation between angle and rotation of prism is nonlinear, making control also nonlinear. Additionally, tolerances, accuracy in wedge angle, alignment errors and temperature and pressure variations affect precision. Benefits of Risley prism beam steering are compact, robust, no coupling, low moment of inertia and low sensitivity to vibrations.

Gratings are lighter, thus higher frequency is possible, but they have dispersion (frequency based effects). Range of motion of Risley prism beam steering systems is typically between 15° and 120° degrees [66], with a frequency of between 75 and 500 Hz, and 30 to 200kHz if rotating [67]–[69]. (100 Hz at 100°+ scan angle [70]) (90° degrees at 200kHz [69]) (100  $\mu\text{rad}$  at designed 6.5kHz [71]) (120° degrees at 50Hz [72]) (69° degrees at 30kHz [73]).

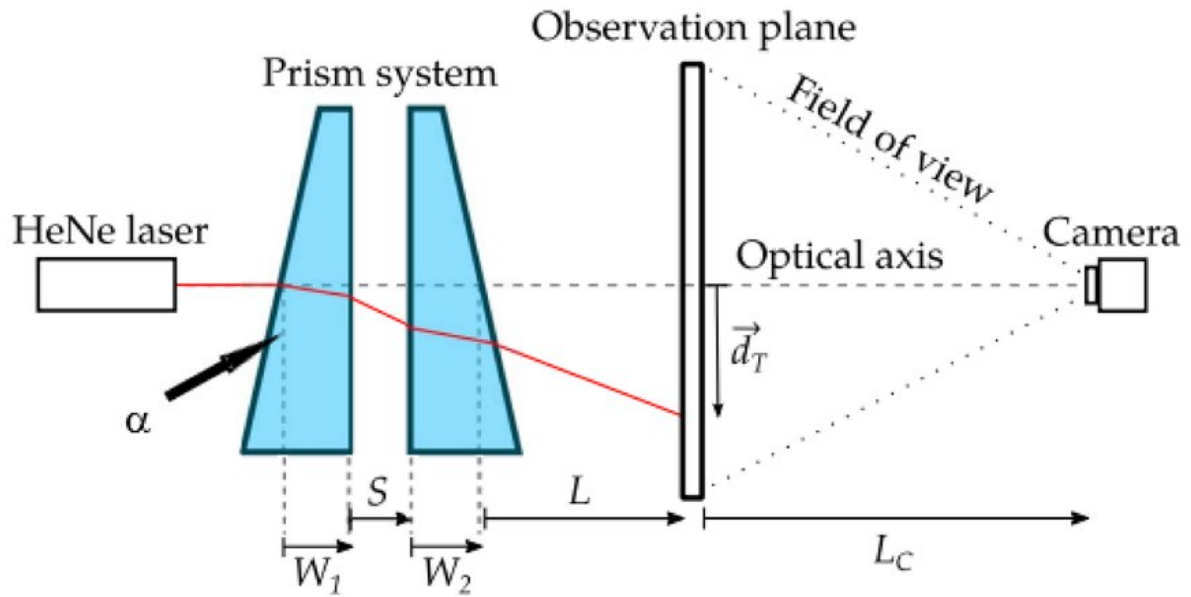


Figure D.11: Risley prism [66]

### Non-mechanical beam steering

Non mechanical beam steering works by changing the phase of wave light per frequency or position, thereby moving a resulting wavefront either in time or position (LC based [74]). TLC is only applicable to polarized light, but relatively slow (100 ms) and limited optical dynamic range. [75] Electro-Optic deflectors have a range of motion of  $\pm 1.5$  mrad at 1kHz frequency [76]. These work by changing the electric field in a crystal through which light beams move, thereby influencing the phase of the light [32]. The accuracy of these EOD is  $0.1\text{-}10 \mu\text{ rad}$ , due to only being influenced by voltage. The maximum angle can be increased by placing several prisms in sequence. Maximum angle from a single prism is a KTN EOD, which has a refraction perpendicular to light direction (see Fig. D.12b). The max angle here is  $\pm 110$  mrad, but lower accuracy (10mrad). KTN introduces astigmatism (single focus point becomes multiple). (GHz is mentioned, but over few degrees if not stacked). The small angles mean low amounts of resolvable points  $N$ , and thus low resolution.

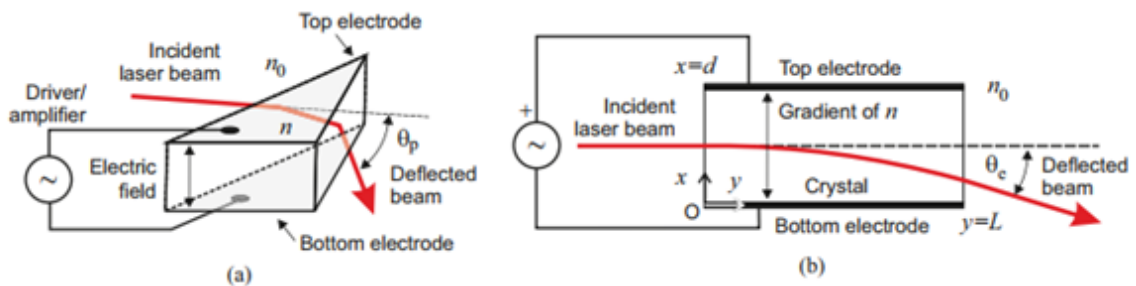


Figure D.12: Electro-Optic Deflector (EOD) workings [32]

Acoustic-Optic Deflectors (AOD) use acoustic waves on a crystal causing a changing refractive index due to rarefaction and compression of the material. This causes a spatial modulation (phase change) to occur which will diffract the input beam. This allows for the creating of light spots at will, in a single plane [77]. AOD is slower, due to the speed difference of sound vs light, but still 40-500 MHz bandwidth [32]. A higher bandwidth however will cause a lower diffraction efficiency, thus bandwidth is limited to not reduce efficiency below 50 to 60%. Same as EOD, small angle thus small resolution. More accurate than EOD, with  $0.15\text{-}1.6$  nrad angular accuracy. Faster than mirror based solutions (4 to 100x), but limited due to efficiency and power handling. Noteworthy is the undefined angle when frequencies are changed. AOD introduce at high scanning speed cylindrical focusing effect. Adding AOD/EOD in front of Galvo will result in a faster and more precise system (see Fig. D.13), allowing for high bandwidth and resolution [32].

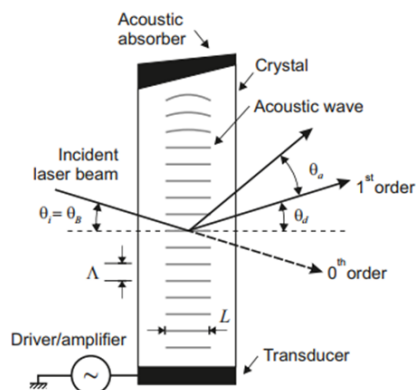


Fig. 3. Typical configuration of an Acousto-Optic Deflector (AOD). Adapted from Zeng et al. (2009).

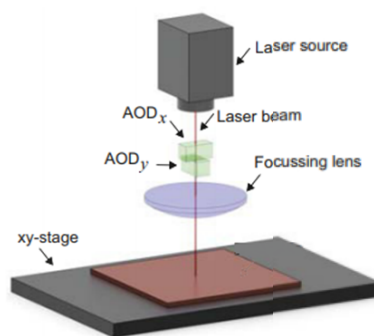


Fig. 4. A two-dimensional scanner can be formed by arranging two AODs orthogonally in series.

Figure D.13: Acoustic-Optic Deflector (AOD) workings [32]

Another option is electro-wetting, where the contact angle changes according to the potential difference between electrolyte liquid and a conductor substrate [34]. i.e. angle of fluid changes which allows for steering and forming. This is a high light efficient solution, since no polarizing occurs. (40Hz frequency, with prism 9.5° to 13.2° degrees)

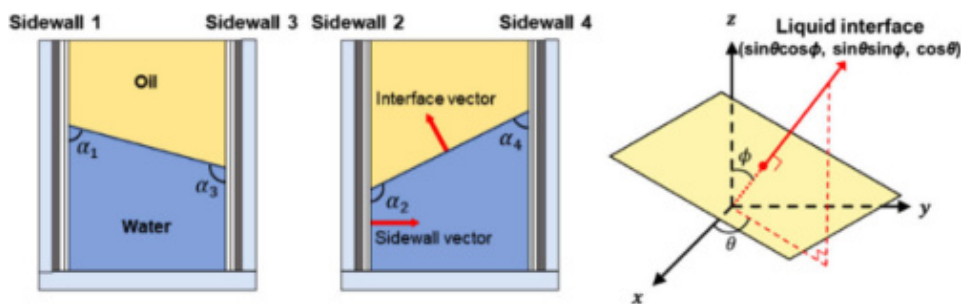


Figure D.14: Electro wetting workings [34]

LCPG use polarization birefringent gratings, which uses liquid crystals to alter phase. These can achieve large angle, up to at least +/- 40° degrees in one direction [35]. Other directions are less (15° degrees). Another option for non-mechanical beam steering is the usage of liquid-based devices. Here the beam is steered using the phase difference caused by the shape of the liquid [34].

